Investigation of Personal Comfort Systems: Experimental Evaluation of Desk and Wearable Fans in Shared Office Environments

Tazia Rahman

A Thesis in

The Department of

Building, Civil, and Environmental Engineering

Presented in Partial Fulfillment of the Requirements

Master of Applied Science in (Building Engineering) at

Concordia University

Montreal, Quebec, Canada

March 2026

CONCORDIA UNIVERSITY

School of Graduate Studies

This is to certify that the thesis prepared

By: Tazia Rahman

Entitled: Investigation of Personal Comfort Systems: Experimental Evaluation of Desk and Wearable Fans in Shared Office Environments

and submitted in partial fulfillment of the requirements for the degree of

Master of Applied Science (Building Engineering)

complies with the regulations of the University and meets the accepted standards with respect to originality and quality.

Signed by the final Examining Committee:

_____ Chair

Chair's name

_____ Examiner

Examiner's name

_____ Examiner

Examiner's name

_____ Supervisor

Dr. Mohamed Ouf

Approved by _____

Chair of Department or Graduate Program Director

_____ 2026 _____

Dean of Faculty

Abstract:

Investigation of Personal Comfort Systems: Experimental Evaluation of Desk and Wearable Fans in Shared Office Environments

Tazia Rahman

Personal Comfort Systems (PCSs), such as desk fans, can reduce perceived warmth through elevated air movement but their spillover effect on nearby occupants remains insufficiently investigated. In addition, few studies have directly compared different fan mechanisms, such as bladed, bladeless desk fans and wearable fans. This study aims to quantify the effects of personal fan (three desk and two wearable fans) configurations and operating speeds on thermal comfort under ASHRAE Standard 55. It further examines zonal cooling performance and cooling efficiency of different fans while assessing vertical air distribution at multiple body levels of the primary occupant and associated localized draught risk to adjacent co-workers. Experiments were conducted in a controlled office space (25 ± 1 °C, 40 ± 5% RH) with a 23-segment adaptive thermal manikin. Results show that whole-body cooling is primarily governed by airflow intensity and distribution. Conventional bladed desk fans produced the strongest cooling but exceeded recommended airspeed limits, whereas USB-powered and bladeless fans maintained guideline airspeeds providing controlled cooling with more uniform zonal Corrective Power (CP). Wearable fans targeting the thermosensitive face–neck region achieved cooling comparable to broader breathing-zone–torso airflow. Co-worker measurements revealed higher draught risk (categories B–C) at rear positions. Although subjective responses in real offices were not assessed, the direct comparison of PCS technologies using manikin-based physiological and airflow measurements provide new insights into the spatial cooling and their influence on overall comfort. The findings also offer guidance for improving PCS performance evaluation methods and optimizing fan-based PCS design for practical implementation in shared environments.

ACKNOWLEDGEMENTS

First and foremost, I would like to express my sincere gratitude to my supervisor, Dr. Mohamed Ouf, for his guidance, mentorship, and continuous support throughout this research. I am especially grateful for the supportive and stimulating research environment he has fostered in the Intelligent Buildings and Cities Lab (IBCL). His insightful feedback and encouragement have been invaluable in shaping this work and my development as a researcher.

I would also like to sincerely thank my examiners for their valuable time and thoughtful comments, which have greatly contributed to improving the quality of this thesis.

I would like to express my heartfelt appreciation to my husband and my son, Farabe Ibn Hossain and Adyaan Bin Farabe, for their unconditional love, patience, and unwavering support. I deeply value the sacrifices they have made that allowed me to pursue and complete this work. Their encouragement and understanding have been a constant source of strength and motivation throughout my academic journey.

Finally, I would like to acknowledge the collaborative and supportive environment provided by my colleagues in IBCL at Concordia University. The engaging discussions, exchange of ideas, and shared learning within the group have greatly enriched my research experience and made this journey both meaningful and enjoyable.

Table of Contents

CHAPTER 1- INTRODUCTION 1…… 1

1.1 Overview ……. 1

1.2 Objective of the study……. 5

1.3 Scope of the study……. 5

1.4 Thesis outline……... 6

CHAPTER 2- LITERATURE REVIEW…… 8

2.1 Thermal comfort theory and the need for localized control…… 8

2.2 PCS application in buildings…… 9

2.3 Classification of PCS based on heat transfer system……... 10

2.3.1 Conduction-Based PCSs…… 10

2.3.2 Convection-Based PCSs……. 11

2.3.2 Radiation-Based PCSs……... 12

2.4 PCS Classification by targeted body region and evaluation approach……. 13

2.5 Standards and guidelines for PCS operation…… 14

2.6 Overview and classification of thermal manikin……. 15

2.6.1 Basic Thermal Manikin…….. 16

2.6.2 Adaptive Thermal Manikin…… 17

2.6.3 Numerical Thermal Manikin…….. 18

2.7 Overview of JOS-3 thermoregulation model…… 19

2.8 Use of fans as PCS in office settings……... 20

2.8.1 Ceiling Fan……. 21

2.8.2 Stand Fan…… 22

2.8.3 Desk Fan……. 23

2.8.4 Wearable fans……. 24

2.9 Methods for evaluating desk fans for whole body comfort and Zonal Cooling….. 25

2.9.1 Human subject-based evaluation methods……. 25

2.9.2 Manikin-based evaluation methods…… 26

2.10 Metrics for quantifying PCS efficiency……... 27

2.10.1 Equivalent Homogeneous Temperature (EHT) …… 27

2.10.2 Corrective Power (CP) …….. 28
2.10.3 Coefficient of Performance (COP) …… 29
2.11 Research gaps and positioning of the present study…… 30
2.11.1 Limitations in comparison of airflow mechanisms (bladed, bladeless, and wearable) of fans…… 30
2.11.2 Limited Understanding of Multi-Region vs. Breathing-Zone Cooling Effects……. 31
2.11.3 Need for multi-height and zonal airflow analysis …….. 31
2.11.4 Lack of co-worker exposure assessment…… 32
2.11.5 Lack of Clarity in PCS standards……... 33
Chapter 3 – METHODOLOGY…… 34
3.1 Thermal Manikin……. 34
3.2 Validation of manikin operating modes for the experiment…… 34
3.3 Cooling Devices……... 38
3.4 Test conditions and protocol…… 39
3.5 Air velocity measurement procedure……... 44
3.6 Determining cooling whole body thermal comfort…….. 46
3.7 Determining cooling efficiency of PCS devices……..... 46
3.8 Analyzing draught risk at the co-worker's location……. 48
3.9 Overall representation of the methodology……..... 49
CHAPTER 4- RESULT AND DISCUSSION……..... 51
4.1 Effect of PCS devices on whole body thermal comfort……... 51
4.1.1: PMV Analysis…… 51
4.1.2 Equivalent Temperature (Teq) Profile……... 54
4.2 Effect of zonal cooling on overall thermal comfort……. 58
4.2.1 Zonal Corrective Power (CP)……. 59
4.2.2 Skin temperature distribution across upper body……... 61
4.2.3 Effect of zonal cooling on whole body thermal comfort……... 62
4.3 Cooling efficiency of the PCS configurations……..... 65
4.4 Air speed Analysis at zonal level……..... 67
4.4.1 Multilevel air speed exposure at primary occupant (P1)…… 67

4.4.2 Spillover effect at Co-worker at P2 and P3…… 69
4.4.3 Draught Risk (DR) analysis……... 71
4.5 Discussion…… 72
CHAPTER 5 - CONCLUSION AND FUTURE WORKS…… 77
5.1 Findings…….. 77
5.2 Implications of this study……... 79
5.3 Limitations……. 79
5.3 Future directions…… 80
References…….. 82
Appendices……. 94

List of Figures

Figure 1: Body-construction concept of JOS-3…… 20
Figure 2: The control concept of JOS-3……... 20
Figure 3: (a) Thermal comfort vote with 24 human subjects], (b) Suitable air speeds at different temperatures in different climate chamber experiments…… 32
Figure 4: Comparison of face skin temperature of manikin (comfort and JOS-3 mode) and human (face-considering the average of chin and forehead)…….. 37
Figure 5: Comparison of neck skin temperature of manikin (comfort and JOS-3 mode) and human (neck) ……. 37
Figure 6: Appearance and designed configurations of the selected PCS devices…… 40
Figure 7: Logged air temperature at experimental office space……... 41
Figure 8: Floor plan of controlled office space and the experimental setup showing manikin placement…… 41
Figure 9: Experimental setup showing manikin and adjacent coworker placement…… 42
Figure 10: Test protocol timeline for Personal Comfort System (PCS) devices including stabilization periods and three fan speed intervals…… 43
Figure 11: Data Capture and selection procedure…… 44
Figure 12: Selected levels for airspeed measurement and anemometer settings……. 45
Figure 13. Cooling scenario with Configuration C2 (Left), C3 (middle) and C6(Right)… 45

Figure 14: Framework of methodology and systematic evaluation……. 50
Figure 15: Predicted Mean Vote (PMV) at Fan off and 10th minute of fan-on conditions. The neutral zone represents the ASHRAE 55 -0.5 < PMV < +0.5…… 52
Figure 16: PMV reduction with increased airspeed levels in desk fan configurations (C1-C5)……. 54
Figure 17(a): Equivalent Temperature (Teq) profile for C1 at three speed levels……... 55
Figure 17(b): Equivalent Temperature (Teq) profile for C2 at three speed levels…….. 55
Figure 17(c): Equivalent Temperature (Teq) profile for C3 at three speed levels……... 56
Figure 17(d): Equivalent Temperature (Teq) profile for C4 at three speed levels…….. 56
Figure 17(e): Equivalent Temperature (Teq) profile for C5 at three speed levels……... 57
Figure 17(f): Equivalent Temperature (Teq) profile for C6 at three speed levels……... 57
Figure 17(g): Equivalent Temperature (Teq) profile for C7 at three speed levels……... 58
Figure 18: Corrective Power (CP) values of different body parts in terms of local heat loss (Watts) across three fan speed settings (low, medium, high)…… 60
Figure 19: Thermal image of upper body segments at high speed for all 7 configurations 62
Figure 20(a): Whole body and zonal CP of desk fans directed toward chest…….. 64
Figure 20(b): Whole body and zonal CP of desk fans angularly (45 degree) directed toward chest ……..……..……..……..……..……..……..……... 64
Figure 20(c): Whole body and zonal CP of wearable fans ……..……..……..... 65
Figure 21: Power input and COP of bladed and bladeless fan configurations ……..... 67
Figure 22: Airspeed at different level for the primary occupant (P1) ……..... 68
Figure 23: Airspeed at different level for the adjacent coworker (P2) ……..... 70
Figure 24: Airspeed at different level for the adjacent coworker (P3) ……..... 70

List of Tables

Table 1: Body parts of the PT Teknik thermal Manikin with respective area (m^2)……. 35
Table 2: Appearance, specifications and setup of the instruments used in the experiment. 36
Table 3: Deviation (%) in skin temperature of manikin (comfort and JOS-3 mode) and human ……..……..……..……..... 38
Table 4: Technical specifications of the selected PCS devices. ……..... 39

Table 5. Clothing insulation values and experimental parameters used for the thermal manikin. ……..……..……..……..…….. 43
Table 6. Comparison of whole-body corrective power in terms of EHT(CP_{EHT}) and Q(CP_Q) from thermal manikin tests across all configurations. ……..……. 66
Table 7: Calculated draught levels (%) at position P2 and P3 for all configurations…….. 72

General Terms

PCS	Personal Comfort Systems
USB	Universal Serial Bus
CP	Corrective Power
HVAC	Heating, ventilation, and air-conditioning
ASHRAE	American Society of Heating, Refrigerating and Air-Conditioning Engineers
PMV	Predicted Mean Vote
PPD	Predicted Percentage of Dissatisfied
PCDs	Personal Cooling Devices
PHDs	Personal Heating Devices
PCM	Phase Change Material
EHT	Equivalent Homogeneous Temperature
CP	Corrective Power
ANSI	American National Standards Institute

ISO	International Organization for Standardization
PI mode	Proportional Integral mode
ADAM	Advanced Automotive Manikin
SAM	Sweating Agile Thermal Manikin
CFD	Computational Fluid Dynamics
VTMs	Virtual thermal manikins
JOS	Joint System Thermoregulation Models JOS
AVA	Arteriovenous Anastomosis
CFIAC	Ceiling-Fan-Integrated Air Conditioning
CFE	Cooling Fan Efficiency
TSV	Thermal Sensation Vote
TCV	Thermal Comfort Vote
PV	Personalised Ventilation
VTCE	Virtual Thermal Comfort Engineering
SAE	Society of Automotive
CP	Corrective Power
COP	Coefficient of Performance

CFE Cooling Fan Efficiency

DR Draught Risk

SD Standard Deviation

Symbols

T_{sk} Skin Temperature

T_{eq}, Equivalent Temperature

P Heat Loss Aj Surface area of each body segment

$T_{sk,j}$ Skin Temperature of each body segment

Q_j Heat loss of each body segments

I_{clo} Clothing Insulation

T_a Local air temperature

v_a Local mean air velocity

T_u Local turbulence intensity

CHAPTER 1- INTRODUCTION

1.1 Overview

Thermal comfort in office spaces has traditionally been maintained through Heating, ventilation, and air-conditioning (HVAC) control strategies, with uniform temperature and humidity within a narrow range throughout the entire space [1][2]. However thermal comfort is highly personalised and decades of research show that it is mostly influenced by metabolism, clothing, posture, activity pattern and sensitivity [3][4][5]. In an open plan office, these differences become particularly evident and centralized control often fails to satisfy all occupants simultaneously [6][7]. Since the occupants are with diverse comfort preferences and thermal neutralities, even an environment optimised for the average occupant still result about 20% of occupants feeling either too warm or too cool [8][9]. To address this limitation, personal comfort system (PCS) has emerged as an occupant-centric technology that provides localised heating and cooling to individual users [10][11]. PCS has been proven of delivering 100% occupant thermal comfort as it allows occupants to fine tune their local thermal environment without conditioning the entire space [12][13][14][15]. Numerous experiments and simulations have shown that acceptable comfort could be achieved at higher setpoints through the incorporation of PCS and thereby HVAC energy consumption could be reduced while improving occupant satisfaction [16][17][18]. In practice, 10-20% cooling energy can be saved through increasing the indoor setpoint temperature by 1-2º C [19][20]. Consequently, PCS are increasingly viewed as a key strategy for achieving energy-efficient and occupant-responsive indoor environments.

Among PCS options, personal desk fans are some of the most widely adopted devices because they are inexpensive, easy to install and provide immediate relieve with increased convective and evaporative heat loss. Desk fans can take advantage of both temporal and spatial alliesthesia, a

pleasant sensation resulting from the alleviation of physiological thermal stress. 'Temporal alliesthesia' occurs during transient shifts in the body as it transitions from non-neutral to equilibrium [21][22][23]. The rapid response from desk fans makes them capable of activating this form of pleasantness in occupants with varied thermal conditions and activity level. 'Spatial alliesthesia' involves simultaneous non-neutral thermal condition on different regions of the body [10][24][25] and can be improved significantly with elevated airspeed on warm environments [11][13][24]. Additionally, the control on local air movements influences the occupants to accept warmer indoor temperatures, particularly when airflow is directed towards exposed regions of the face and upper body [17]. However, despite all the advantages of desk fan, it can increase the risk of local overcooling with excessive air movement and decrease comfort even when overall thermal sensation improves [26]. Another drawback is the airflow coming from the PCS can noticeably modify the micro-environment of nearby coworkers, often leading to the risk of draught discomfort. This spillover effect to the coworker is one of the major limitations of implementing desk fan based cooling strategies in open plan workspace, that remains relatively less studied.

In parallel with research on conventional desk fans, recent studies have increasingly focused targeted cooling to specific segments of the human body with wearable cooling systems (e.g., neck and face fans) as an alternative PCS approach that minimizes disturbances to surrounding occupants. Waseem [27] shows that the portability and negligible energy use of wearable cooling systems have increased research trends almost 20 times higher over the past two decades. These wearable cooling solutions are generally divided into two categories – passive (e.g. radiative cooling textiles) and active (e.g. fan assisted ventilation garments). While radiative cooling textiles and ventilation garments are effective [28][29], they often restrict movement [30] or introduce hygiene concerns due to the recirculated air contaminated by sweat and body odor [29]. On the

other hand, lightweight wearable fans targeting the face and neck regions have emerged as a promising alternative. Although the face and neck account for only 5.5% of the body's surface area, physiological and thermoregulatory studies show that cooling these zones can expand the acceptable indoor temperature boundaries [31]. Cotter and Taylor further demonstrated that the hedonic thermal responses of face and neck are stronger than any other body parts and even small cooling interventions can produce disproportionately large improvement in overall comfort [32]. Additionally, face and neck cooling via lightweight fans has shown reductions in local skin temperature up to 2.1ºC and moderated thermal sensation votes allowing the HVAC set-point elevations up to 32 ºC [29].

Despite this growing body of evidence, a systematic comparison between wearable face and neck fans and conventional desk fans has not yet been thoroughly investigated in an office-like environment. Conventional bladed and bladeless desk fans typically provide airflow to the breathing zone, torso, and hands, while wearable devices primarily deliver targeted cooling to the face and neck regions. While the thermo-sensitivity of the face and neck is well established, it remains unclear whether low-energy, targeted cooling at breathing zone by wearable devices can achieve whole-body thermal comfort comparable to that provided by conventional desk fans. Furthermore, the relative thermal comfort performance of these different PCS technologies have not been evaluated within a unified experimental framework.

In addition, to enable the use of air movement as a comfort strategy, ASHRAE standard 55 limits the airspeed between 0.3-0.8 m/s when a desk fan is directed toward head, face or upper body [33]. This practical airspeed range allows to balance the cooling benefits of increased convection with the potential risk of draught discomfort of the primary user and nearby occupants. However, in the elevated airspeed section the same standard mentions that there is no upper speed limit if the

occupant has direct control, which introduce a degree of ambiguity in practical applications. When occupants adjust the fan speed according to their preference specially beyond the threshold limit, the resulting airflow may become highly non-uniform, with very high velocities directed toward the upper body and head region while the lower body receives minimal airflow [6]. Such conditions may introduce local discomfort and may also affect nearby co-workers who are exposed to unintended air movement.

Despite the increasing adoption of desk fans as PCS, the impact of desk fan airflow on adjacent occupants in an energy conscious open plan office settings remain poorly quantified. Previous research highlights that individual environmental control in open plan office can conflict with shared environmental quality [7]; however, no experimental studies explicitly link desk-fan configurations with airflow spillover and coworker drought risk across multiple heights. This gap is particularly important in practice, as PCS adoption in office is often limited by complaints from nearby occupants who experience unwanted air movements without having personal control. Therefore, A combined analysis of average and local airspeed distribution towards primary occupant, together with potential exposure of the adjacent coworker, is essential for evaluating the practical application of ASHRAE standard 55 guidelines in real-world shared office settings.

Against this background, the overarching goal of this thesis is to experimentally evaluate and compare the thermal performance, airflow characteristics, and shared-environment impacts of non-wearable and wearable PCS in an energy conscious open-plan office setting. This analysis aims to inform evidence-based guidelines for efficient and socially acceptable occupant-centered thermal control.

1.2 Objective of the study

The present study aims to provide an integrated experimental assessment of PCS performance in an open-plan office context. The objectives of this study are:

1. Quantify the effects of personal fan configurations (air distribution mechanism and placement of bladed, bladeless, and wearable fans) and operating speeds on occupant thermal comfort.
2. Evaluate the zonal cooling performance of each fan configuration and examine how localized cooling influences whole-body thermal comfort.
3. Quantify and compare the cooling efficiency of the different fan types across operating conditions.
4. Assess vertical air distribution at multiple body levels to evaluate overcooling risk for the primary occupant and the associated localized draught risk to adjacent co-workers.

1.3 Scope of the study

This research presents a comprehensive experimental evaluation of airflow mechanism and thermal comfort PCS in open-plan office environments with a thermal manikin. It presents a comparative evaluation of different airflow mechanisms, including direct airflow from conventional desk fans, split airflow generated by dual small bladed fans, diffused airflow from bladeless fans, and targeted airflow from wearable cooling devices. In addition, a multi-height airflow measurement structure is developed to better understand zonal airflow exposure at different body levels and its influence on localized and whole-body thermal comfort. The research also quantifies airflow spillover and associated draught risk at adjacent location of coworkers, providing insights into how PCS operation can affect nearby occupants in shared office settings.

The analysis is based on objective physiological measurements from a non-sweating thermal manikin and airflow data measured at different locations in the office space. The scope therefore includes assessment of zonal and whole body cooling effects, spatial airflow distribution and spillover of the desk fans in shared office space.

1.4 Thesis outline

Chapter 1 highlights the significance of PCS, particularly desk fans and wearable cooling devices, as energy-efficient solutions and outlines the challenges associated with non-uniform airflow and potential draught exposure to nearby occupants in shared office spaces. The research objectives and scope of the study are presented are presented based on the background.

Chapter 2 reviews the existing research related to thermal comfort theory, the application of PCS in buildings and operating principles of thermal manikin. It summarizes commonly used human-subject and thermal manikin based evaluation methods, along with key performance metrics and concludes by identifying research gaps that motivate the present study.

Chapter 3 explains the experimental setup, environmental conditions of the controlled office space, criteria for designing the fan configurations, and measurement procedures for airflow distribution. In addition, the analytical methods used to calculate thermal comfort indices, cooling efficiency, and draught risk are presented.

Chapter 4 presents the experimental results and analyzes the thermal comfort performance of the tested PCS configurations. It evaluates both whole-body and zonal cooling effects and explores airflow spillovers and draught risk at nearby co-worker locations to assess the practical implications of PCS use in shared office environments.

Chapter 5 summarizes the key findings of the study and discusses their implications for the design and application of PCS in office environments. The chapter also discusses the limitations of the present experimental framework and suggests directions for future research. Finally, recommendations are provided for improving PCS design and developing clearer guidelines for their implementation in shared indoor spaces.

CHAPTER 2- LITERATURE REVIEW

This chapter reviews existing studies on the application and performance evaluation of PCS, including both human subject and thermal manikin–based investigations. It summarizes the key methods and metrics used to assess PCS effectiveness, along with the guidelines provided in standard. The chapter also discusses the limitations of current PCS research and the gaps in existing thermal comfort standards and establish the need for a comprehensive assessment framework.

2.1 Thermal comfort theory and the need for localized control

In literature, thermal comfort is defined as 'condition of mind that expresses satisfaction with the thermal environment' [33][34]. In practice, it refers to how comfortable the occupant is feeling with the surrounding thermal condition. Acceptable indoor environment is defined by ASHRAE standard 55 by integrating environmental parameters such as air temperature, airspeed and radiant temperature with physical variables like clothing insulation and metabolic rate. Two primary frameworks are widely used to understand and predict human thermal comfort. First one is the heat balance approach which considers the human body as physical system and assess comfort based on the balance between metabolic heat production and heat loss between surrounding environment through conduction, convection, radiation and evaporation. PMV-PPD model [26] and multi-node thermoregulation model [35] focusing mainly of physiological and environmental aspects, is the prominent example of this approach. The second framework is the adaptive thermal comfort approach, where comfort is viewed as a dynamic and context-dependant process. This approach explains that the users actively adapt their environment through behavioral changes, such as opening windows, modifying clothing level or operating PCSs, as well as physiological adjustments [4][36]. Humphreys and Nicol [37] described this adaptive process clearly stating, "If a change occurs such as to produce discomfort, people react in ways which tend to restore their

comfort". De Dear and Brager [4] established that adaptive thermal comfort model is mostly applicable in naturally ventilated buildings, where indoor condition is greatly depended to the outdoor environment and occupant control.

When the adaptive model was introduced into ASHRAE standard 55, Brager and Olsen [38] explored an important limitation of uniform thermal control, mentioning even when the indoor condition satisfies the 80% acceptability criterion, a significant fraction remains dissatisfied. Individual control was found to be the most effective way to address the personal differences in comfort preferences. Based on this concept, Zhang [39] introduced a thermal comfort model for non-uniform and transient environment. Her work demonstrated that the thermal sensation and overall thermal perception is highly dependent on local thermal sensation, with the head and hands being most sensitive in warm conditions and the hands, arms, and feet in cool conditions. The study identified that targeted cooling or heating at these thermally sensitive zones can notably enhance thermal comfort, even when the ambient temperature falls outside the conventional comfort zone. These insights contributed to the development of energy efficient PCSs to provide direct heating cooling to the occupants [40][41]. The users can modify their thermal conditions according to their individual preferences with these approaches and reduce the overall HVAC energy demand. In this context, PCSs can be considered as practical devices that support adaptive behavior in modern buildings, bridging the gap between conventional heat-balance models and real-world comfort needs in energy efficient manner.

2.2 PCS application in buildings

Arens [42] defined PCSs as technologies that deliver localised heating, cooling or ventilation directly to the occupant without relying on the central HVAC system. PCSs can be divided into

two main categories, Personal Cooling Devices (PCDs) and Personal Heating Devices (PHDs), and these categories they were further classified based on their characteristics and targeted area. PCSs can also be distinguished by systematic classification considering three key aspects: primary heat transfer mechanism, targeted body segment and evaluation approach and subject response. A wide range of PCS technologies for both heating and cooling applications has been reported in extensive literature studies. Rawal [42] conducted a comprehensive review of more than 150 PCS studies and classified systems based on operating mode, control strategy, and targeted body region.

2.3 Classification of PCS based on heat transfer system

Categorising the PCSs in terms of heat transfer mechanism, conduction, convection and radiations is the most used approach in the literature. This outline provides a physical basis for evaluating and comparing the efficiency of different heating and cooling devices providing a clear understanding how various PCS technologies influence human thermoregulatory system and zonal thermal sensation.

2.3.1 Conduction-Based PCSs

Conduction based PCSs moderate thermal comfort through direct contact between device and human skin, allowing heat to be transferred through contact surface. In cooling PCS category covers cooling vests with phase change material (PCM) [43][44][45], cooling pads and chairs [1], and thermally conductive textiles, that absorb sensible or latent heat from the skin [46][47]. Among these examples, PCM based systems are particularly effective because they are able to absorb and release thermal energy during phase transition that stabilizes local skin temperature and enhances perceived comfort in warm environment. A number of studies have reported enhanced thermal sensation and overall comfort with the use of conduction base PCSs, especially under transient

condition and high heat exposure [43][44][45][46][47][48]. However, the cooling performance of conduction based PCS depends largely on factors like contact area, duration of thermal capacity, material properties. The cooling effect gradually weakens as the PCM completes the phase transition [47]. As a result, these systems are generally suitable for temporary task specific cooling, and their real world applicability is also challenged by added weight, bulkiness, regeneration time, and non-uniform cooling distribution.

For heating applications, conduction-based PCSs include heated chairs [49][50][41][51] heated cushions [1][52], backrests [53], heated desk surfaces and shoe insoles [17][54], which provide direct warmth to body segments that are highly sensitive to cold [55][56][59, 60]. These systems were found highly effective in improving the overall thermal comfort as warming body segments such as lower back, thigh and feet can substantially improve comfort even in cool indoor environment. In addition to their comfort benefits, they offer a major energy advantage requiring significantly less energy compared to increasing the temperature of the entire room.

2.3.2 Convection-Based PCSs

Convection-based PCSs improve comfort sensations by increasing local air movement, which enhances convective and evaporative heat loss from the body and the surrounding environment. This approach is the most widely used and practically implemented PCS type, especially for cooling applications. Common examples include ceiling fans, pedestal fans, desk fans, wearable fans, and localized air terminals [42]. Convective cooling PCSs are markedly efficient in warm environments, especially for occupants engaged in sedentary activities. The increased air velocity near the skin significantly enhances heat dissipation and sweat evaporation in this case [19]. Both simulation and experimental studies have demonstrated that personal fans extend cooling setpoints

substantially, often by approximately 1–3 K, without compromising acceptable comfort level [8][19].

Despite these advantages, convection-based PCSs are likely to introduce important challenges related to uneven airflow distribution and local draught risk. Elevated air jet directed to sensitive body segments such as the face, neck, or hands may cause unwanted discomfort, specifically under energy conscious ambient conditions [3]. In addition, airflow jets from desk or pedestal fans can extend beyond the primary user, leading to airflow spillover and unwanted exposure of nearby coworkers [42]. In heating mode, convection-based PCSs typically include small desktop heaters and localized warm-air units, that create a small thermal microclimate around the occupant. While these systems effectively provide local warmth, their efficiency depends strongly on airflow direction, temperature, and distance from the users. It may also lead to localized dryness or overheating if not properly controlled [56].

2.3.3 Radiation-Based PCSs

Radiation-based PCSs operate by influencing the exchange of radiant heat between the human body and surrounding surfaces. Examples of cooling technologies are radiant cooling panels [57][58] and radiative cooling textiles [59], which promote greater long-wave heat loss from the body. Recent development in this field focuses on advanced materials designed to improve infrared emission while limiting solar heat gain. This allows passive or low-energy cooling without the need for increased air movement. Radiative cooling is suitable in environments where air movement is undesirable, such as quiet workplaces or healthcare spaces. However, the performance of radiative PCSs is highly dependent on specific factors such as surface temperatures and clothing insulation [42].

For heating, radiation-based PCSs include infrared radiant panels [58], radiant foot warmers [18][60], and localized radiant heaters [61], which directly warm exposed body surfaces through radiant heat transfer. These systems are especially effective in warming exposed body regions, especially to feet and lower extremities, and can achieve high acceptance levels with minimal impact on overall air temperature [62].

2.4 PCS Classification by targeted body region and evaluation approach

Another way to effectively classify the PCSs is based on the body zones they target. As different body regions do not contribute to the overall thermal perception equally, the abovementioned PCS technologies are sometimes classified as how they provide cooling and heating to localized areas. This classification aligns well with the segmented evaluation conducted on local body parts through human subjects or manikin. However, in practice, many modern PCS concepts are hybrid systems that combine multiple heat-transfer mechanisms and target several body regions simultaneously. Examples include systems combining convective and radiative heating/ cooling, or integrated solutions such as heated chairs with leg or foot warmers, which reduce sensitivity to individual variability [56][63].

Beyond physical classification and PCSs are sometimes categorized based on how their performance is evaluated. Human-subject studies typically assess thermal sensation votes, comfort votes, and preference responses. Sometimes physiological indicators such as skin temperature or heart rate are also considered [31]. In contrast, manikin-based studies use segmental heat loss, equivalent homogeneous temperature (EHT), and corrected power (CP) to quantify localized thermal effects under controlled conditions [14][17][40]. Current studies increasingly advocates

for multi-metric classification and evaluation frameworks that integrate subjective comfort, physiological response, and energy performance [64]

2.5 Standards and guidelines for PCS operation

ASHRAE Standard 55 [33] is a widely accepted international standard for thermal comfort which is sponsored and controlled by the American Society of Heating, Refrigerating and Air-Conditioning Engineers (ASHRAE) and co-sponsored by the American National Standards Institute (ANSI). The standard is similar to ISO 7730 [34] and is based on PMV [3]. Nevertheless, the ASHRAE standard was the first international standard to include an adaptive approach. Under extensive work by de Dear and Brager, and using data from ASHRAE project RP884, adaptive criteria for free-running buildings were developed [47]. ASHRAE standard employs the relation between indoor comfort temperature and outdoor temperature to describe acceptable ranges for indoor temperature in naturally ventilated buildings.

The 2023 edition of ASHRAE Standard 55, guidelines and provisions for the application of PCS are included. ASHRAE standard 55 defines PCS as localized heating or cooling systems that occupants can directly control and that can produce a meaningful modification in thermal sensation. For cooling applications, the standard specifies that a PCS must be capable of achieving at least a –0.5 change in PMV at design cooling conditions. This requirement also includes several equivalent mechanisms, including a reduction in average air temperature by 3 °C, a reduction in mean radiant temperature by 3 °C, or an increase in average air speed by at least 0.3 m/s. In the case of air-movement-based PCS such as desk fans aimed at the head, face, or upper body, ASHRAE standard 55 prescriptively limits the acceptable operational range at 0.36–0.8 m/s. For other cooling PCS, such as cooled chairs, the standard specifies a minimum heat extraction

capacity of 20 W from the body, thereby translating thermal comfort impact into an equivalent power-based metric.

For heating purpose, ASHRAE standard 55 specifies that PCS must provide at least a +0.5 modification in PMV under designed heating conditions. Other criteria are an increase in air temperature or mean radiant temperature by 3 °C, or by using devices with defined heating output such as 6 W for footwarmers and 14 W for heated chairs. The standard also emphasizes that PCS must either be evaluated by the criteria listed in guideline table [Table 6-2] or demonstrate an equivalent minimum corrective power of ±2 °C. This recommendations provide a baseline for evaluation of PCS effectiveness on the human body and provide a quantitative framework for incorporating PCS into thermal comfort compliance.

2.6 Overview and classification of thermal manikin

Thermal manikins are specifically developed as anthropomorphic instruments to simulate thermal interaction between human body and the surrounding environment under controlled conditions [65][66][67][68][69]. They provide objective and repeatable data that complement subjective human studies and are particularly valuable for evaluating thermal comfort in buildings, vehicles, and clothing systems [66][67][68][69]. Modern thermal manikins are designed to replicate human body geometry, heat production, and heat loss mechanisms. They are typically segmented, allowing independent control of individual body parts to represent non-uniform heat transfer across the body [66][70][71][72][73]. Advanced manikins may also incorporate human thermoregulation models, enabling more realistic assessment of thermal comfort in complex and non-uniform environments [65][67].

Manikins were originally developed to measure clothing thermal insulation and have long been used to measure heat transfer between human body and its environment [74][75]. Early developments, like the standing manikin by Winslow and Herrington [76] and Toda's copper manikin, laid the foundation for modern applications. Today, the evaluation of clothing insulation and moisture vapor resistance remains a key application of thermal manikins [65][69][77][78]. In addition, thermal manikins are extensively used to assess HVAC performance and indoor thermal environments, allowing detailed investigation of factors that strongly affect thermal comfort such as vertical temperature gradients, radiant asymmetry, and local airflow [70][79][80][81]. Recent literature identifies three primary types of manikins used in thermal comfort and heat transfer research: basic thermal manikin, adaptive thermal manikin, and numerical thermal manikin.

2.6.1 Basic Thermal Manikin

Basic thermal manikins are physical devices designed to simulate the human body's shape and heat production and could be divided as non sweating and sweating thermal manikin. Non-sweating thermal manikins are designed to simulate human sensible heat exchange by maintaining a controlled surface temperature. It allows to quantify the dry heat transmission parameters such as thermal insulation (clo), convective and radiative heat loss, and Equivalent Homogeneous Temperature (EHT) under steady environmental conditions [34][82]. These manikins are widely used in building science and PCS research because they provide highly repeatable and stable measurements. On the other hand, sweating thermal manikins are incorporated with controlled water supply through a permeable skin to simulate human sweat. It enables direct measurement of both sensible and latent heat loss as well as clothing evaporative resistance (Ret) [77][83]. Sweating thermal manikins are commonly used to measure clothing evaporative resistance [84][85][86] as they provide a more physiologically realistic representation of human

thermoregulation, particularly in hot conditions where evaporation dominates total heat dissipation [87][88]. However, sweating manikins are more complex to operate and require careful control of sweat rate, uniform wetting, and environmental conditions to ensure measurement accuracy and repeatability [87]. Therefore, non-sweating manikins are preferred for controlled evaluation of sensible heat transfer and PCS performance, while sweating manikins are more suitable for comprehensive assessment of comfort and evaporative cooling under realistic thermal stress conditions.

Traditionally, thermal manikins are used with three different control modes: constant skin surface temperature (PI) mode; constant heat flux mode; and the comfort mode. In PI mode, each body segment of the thermal manikin is controlled to maintain a target skin temperature. The controller continuously compares the measured skin temperature with the setpoint and adjusts the heating power accordingly [89][90]. In locked power mode, the heating input for each segment is kept constant and does not respond to environmental changes. As a result, skin temperatures are free to vary depending on local thermal influence. In comfort mode, the manikin operates using a physiologically based control strategy instead of maintaining fixed skin temperatures. Segmental heat loss is governed by a comfort equation producing heat flux and skin temperature values representing a comfort driven human [89].

2.6.2 Adaptive Thermal Manikin

Adaptive thermal manikins enhance the capabilities of conventional manikins by integrating human thermoregulation models and enabling their application under transient thermal conditions [65][67]. These systems dynamically regulate segmental heat output and skin temperature to simulate physiological responses such as vasoregulation, sweating, and shivering in response to

changing environmental conditions. Adaptive manikins provide a more realistic representation of human thermal response in non-uniform and transient environments than basic control modes by coupling it with a multi segmental thermoregulation control. Adaptive manikins have been developed and evaluated in several studies, including those by Psikuta [91], Rugh [92], and Yang [93]. The coupled thermoregulatory models applied in these studies include the model developed by Huizenga [94], the Fiala model [95] and its revised UTCI-Fiala model [35], as well as the 65 multi-node (65MN) model [96]. The manikins used include ADAM (Advanced Automotive Manikin) [92], Newton [97], and SAM (Sweating Agile Thermal Manikin) [98]. In addition, Foda and Sirén [99][100] employed the MSP model developed based on the original Pierce model [101] with the thermal manikin 'Therminator', while Shinoda [102] applied the JOS-3 model developed by Takahashi [103] with a PT Teknik thermal manikin to assess individual thermal responses under transient environmental conditions.

2.6.3 Numerical Thermal Manikin

Numerical thermal manikins are computational models that leverage techniques such as Computational Fluid Dynamics (CFD) to simulate the thermal exchange between a virtual human body and its environment [65][104]. Numerical manikins exist entirely within a software environment, allowing simulations of complex scenarios that are difficult or impossible to replicate physically [65]. These virtual manikins can be coupled with human thermal models to visualize thermal comfort, investigate indoor air quality, and analyze pollutant exposure reduction in personalized ventilation systems [105]. Advanced virtual thermal manikins (VTMs) are equipped with breathing functionality, that can simulate the flow interaction in the breathing zone and provide valuable insights into indoor air quality and occupant thermal comfort [104].

2.7 Overview of JOS-3 thermoregulation model

JOS-3, developed by Takahashi [103], is a human thermoregulation model based on the lumped-parameter model of Stolwijk [106]. It was derived from earlier versions including the 65MN model [104] and the Joint System Thermoregulation Models JOS [107] and JOS-2 [108]. Compared to previous JOS models, JOS-3 incorporates additional features such as basal metabolic rate estimation, aging effects on thermoregulation, and shivering and non-shivering thermogenesis. The model can be personalized with respect to sex, age, body composition, and cardiac activity, allowing evaluation of a wide range of populations. Figure 1 shows the concept of JOS-3, a multi-node human thermoregulation model derived from Stolwijk's framework and its predecessor JOS-2. The model represents the human body using 85 nodes distributed across 17 anatomical segments, including the head, torso, arms, and legs. Each segment is composed of layered nodes representing blood, core, muscle, fat, and skin, with varying composition by body region. Blood flow is modeled through arterial, venous, and superficial venous pools, with arteriovenous anastomosis (AVA) included in the hands and feet to capture peripheral thermoregulation. To improve prediction accuracy the head and pelvic are modeled with additional layers. This detailed multi-layer; multi-segment structure enables realistic simulation of heat transfer and physiological responses under non-uniform thermal conditions.

The JOS-3 model is implemented in Python-3 [109] to enable real-time coupling with the thermal manikin control software. In the adapted framework, the internally calculated sensible heat loss terms are suppressed, and the segmental heat loss measured by the thermal manikin is inputted directly to the JOS-3 model as skin heat loss. The model then computes the corresponding skin temperatures, which are returned as dynamic setpoints for the manikin surface temperature control

using an existing PI controller [102]. A conceptual illustration of the control framework is given in Figure 2.

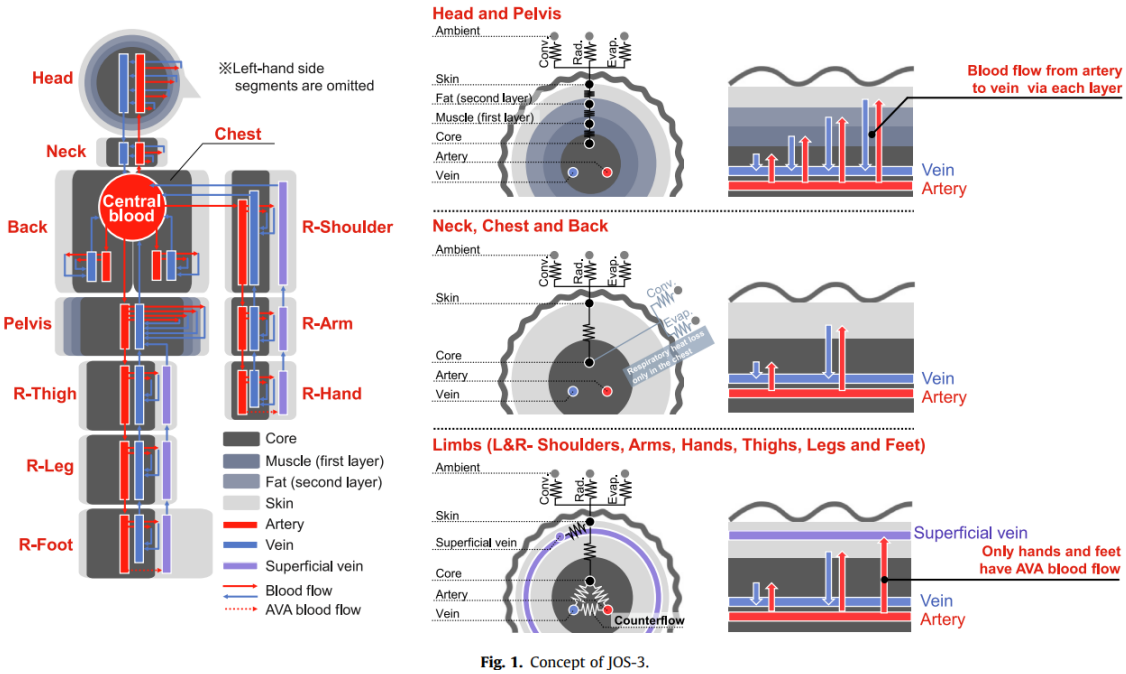

Figure 1: Body-construction concept of JOS-3 [103]

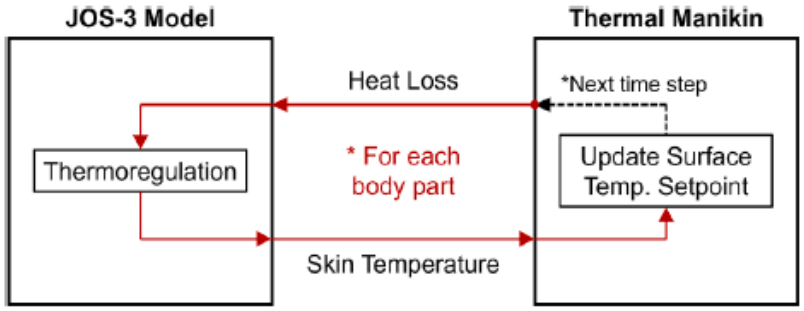

Figure 2: The control concept of JOS-3 [102]

2.8 Use of fans as PCS in office settings

The integration of ceiling, desk, and stand fans with mechanically air-conditioned spaces has been widely documented to enhance occupants' thermal comfort and reduce overall cooling energy demand. By increasing air movement and promoting convective and evaporative heat loss from

the body, these fan-assisted strategies allow for higher thermostat setpoints without compromising perceived comfort. However, despite their proven benefits, each fan type exhibits distinct performance characteristics, operational advantages, and potential limitations related to airflow distribution, noise, draught risk, and shared-space impacts. The effectiveness and associated drawbacks of these fans are therefore summarized in the following sections.

2.8.1 Ceiling Fan

Both laboratory and field studies demonstrate that ceiling fans can maintain acceptable comfort at elevated indoor temperatures (26–31 °C) by increasing local air movement and enhancing convective heat loss. Studies reported that occupants remained thermally comfortable at 28 °C and 31 °C when using personal ceiling fans, and that personal control over fan speed significantly improved comfort perception, highlighting the importance of user control and expectations [110][111]. Lipczynska [112] found that the most comfortable office condition occurred at 26 °C with operating ceiling fans, compared to a conventional setpoint of 23 °C, increasing thermal acceptability from 59% to 91% and significant energy savings (~44 kWh/m²·year). From an airflow perspective, CFD and experimental studies show that ceiling fan performance is highly influenced by rotation speed, which controls airflow circulation and convective heat transfer around the body [113]. Zhai [114] further established that, with occupant control, increased air speed from ceiling fans significantly improves thermal comfort and perceived air quality in warm-humid environments, enabling acceptable comfort at temperatures up to 30 °C. Advanced concepts such as Ceiling-Fan-Integrated Air Conditioning (CFIAC) also confirm that fan-assisted airflow can provide thermal comfort at higher setpoints compared to conventional systems at lower temperatures, despite non-uniform airspeed distributions [115][116][117]. Although ceiling fans are effective at improving overall comfort, they typically generate room-scale air movement,

which can increase the risk of unwanted draft or cross-exposure for nearby occupants in shared spaces [118]. In this context, ASHRAE Standard 55 emphasizes the importance of occupant control for elevated air speed and more localized solutions, such as desk fans, which could offer better individual control and acceptability in open-plan office environments.

2.8.2 Stand Fan

The performance of stand and pedestal fans as personal cooling systems have been evaluated by several studies, that highlighted their effectiveness and energy-saving potential. Sun [119] to assesses thermal comfort under different indoor temperatures (22–30 °C) and fan speed settings with combined human subject and manikin tests. Results demonstrated that stand fans significantly enhance convective heat transfer and provide noticeable cooling effects, enabling comparison with conventional air-conditioning in terms of energy performance. Relatable results were found by Muhammad [120] with a Peltier-based bladeless pedestal fan, showing that integrating thermoelectric modules can further improve cooling efficiency, achieving up to 22% temperature decrease and significant energy savings compared to traditional pedestal fans and air conditioners. Yang [121] introduced the Cooling Fan Efficiency (CFE) index based on thermal manikin experiments, which relates whole-body cooling effect to power consumption. He found that although stand fans consume electrical energy, brushless DC stand fans can achieve up to three times higher efficiency than conventional AC fans. However, user preference and comfort perception under the resulting non-uniform airflow fields at elevated temperatures were not explicitly addressed. Kim [122] identified thermally comfortable operating conditions for stand fans in warm environments, showing that elevated air movement can extend the acceptable comfort range beyond that defined by ASHRAE Standard 55 for uniform airflow conditions. Nevertheless, some studies have also reported that high-velocity air jets may increase the risk of

draught discomfort and eye irritation, indicating potential limitations of pedestal fans as personal cooling devices [123].

2.8.3 Desk Fan

Desk fans increase the acceptable thermal comfort range, consistent with the Adaptive Comfort Model and local thermal comfort principles [124]. For instance, a field study in a zero-energy office building in Singapore reported a 36% reduction in cooling energy consumption following the installation of ceiling and desk fans, while maintaining high levels of occupant comfort and satisfaction [125]. Desk fans also facilitate individualized thermal control in shared office environments, enhancing overall comfort and satisfaction [126]. Air velocities between 0.2 and 0.8 m/s at the occupant level are generally effective for enhancing thermal comfort [127], although draught and discomfort could occur depending on individual sensitivity and fan placement [127] [128]. To identify the upper acceptable indoor temperature limits with PCSs, various studies have implemented desk fans while gradually increasing thermostat setpoints. Shetty [129] and Lipczynska [112] increased the temperature from 23 °C and found that 27 °C was not acceptable in office environments. Based on this result, Kent [118] evaluated a setpoint of 26.5 °C with desk fans for over three weeks and reported high occupant satisfaction. Other evaluations have shown that desk fans provide cooling performance comparable to other personal comfort systems (PCS) [130]. Udayraj [131] reported similar overall comfort and skin temperature responses between desk fans and ventilation clothing, while Yingdong [132] demonstrated that desk fans are highly energy-efficient, although hybrid systems combining radiant cooling and desk fans can further extend the comfort range at the expense of higher energy consumption. Meiling [133] found that low-power desk fans (maximum 3 W) meaningfully improved thermal comfort, thermal sensation, and observed air quality in warm-humid conditions (26–30 °C), with user-controlled airflow

providing superior comfort. Although barriers such as noise, perceived unintended draught, and lack of integration guidelines remain, ongoing research continues to optimize their application, including investigations into distribution to maximize comfort while minimizing adverse physiological effects [124][125].

2.8.4 Wearable fans

Wearable face and neck fans enhance thermal comfort primarily by increasing local convective and evaporative heat loss at thermally sensitive regions, particularly the face and neck, which play a critical role in thermal perception. Researches have demonstrated that, in warm condition, these devices can reduce local skin temperatures at the forehead, face, and neck by up to approximately 2.1 °C, accompanied by significant improvements in both local and whole-body thermal sensation and comfort votes [134]. Similarly, occupational and chamber-based studies have shown that wearable neck fans improve whole-body thermal comfort by providing targeted cooling to exposed upper-body regions, although excessive or uneven airflow may lead to localized overcooling or thermal asymmetry depending on airflow intensity and distribution [135][136]. Physiological investigations further established that localized facial and neck cooling can substantially reduce perceived heat stress and discomfort even without significant reductions in core body temperature. This highlights the strong effect of upper-body thermal receptors on whole-body comfort perception [29]. Despite these established benefits, studies directly comparing the effectiveness of localized head–neck cooling with combined head–neck–torso cooling strategies in office environments remain limited, indicating the need for further research to quantify their relative contributions to whole-body and zonal thermal comfort.

2.9 Methods for evaluating desk fans for whole body comfort and Zonal Cooling

The principal methodological approaches used to evaluate desk fans for whole-body thermal comfort and zonal cooling varies significantly. The human subject and manikin based methods, are discussed in the following sections.

2.9.1 Human subject-based evaluation methods

Human-subject studies evaluating desk fans as PCSs commonly combine physiological measurements and subjective questionnaires to assess both whole-body thermal comfort and zonal cooling performance. Udayraj [131] measured heart rate (HR) and local skin temperatures to calculate mean skin and torso temperatures. Questionnaire-based perceptual responses were used to assess whole body thermal comfort, including thermal sensation vote (TSV), thermal comfort vote (TCV), and air movement acceptance. Local skin temperature measurements revealed that desk fans provided greater cooling at exposed regions (forehead, forearms, and hands), while ventilation clothing reduced torso temperatures more effectively. Similarly, Yingdong [132] used questionnaire-based thermal sensation and acceptance votes to assess whole-body comfort and showed that desk fans provided energy-efficient cooling at temperatures up to 30 °C.

Similar approaches have also been adopted in several studies. Tang [1], Ilmiawan [128] and Wang [137] primarily depend on subjective questionnaires to evaluate thermal sensation, comfort, and acceptance under desk fan operation, while physiological indicators such as skin temperature were used to quantify localized cooling effects. Norouziasl [127] integrated physiological monitoring, including skin temperature and biometric responses, with subjective feedback to assess comfort and airflow effectiveness. Field studies by Kent [125] Wegertseder-Martinez [138], and André [126] evaluated whole-body thermal comfort and satisfaction using occupant surveys with desk

fan. In addition, Lu and Hameen [139] and Yu [140] incorporated subjective feedback with non-intrusive sensing and comfort modeling to assess personalized thermal comfort in office environments. Overall, these studies demonstrate that with human subjects, whole-body thermal comfort is primarily addressed using subjective questionnaire-based metrics, such as TSV, TCV, and comfort acceptance. Zonal cooling performance is evaluated using physiological measurements, specifically local skin temperature, mean skin temperature, and torso temperature, with heart rate occasionally used as a supplementary indicator.

2.9.2 Manikin-based evaluation methods

Thermal-manikin studies on desk fans/personal fans typically estimate whole-body thermal comfort by converting measured manikin dry-heat exchange into manikin-based equivalent temperature (T_{eq}) and, PMV-from-manikin [75]. Cooling effect of the fan is then reported as a whole-body T_{eq} reduction or an efficiency metric [141]. For zonal cooling, studies principally rely on segmental heat loss (W or W/m²) and local EHT derived from segment dry-heat loss under non-uniform airflow [142]. Desk-fan performance has also been evaluated in workstation microclimate systems, where a breathing thermal manikin is used to quantify body cooling and the asymmetry created by airflow sources such as desk-mounted fans and desktop PV terminals [143] as well as ductless PV used with desk fans [144]. Several chamber and modeling studies further quantify fan-driven cooling through manikin heat-loss differences and convective heat-transfer coefficients by body segment [145]. In the broader manikin based PCS studies EHT and CP is frequently applied to desk-fan benchmarking. This parameters are used to express local and whole-body cooling/heating as the difference in segment/whole-body heat loss relative to a reference case (CP). This supports device-to-device comparisons under identical ambient conditions. Practical evaluations also report “cooling power” as the increment in sensible heat loss attributable to the

fan, which can be summarized at whole-body and segment levels [146]. Finally, desk-fan configurations are commonly included in PCS development and validation work using controlled chambers where the primary outputs remain segmental and whole-body heat loss, optionally paired with derived EHT/T_{eq} to express comfort-equivalent temperature shifts [147], [148].

2.10 Metrics for quantifying PCS efficiency

2.10.1 Equivalent Homogeneous Temperature (EHT)

Virtual Thermal Comfort Engineering (VTCE) was developed to predict occupant thermal comfort in highly non-uniform environments by integrating a human thermophysiological model with the concept of EHT [149]. The VTCE model considers the human body as 16 anatomical segments, each divided into core, muscle, fat, skin, and clothing layers, allowing prediction of local and whole-body thermal comfort based on segmental heat exchange. According to SAE Standard J2234, EHT is defined as "the uniform temperature of an imaginary still-air enclosure in which a person would exchange the same dry heat by radiation and convection as in the actual non-uniform environment," assuming identical posture, activity, and clothing insulation [150]. This definition provides a tangibly significant basis for comparing thermal environments with spatially varying airflow, radiation, and temperature distributions. Based on this framework, segmental EHT profiles were introduced by Wyon [151] derived from thermal manikin measurements to quantify sectional heat loss to diagnose thermal asymmetry in vehicle cabins. Similarly, Nielsen [152] identified zonal distribution of segmental EHT values and the difference between maximum and minimum segmental EHT (ΔEHT) as reliable indicators of local discomfort and whole-body thermal imbalance in non-uniform environments. Hepokoski [153] further confirmed the application of EHT in transient and asymmetric conditions. He emphasized its usefulness as a

simplified parameter for predicting human thermal perception when coupled with thermal manikin measurements, also explaining the limitations in representing active physiological thermoregulation.

Later studies extended the application of EHT to building PCS evaluations. Barna and Bánhidi [154] used thermal manikin-derived EHT to investigate the combined effects of radiant asymmetry and warm floor exposure on local and whole-body discomfort. Luo [17] incorporated both localized and whole-body EHT to calculate CP, demonstrating that PCS devices such as cooled chairs could offset ambient temperature increases of up to 2 K individually and up to 4.2 K when combined with other PCS technologies. More recently, Li [90] applied EHT-based CP analysis to quantify segmental heat loss and evaluate the performance of personal heating systems using a thermal manikin, validating the applicability of EHT as a comprehensive metric for assessing zonal and whole-body thermal responses. These studies establish EHT as physically grounded and widely adopted metric for evaluating local and whole-body thermal comfort under non-uniform thermal conditions, especially when combined with thermal manikin measurements and thermophysiological models.

2.10.2 Corrective Power (CP)

Zhang [10] introduced the concept of CP to understand the level to which a PCS can “correct” a warm or cool ambient environment toward thermal neutrality. CP is defined as the difference between two ambient temperatures at which the same thermal sensation is achieved: one under a reference condition without PCS and the other with PCS in operation. CP can be obtained from subjective survey responses and expressed in terms of comfort votes (CP-C) or thermal sensation votes (CP-S), using the respective voting scale units. These metrics quantify the comfort and

sensation differences between occupants exposed to PCS and no-PCS condition. She analyzed CP values from 42 PCS studies, encompassing air-jet systems directed at the upper body, ceiling fans, large fans or window-based airflow, and various heating and cooling PCS evaluated using both human subjects and thermal manikins. Their findings demonstrated that CP improvement through PCS and enhanced air movement enables substantial energy savings by allowing relaxed zone temperature setpoints and reduced HVAC intensity. With potential savings exceeding 30% of total building HVAC energy, these strategies simultaneously increasing the fraction of satisfied occupants toward nearly 100%. Building on this framework, Li [90] calculated whole-body EHT and CP to compare the corrective performance of four personal heating strategies under different environmental conditions. Luo [17] further extended the concept by expressing CP in watt units, representing the difference in body heat loss between PCS-assisted and reference conditions, and introduced a device-level Coefficient of Performance (COP) to evaluate the energy efficiency of PCS devices. Based on Zhang's CP concept, Veselý [155] et al. proposed Corrective Power Efficiency (CPE), defined as the power required to compensate for one unit of thermal sensation, and applied it to compare the cooling efficiency of chair, desk, and floor-based heating systems, both individually and in combination. Similarly, He [156] introduced the Corrective Energy and Power (CEP) index, defined as the ratio between the energy consumption required to correct thermal sensation from a non-neutral to a neutral state to assess the cooling efficiency of retrofitted houtong systems widely used in China as personal heating devices.

2.10.3 Coefficient of Performance (COP)

In PCS research, COP is used to express how much personal heating/cooling a device delivers per unit of electrical input. This performance is often quantified using CP which represents the PCSs ability to shift the thermal condition towards comfort zone. [33]. Building on this framework,

Zhang [10] synthesized CP results across several PCS types and highlighted CP as a practical bridge between comfort effectiveness and energy metrics such as COP. Using controlled evaluations of multiple low-power PCS devices (e.g., heated/cooled chair surfaces and local air movement), Luo [17] explicitly paired CP with COP and reported combined heating and cooling cooling illustrating that PCS can provide substantial comfort correction with very small device power when compared on an output-per-input basis. In fan-based PCS, "cooling output" is better represented as an equivalent temperature/comfort shift rather than refrigeration heat removal. Considering that, Schiavon and Melikov [141] proposed the Cooling Fan Efficiency (CFE) index (cooling effect measured with a thermal manikin divided by fan power). CFE is often used as an efficiency analogue to COP for air-movement devices. The literature treats COP as a device-level efficiency measure that complements CP by linking comfort benefit to power demand.

2.11 Research gaps and positioning of the present study

Desk fans have been broadly researched as an energy-efficient PCS, demonstrating their ability to improve comfort metrics and extend acceptable indoor temperature setpoints while consuming minimal energy. However, several important limitations remain in the existing literature.

2.11.1 Limitations in comparison of airflow mechanisms (bladed, bladeless, and wearable) of fans

The effectiveness of desk fans is widely accepted in literature studies but most of them focused on conventional bladed desk fans. The effect of bladeless fan on thermal comfort improvement remains under investigated. Similarly, wearable face and neck fans have been shown to provide effective localized cooling with significant improvements in thermal comfort. However, most existing studies have evaluated these technologies independently, and direct comparisons between

bladed desk fans, bladeless desk fans, and wearable fans remain limited. In particular, the influence of differing airflow structures, such as concentrated jet flow by bladed fan versus diffused or targeted local airflow provided by bladeless and wearable fans respectively, on cooling efficiency and physiological response has not been systematically quantified.

2.11.2 Limited Understanding of Multi-Region vs. Breathing-Zone Cooling Effects

Since thermal comfort is strongly influenced by local heat exchange at different anatomical regions, particularly the head, torso, and extremities, accurate assessment of PCS performance requires analysis of zonal heat under different airflow mechanisms. Furthermore, there is a lack of comprehensive analysis comparing multi-region cooling (e.g., breathing zone–torso–hand) with breathing-zone-dominant cooling in terms of whole-body thermal comfort improvement. Addressing these gaps is essential for developing evidence-based guidelines for selecting and optimizing PCS in shared office environments.

2.11.3 Need for multi-height and zonal airflow analysis

Most desk-fan research has concentrated on enabling higher cooling setpoints—often above 28 °C, but incorporation of desk fans with zonal airflow distribution in energy conscious open plan office space remains limited. He [133] showed that at 26ºC, when the airspeed was 1.5 m/s, 70% of occupants found it acceptable though 50% of occupants mentioned slightly cool' in thermal comfort vote (Figure 3a). Huang [157] highlighted that within the 24–26 °C range, most occupants prefer airspeed below 1 m/s (Figure 3b). However, these single-point or average air velocity measurements, which do not adequately capture the vertical and spatial distribution of airflow experienced by the occupant. Detailed multi-height airflow and zonal cooling analysis in energy

conscious shared office is therefore essential to understand the spatial cooling characteristics of PCS devices and their influence on both local and whole-body thermal comfort.

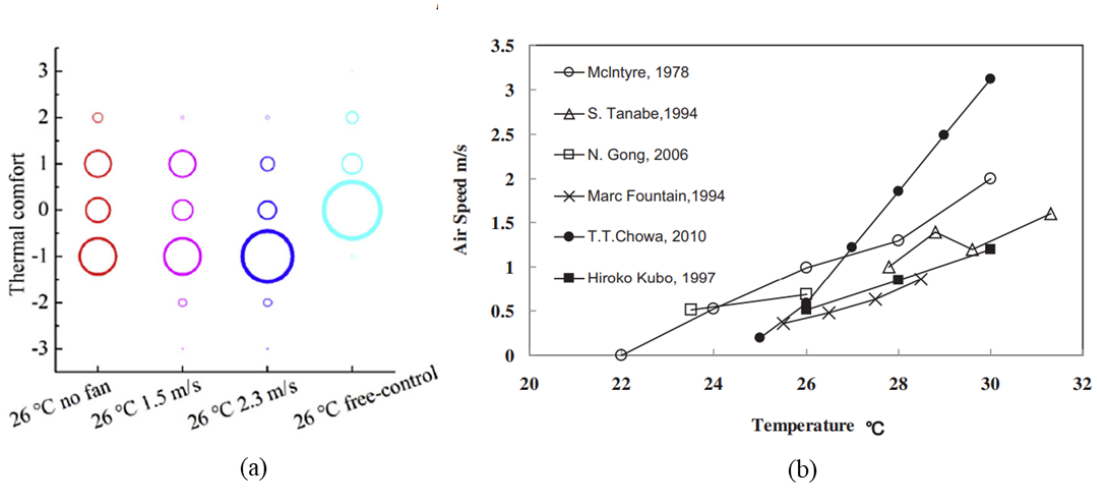

Figure 3: (a) Thermal comfort vote with 24 human subjects [133], (b) Suitable air speeds at different temperatures in different climate chamber experiments [157]

2.11.4 Lack of co-worker exposure assessment

Although desk fans are considered to provide localized cooling to the users, the generated airflow can extend beyond the primary occupant and create unintended air movement and draught discomfort for the adjacent occupants. Despite this practical relevance, most desk fan studies have focused exclusively on the primary occupant and overlooked the systematical evaluation of airflow distribution or draught risk at nearby workstations, especially when the primary occupant is elevating the airspeed beyond recommended limit. This drawback restricts the applicability of desk fan in shared environments. Quantifying multilevel airflow exposure at co-worker locations is therefore required to ensure that PCS devices provide localized comfort without negatively affecting surrounding occupants.

2.11.5 Lack of Clarity in PCS standards

Existing thermal comfort standards, such as ASHRAE Standard 55, incorporates the use of PCSs and provide guidelines for PCS application. However, these standards primarily specify acceptable ranges of average air velocity and overall thermal comfort conditions and do not provide detailed guidance on airflow measurement framework, vertical air speed variation, or zonal effects. Furthermore, the standards do not explicitly address emerging PCS technologies such as wearable fans or differentiation between different types of desk fans. This lack of detailed performance evaluation criteria limits the ability to objectively compare PCS technologies and optimize their design and application.

To address these research gaps, the present study provides a comprehensive evaluation of desk fans representing different airflow mechanisms: direct airflow generated by conventional bladed desk fans, diffused airflow produced by bladeless fans, and targeted airflow delivered by wearable face and neck fans. using a thermal manikin under controlled environmental conditions.

CHAPTER 3- METHODOLOGY

This chapter presents the experimental framework designed to evaluate the performance of the selected PCS devices. It summarizes the technical specifications of each device, defines the environmental conditions of the controlled office space, and outlines the structured experimental protocols employed consistently across all test scenarios. In addition, this section details the analytical methodology used to quantify cooling effectiveness and draught discomfort, including the derivation of EHT, CP and DR metrics for comparative performance assessment.

3.1 Thermal Manikin

A non-sweating thermal manikin developed by PT Teknik [89] designed to replicate human body heat and respond to environmental conditions, mimicking real-life thermal behavior was used for our experiment. The manikin represents an average Scandinavian male with a height of 1.75m. The body is divided into 23 individually controllable segments that are presented in Table 1 with respective area (m^2). Each body segment can be controlled to maintain the same surface temperature or to be equivalent to the skin temperature of a person at a state of thermal neutrality [75]. The manikin's accuracy level is ±0.2k for temperature and 1% for the heat flux and has a resolution of 0.1 K and 0.1 W/m2 respectively. The manikin was calibrated prior to the measurements.

3.2 Validation of manikin operating modes for the experiment

Several studies have demonstrated that although thermal manikins can be operated in constant temperature, constant heating power, or comfort modes, accurately replicating human thermo-physiological behaviour requires coupling the manikin with an advanced thermoregulation model [30][31][32]. In the present study, the objective was to quantify changes in PMV, T_{eq}, and P

following the activation of PCS devices, so either the Comfort mode or the JOS-3 thermoregulation mode had to be selected.

Table 1: Body parts of the PT Teknik thermal Manikin with respective area (m^2)

Zone Split of the Thermal Manikin	Manikin Segments	Area (m^2)
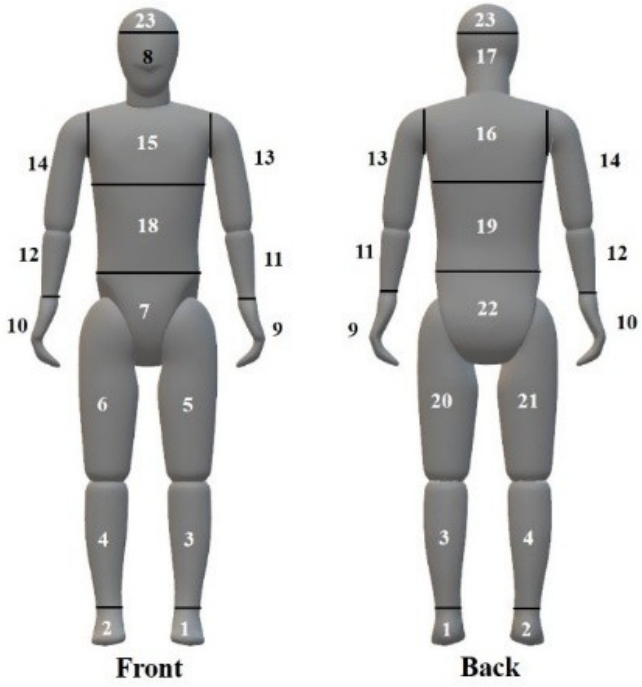	1. L. Foot	0.053
	2. R. Foot	0.053
	3. L. Foreleg	0.115
	4. R. Foreleg	0.115
	5. L. Front Thigh	0.0957
	6. R. Front Thigh	0.0957
	7. Pelvis	0.038
	8. Face	0.04
	9. L. Hand	0.0432
	10. R. Hand	0.0432
	11. L. Forearm	0.043
	12. R. Forearm	0.04
	13. L. Upper arm	0.083
	14. R. Upper arm	0.083
	15. Chest	0.0894
	16. Upper Back	0.0894
	17. Neck	0.04
	18. Stomach	0.0894
	19. Lower Back	0.0894
	20. L. Back Thigh	0.0957
	21. R. Back Thigh	0.0957
	22. Back side	0.078
	23. Scull	0.0544

Although previous research has shown that thermoregulation-coupled manikins closely approximate human thermal responses, a preliminary validation experiment was conducted with manikin and human skin temperature to verify this assumption under the present experimental conditions. Human skin temperature measurements were obtained using iButton data loggers which function as an integrated temperature and humidity logging system. The instruments used in different segments of this experiment are presented in Table 2.

Table 2: Appearance, specifications and setup of the instruments used in the experiment

Device Appearance	Features		Setup
	**Instrument:**	**Ibutton**	
	Model:	DS1923-F5# Hygrochrons	
	Measured Parameters:	Temperature Humidity	
	Range:	-20°C to +85°C	
	Accuracy	±0.5°C	
	Resolution	0.5°C	
	**Instrument:**	**Omnidirectional hotwire Probe**	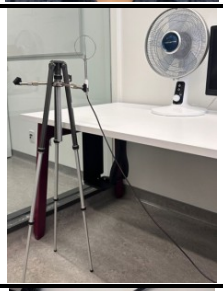
	Model:	NESA	
	Measured Parameters:	Airspeed	
	Range:	0.1-5m/s	
	Accuracy	±0.1m/s	
	Resolution	0.01 m/s	
	**Instrument:**	**Data Logger**	
	Model:	Onset HOBO MX1105	
	Measured Parameters:	-	
	Range:	0 to 20.1 mA	
	Accuracy	±2% of reading	
	Resolution	0.3µA	
	**Instrument:**	**Plug load logger**	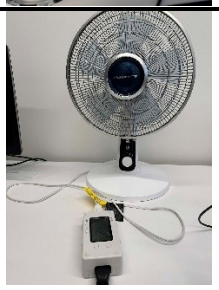
	Model:	Hobo UX120-018	
	Measured Parameters:	Energy input	
	Range:	-	
	Accuracy	0.5%	
	Resolution	Volts: 10mV Amps: 0.1mA	

The iButtons were attached to the skin using Leukotape at three locations: forehead, chin, and neck. Skin temperature at each site was recorded at one-minute intervals. The average of the forehead and chin temperatures was used to represent facial skin temperature. The experiment was conducted under identical environmental conditions using a bladed desk fan operating at medium speed. Measurements were performed for a human subject as well as for the thermal manikin

operating in both Comfort mode and JOS-3 mode. The comparative skin temperature responses of the human subject and the two manikin modes are presented in Figures 4 and 5 and the percentage of error in steady and transient state is shown in Table 3.

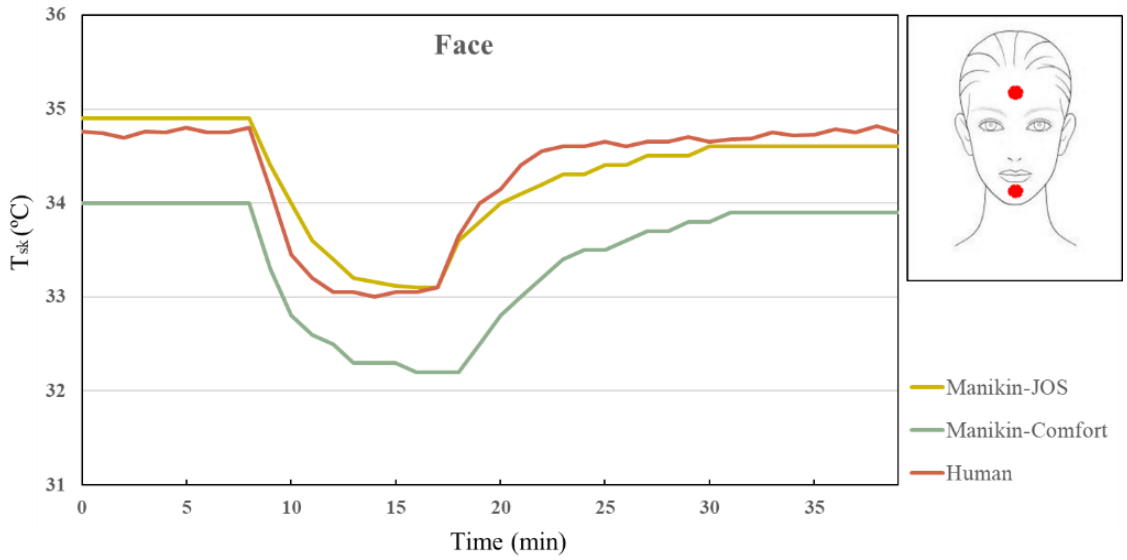

Figure 4: Comparison of face skin temperature of manikin (comfort and JOS-3 mode) and human (face-considering the average of chin and forehead)

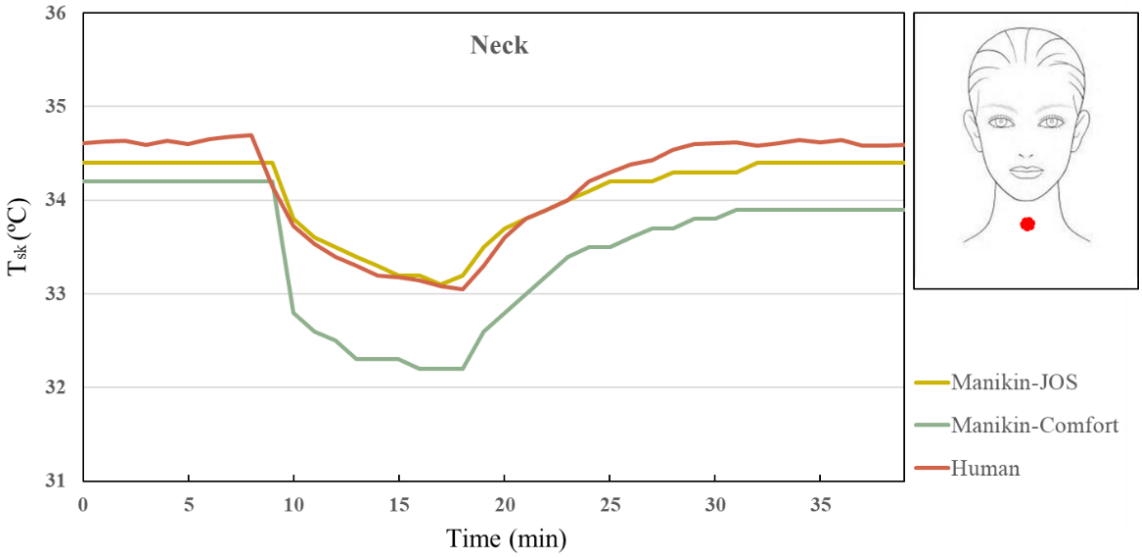

Figure 5: Comparison of neck skin temperature of manikin (comfort and JOS-3 mode) and human (neck)

Table 3: Deviation (%) in skin temperature of manikin (comfort and JOS-3 mode) and human

State	Steady State		Transient	
Manikin-mode	**JOS-3**	**Comfort**	**JOS-3**	**Comfort**
Face	0.41	2.3	0.59	2.89
Chin	0.64	1.6	0.38	2.41

The results indicate that the JOS-3 mode exhibits substantially lower deviation from human skin temperature compared to the Comfort mode. Specifically, the deviation between manikin and human skin temperature for JOS-3 was 0.18% under steady-state conditions and 0.91% during transient conditions (fan activation and transition toward thermal neutrality). In contrast, the Comfort mode showed deviations of 2.12% and 2.06% for steady-state and transient conditions, respectively. Based on these findings, all subsequent experiments were conducted using the JOS-3 mode.

3.3 Cooling Devices

Three types of desk fans were selected to represent a range of airflow delivery strategies commonly used in PCS: a conventional bladed desk fan, two small USB bladed desk fans, and a bladeless desk fan. The conventional bladed fan delivers a high-coverage, direct airflow, with a maximum airflow rate of approximately 1,589 ft^3/min, allowing concentrated air delivery toward the occupant [158]. Each USB desk fan uses a seven-blade design and provides a maximum outlet airspeed of approximately 15.4 ft/s [159]. Two USB fans were intentionally selected to examine the effect of dividing a single high-momentum airflow jet into multiple smaller jets, thereby assessing potential reductions in airflow intensity and spillover. The bladeless desk fan produces a diffused and more uniform airflow through an enclosed air-amplification mechanism, resulting in gentler air delivery with reduced turbulence [160]. The face fan incorporates dual 360º rotating

axial brushless DC motor-fans, while the neck fan uses two 5cm centrifugal brushless DC fans that circulate air through 76 micro-vents. Both devices operate using built-in rechargeable lithium batteries [160][161]. Specifications of all devices are summarized in Tabe 4 and designed configurations are presented in Figure 6.

Table 4: Technical specifications of the selected PCS devices

Type:	Air velocity:	Weight:	Dimension (in):	Control mode:	Oscillation:	Noise Level:	Power Source:
Bladed	Level 1-4	6.53 lb	11.02x 11.81 x 9.06	Manual Knob	up to 120°	38dB (max)	AC
USB powered	Level 1-3	0.5lb	1.5D x 5W x 6.1H	Push Button	No	35dB (max)	AC
Bladeless	Level 1-9	6.61 lb	25.4Dx 25.4W x 59.7H	Remote/ Touch	Yes	32 dB	AC
Face Fan	Level 1-3	0.375 lb	6.35D x 19W x 12.7H.	Button	No (manual rotation)	25 dB	2500mAh batteries
Neck fan	Level 1-5	0.119 lb	19.7D x 19.8W x 6H	Button	No	25 dB	4000mAh batteries

3.4 Test conditions and protocol

Experiments were conducted in a controlled office space located at Concordia University, Montreal, Canada, designed to replicate realistic office thermal conditions while ensuring precise control of environmental variables. The internal dimensions of the chamber are 3.6 m × 2.9 m × 2.7 m (length × width × height), representing a typical small office space. The air temperature was maintained at 25 ± 1 °C throughout each test using a wall-mounted thermostat with continuous monitoring to ensure stability. The temperature profile during one trial is presented in Figure 7. The background air velocity in the chamber was maintained at approximately 0.1 m/s, which falls within the range defined as still air conditions according to established thermal comfort standards and previous PCS research. The relative humidity was at 40 ± 5%.

Figure 6: Appearance and designed configurations of the selected PCS devices

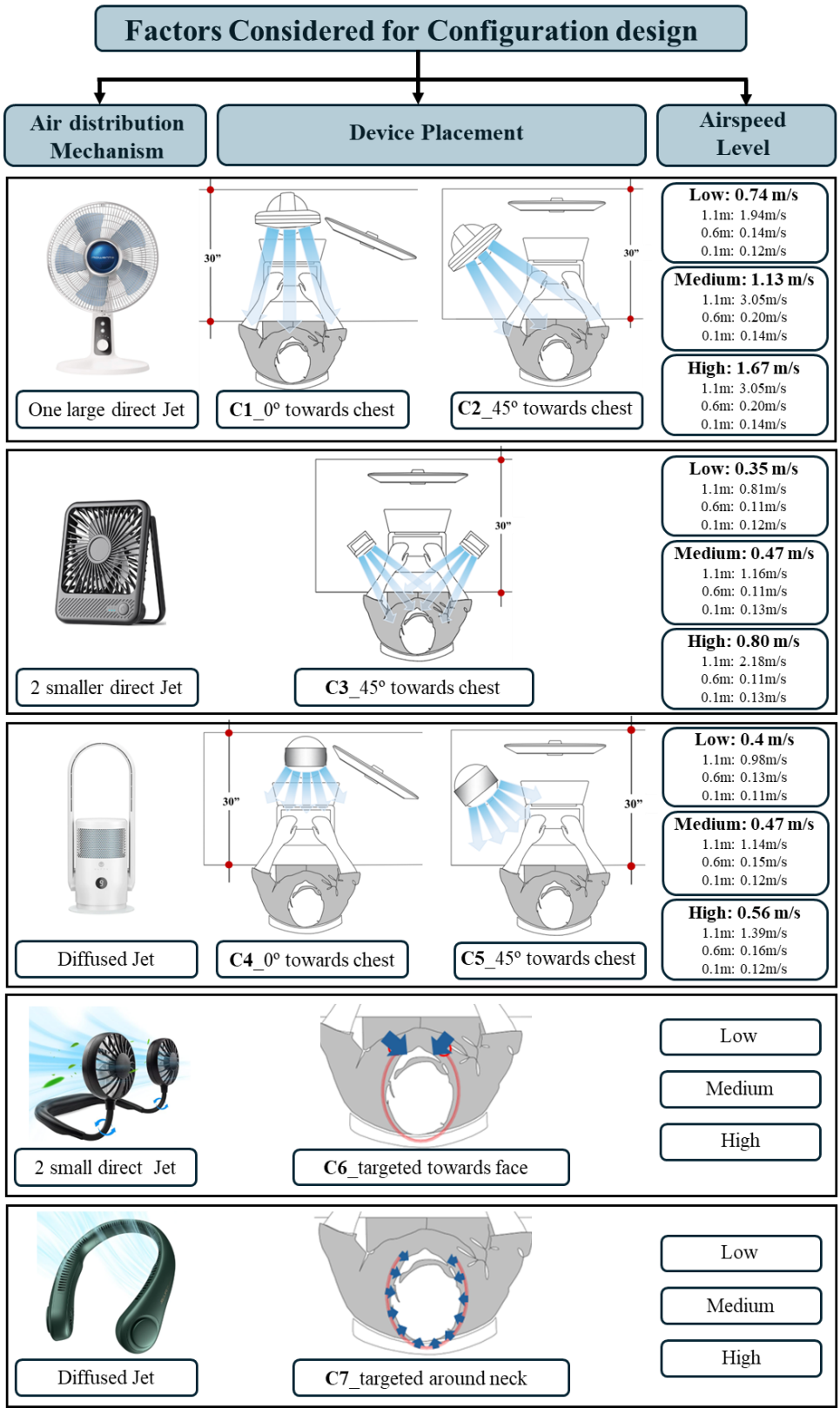

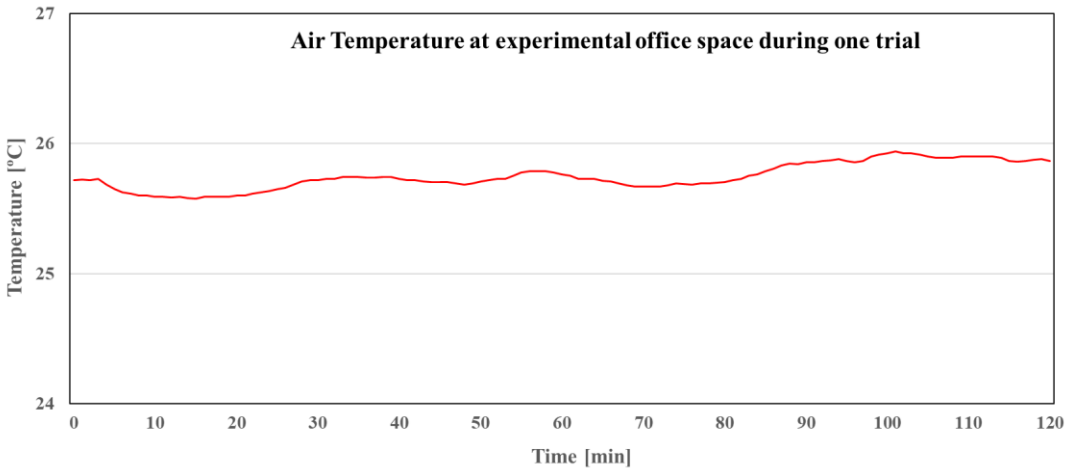

Figure 7: Logged air temperature at experimental office space

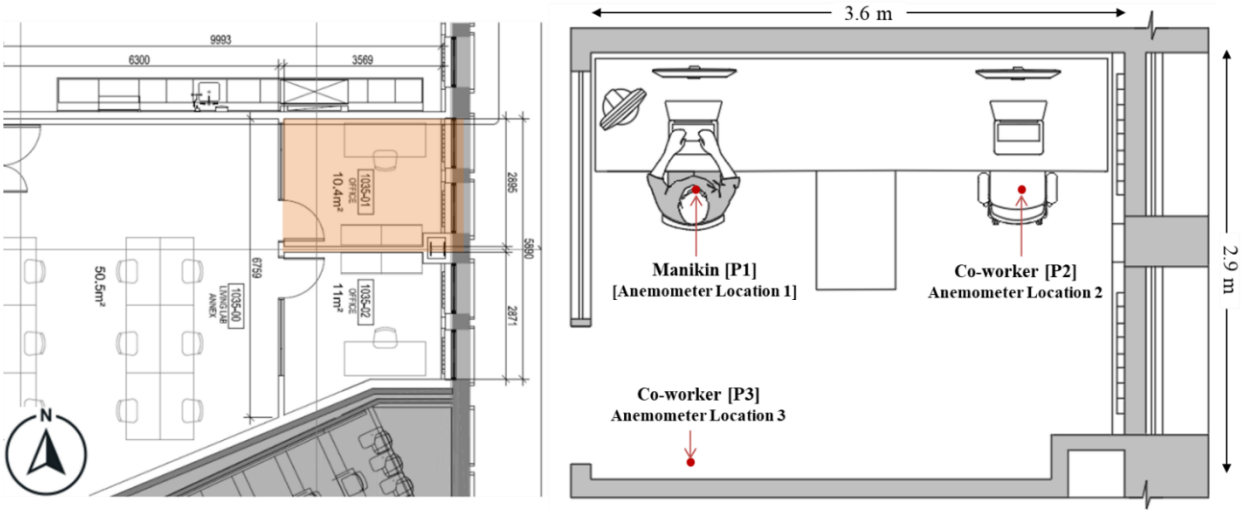

Figure 8: Floor plan of controlled office space and the experimental setup showing manikin placement

The thermal manikin was seated at an office desk designed for two occupants, reflecting a realistic shared-workspace scenario commonly found in open-plan offices. This configuration was selected to enable investigation of localized cooling effects and potential airflow spillover toward adjacent workstations. To eliminate the influence of solar radiation and external heat gains, all experiments were conducted during late evening hours. In addition, the chamber windows were fully covered with opaque black curtains, effectively blocking external radiation. This measure was taken to

reduce radiant temperature asymmetry and keeping interior surface temperatures remained close to the ambient air temperature. The floor plan of the environmental chamber and the detailed experimental setup, including manikin placement and fan configurations, are shown in Figure 8 and 9.

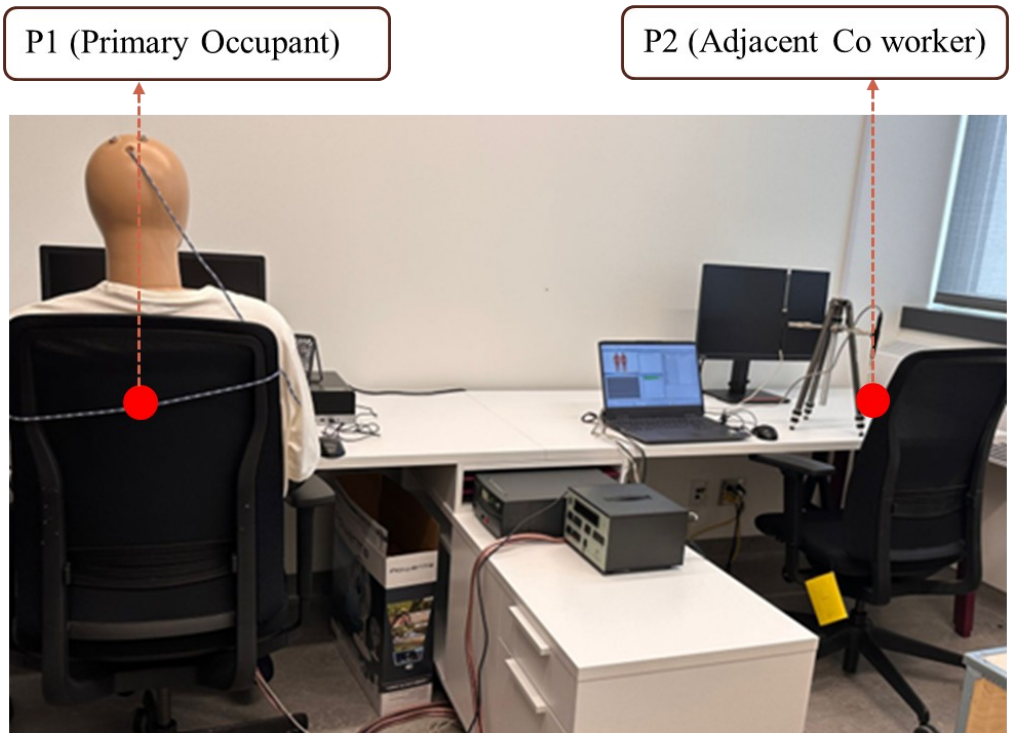

Figure 9: Experimental setup showing manikin and adjacent coworker placement

The thermal manikin was dressed in standard office clothing corresponding to an overall insulation level of approximately 0.5 clo, representing typical summer office attire. Clothing insulation values for individual garments and their combinations were determined using established clo estimation procedures based on ASHRAE standards, and the detailed segmental insulation values are summarized in Table 5. During all experiments, the manikin operated in JOS-3 control mode, which simulates human thermoregulatory responses and enables calculation of equivalent temperature, predicted thermal sensation, skin temperature, and heat loss based on segmental heat balance.

Table 5. Clothing insulation values and experimental parameters used for the thermal manikin

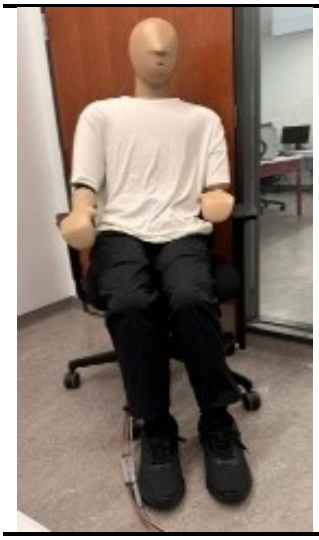

Summer Clo (0.5)
Short Sleeve Tshirt (0.17)
Men's brief (0.04)
Trouser-thin (0.15)
Ankle length socks (0.02)
Thin sole shoe (0.02)
Office chair (0.1)

Experimental Parameters
Age: 35 years
Weight: 70 kg
Body Fat: 18%
Cardiac Index: 2.643 l/min/m^2
MET: 1.2

21 cooling cases of seven above mentioned configurations in three speed levels were experimented. Each test scenario lasted for 210 min and consisted of one PCS configuration in three speed levels along with two intervals for stabilisation. All the test scenarios were repeated four times. PMV, T_{eq}, T_{sk} and P were recorded at 1 min interval. Test protocol is presented in Figure 10. After each 10-minute cooling period, the changes in Tsk, P, T_{eq} and PMV were recorded. Trials exhibiting a standard deviation greater than 10% were considered unstable and were therefore discarded and repeated. The data capture and trial selection process is illustrated in Figure 11.

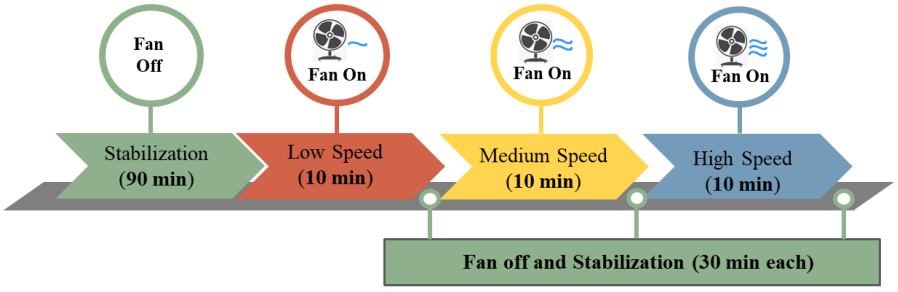

Figure 10: Test protocol timeline for Personal Comfort System (PCS) devices including stabilization periods and three fan speed intervals

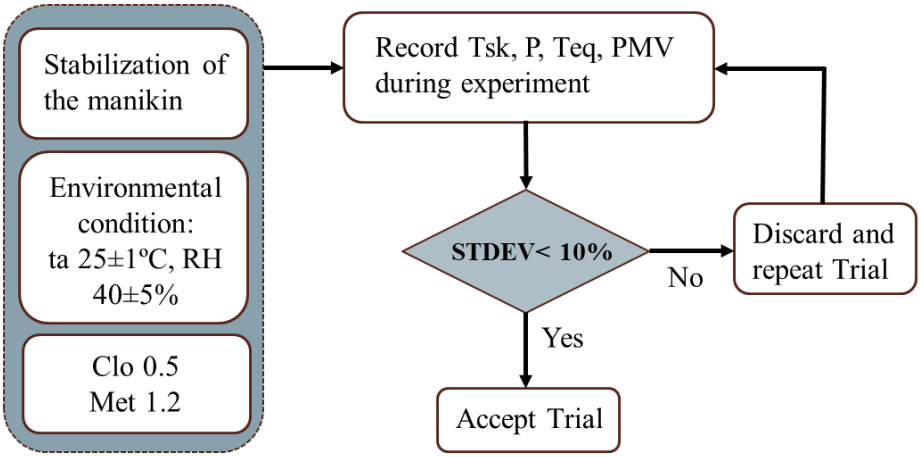

Figure 11: Data Capture and selection procedure

3.5 Air velocity measurement procedure

The mean air velocity generated by each fan configuration was determined by averaging airspeed measurements collected at three representative vertical levels corresponding to key occupant body regions: 1.1 m (head), 0.6 m (seated), and 0.1 m (ankle) level. An omnidirectional airspeed logger was used to measure local air velocity, and data were logged using a data logger (presented in Table 12). To ensure consistent sensor positioning and measurement repeatability, the omnidirectional airspeed probe was mounted on a height-adjustable tripod, allowing precise alignment of the sensor at each measurement height without disturbing the surrounding airflow field. At each measurement location and height, airspeed data were recorded for a duration of 10 minutes at one-minute intervals, yielding sufficient temporal resolution to account for short-term airflow fluctuations and fan-induced turbulence. The arithmetic mean of the three height-specific measurements was used to represent the mean air velocity at each location for a given fan configuration and speed setting. The selected levels and setup of airspeed measurement is shown in Figure 12. Three cooling configurations are presented in Figure 13.

The primary occupant measurement position was designated as P1 and located at the seated position of the thermal manikin. This position represents the direct exposure zone where the PCS was intended to provide localized cooling. To assess airflow spillover toward adjacent occupants in a shared office environment, a second measurement position, P2, was defined at a lateral distance of 2.1 m from P1, to evaluate unintended air movement and potential draught risk experienced by a coworker seated beside the primary user.

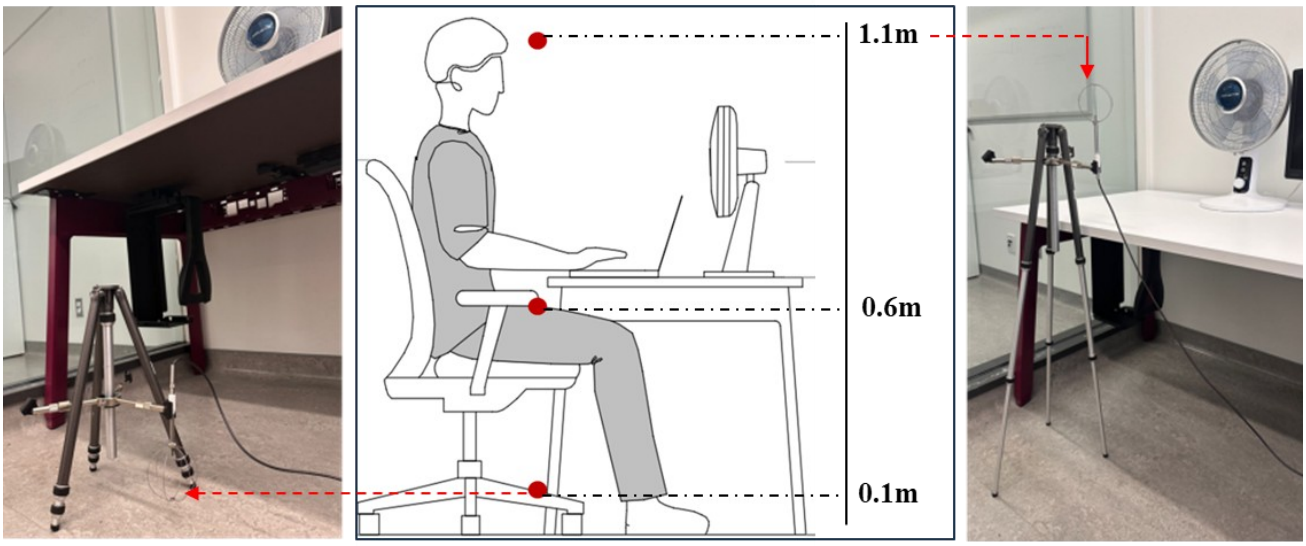

Figure 12: Selected levels for airspeed measurement and anemometer settings

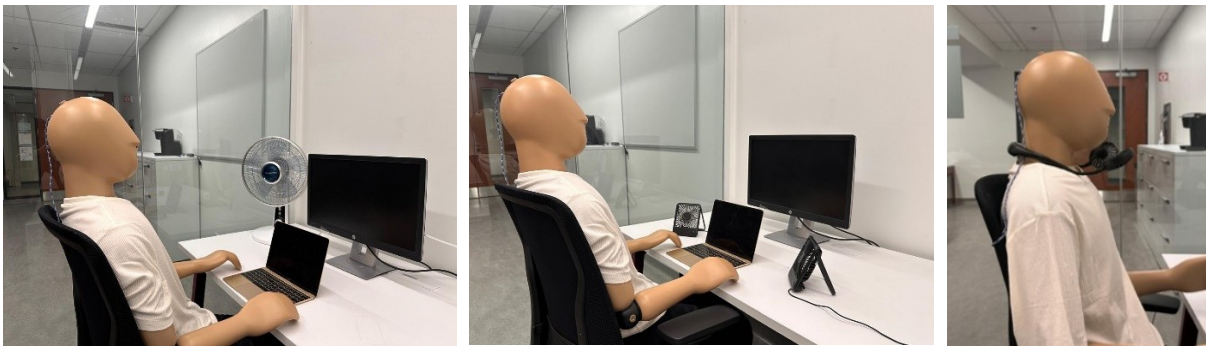

Figure 13. Cooling scenario with Configuration C2 (Left), C3 (middle) and C6(Right)

Although the experimental office space was designed for two occupants, an additional measurement location, P3, was introduced to capture rearward airflow propagation. P3 was

positioned 1.9 m downstream of the primary occupant, representing a coworker seated behind the primary workstation, a common arrangement in open-plan offices. This third position enabled quantification of airflow spillover in the downstream direction and provided insight into how different fan configurations influence air distribution beyond the immediate user zone. The Location of P1 and P2 is shown in Figure 8.

3.6 Determining cooling whole body thermal comfort

The thermal manikin is equipped with an integrated thermophysiological and heat-balance model that enables the calculation of T_{eq} and PMV directly from the measured heat exchange data. These parameters are computed automatically by the manikin software based on the fundamental heat balance between the manikin surface and the surrounding environment, including convective and radiative heat transfer. The embedded model uses segmental heat loss measurements, environmental conditions, and predefined physiological assumptions to determine the equivalent uniform temperature that would produce the same dry heat loss as the actual non-uniform environment. Similarly, PMV is estimated using established thermal comfort equations that relate heat balance to predicted human thermal sensation. The governing equations and theoretical framework underlying these calculations are described below.

3.7 Determining cooling efficiency of PCS devices

The localized thermal effects produced by PCS is quantitatively described using the concept of EHT [42][43][44]. A higher EHT corresponds to a warmer perceived thermal environment, whereas a lower EHT indicates a cooling effect. Thermal manikins are commonly employed to measure EHT under controlled laboratory conditions. For PCS evaluation, in order to capture the spatial variability of localized heating and cooling, segmented thermal manikins are essential. In

this experiment, the thermal manikin with independently controlled 23 body segments (j), each associated with a known surface area Aj (m^2) is being used. During experiments, the skin surface temperature of each segment and whole body, ($T_{sk,j}$ and T_{sk}) and the corresponding heat loss rate (Q_j and Q) (W) is continuously recorded. Based on these measurements, the whole-body EHT is calculated using Equation 1, where I_{clo} denotes the clothing insulation of the respective body segment under reference conditions, and the factor 0.155 is used to convert clothing insulation from clo units to thermal resistance units ($K \cdot m^2 \cdot W^{-1}$).

Whole-body EHT is subsequently determined using Equation (1), in which the total body heat loss (Q), total body surface area (A), and overall clothing insulation (Iclo) are used. This aggregated metric provides a single value representing the global thermal sensation of the occupant under non-uniform PCS exposure.

$$EHT_{whole\text{-}body} = T_{sk} - \frac{Q}{A} x\ I_{clo}\ x\ 0.155 \qquad (1)$$

EHT data have often been converted into CP to quantify the effectiveness of PCS devices. CP reflects the capacity of a PCS to shift the local or overall thermal environment toward an occupant's thermal neutrality. As defined in Equation (2), CP is calculated as the difference between EHT values measured with PCS operation and those obtained under reference conditions without PCS.

$$CP_{EHT} = EHT - EHT_{reference} \qquad (2)$$

CP can also be expressed in watt units, representing the direct change in human body heat loss induced by PCS exposure. $CP_{Q,j}$ is calculated from the difference in measured heat loss rates between PCS and no-PCS conditions, multiplied by the corresponding body segment area (Equation 4). At the whole-body level, CPQ is obtained by substituting segment-level heat loss with total body heat loss. A device-level COP may be defined to evaluate the energy efficiency of

PCS devices. COP is calculated as the ratio between the thermal corrective power achieved (in watts) and the electrical power input required to operate the device (Equation 4). This indicator provides a direct measure of how effectively a PCS converts electrical energy into perceived thermal benefit for the occupant.

$$CP_{Qj} = A_j \times (Q_j - Q_{j\_reference}) \text{ (W)} \quad (3)$$

$$COP = \frac{CP}{Power\ input} \quad (4)$$

3.8 Analyzing draught risk at the co-worker's location

Draught is widely recognized as the most common cause of local thermal discomfort in indoor environments and is defined as an undesired local cooling of the human body resulting from air movement. Unlike general thermal sensation, which reflects whole-body comfort, draught represents a highly localized phenomenon that primarily affects thermo-sensitive body regions such as the neck, head, ankles, and upper torso. Even under thermally neutral or slightly warm conditions, excessive air movement across these regions can induce sensations of overcooling and lead to occupant dissatisfaction.

To quantitatively describe draught-related discomfort, Fanger and Christensen, followed by Fanger et al. [3][45], developed a predictive model that has since been adopted by international standardization bodies, including ASHRAE Standard 55 and ISO 7730, as the most appropriate framework for estimating zonal discomfort caused by air movement. In this model, draught discomfort is expressed as the Draught Rate (DR), defined as the predicted percentage of occupants likely to feel dissatisfied due to unwanted air movement. DR is calculated using Equation (6), which incorporates the combined effects of local air temperature, mean air velocity, and turbulence intensity:

$$DR = (34 - t_a)\,(v_a - 0.05)^{0.62}\,(0.37 \times v_a \times T_u + 3.14) \quad (6)$$

where DR is the draught rate (%); t_a is the local air temperature (°C), v_a is the local mean air velocity (m/s) and Tu is the local turbulence intensity (%). This formulation reflects the fact that draught discomfort increases not only with higher air velocities but also with lower air temperatures and greater flow fluctuations.

According to ASHRAE 55 and ISO 7730, the applicability of this model is subject to several constraints. It is valid only for indoor environments where the local air temperature lies between 20 and 26 °C and the mean air velocity ranges from 0.05 to 0.5 m/s. Furthermore, the model is intended for occupants engaged in predominantly sedentary activities and experiencing an overall thermal sensation close to neutrality [26][43]. These assumptions are consistent with typical office conditions, making the draught model particularly relevant for assessing comfort risks associated with air movement generated by personal comfort systems.

ISO 7730 further classifies indoor environments into three comfort categories based on acceptable DR levels. Category A, representing the highest comfort standard, requires a draught rate below 10%; Category B permits DR values below 20%; and Category C, the lowest acceptable category, allows DR values up to 30% [47]. These thresholds provide a practical framework for evaluating and comparing localized draft risk in different indoor scenarios and are widely used in both experimental studies and building performance assessments.

3.9 Overall representation of the methodology

The overall methodology and systematic evaluation process of different personal fan configurations based on airflow structure (targeted, direct, and diffused) and orientation are summarised in Figure 14.

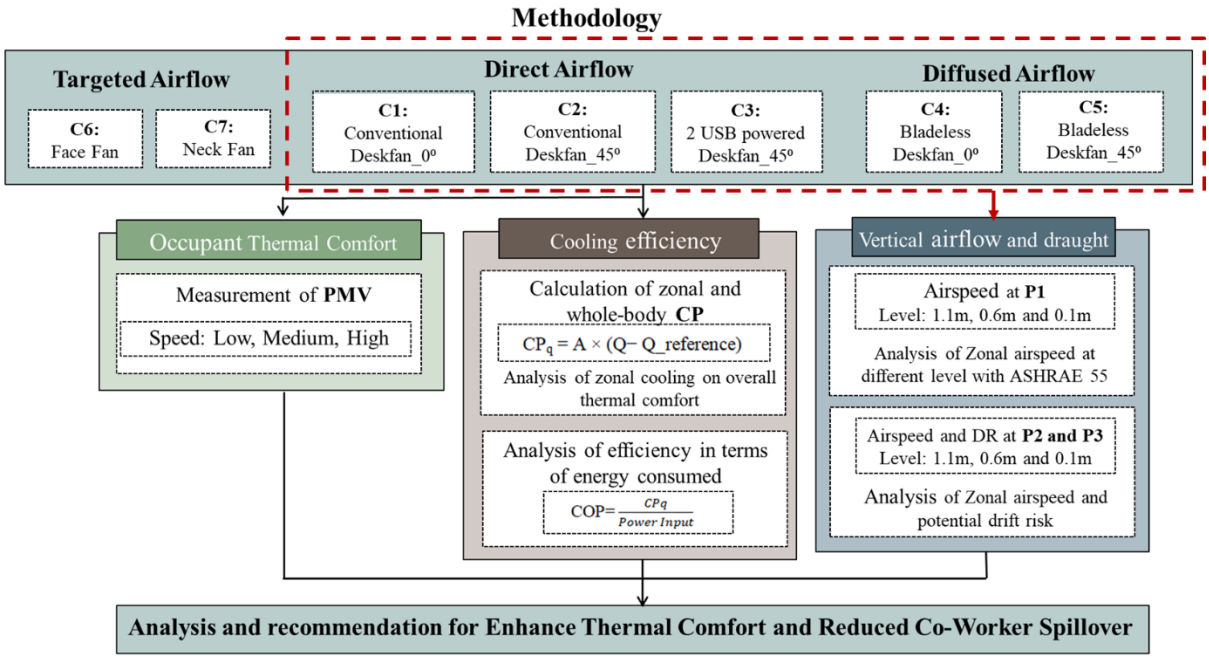

Figure 14: Framework of methodology and systematic evaluation

Seven configurations—including conventional desk fans, bladeless fans, USB fans, and wearable face and neck fans—are tested under multiple speed settings (low, medium, and high). The assessment framework integrates three main components: occupant thermal comfort, cooling efficiency, and energy efficiency. This structured approach enables a comprehensive comparison of configurations to identify solutions that maximize zonal and whole-body comfort while minimizing energy use and airflow spillover in energy conscious shared office environments.

CHAPTER 4- RESULT AND DISCUSSION

This chapter presents the experimental results and analysis of thermal comfort performance associated with seven PCS configurations. It examines both whole-body and localized thermal effects of the primary user and unwanted airflow spillover experienced by adjacent co-workers. The findings are further interpreted in zonal cooling effect, cooling efficiency and draught risk, providing a combined assessment of desk fan effectiveness and shared-environment impacts.

4.1 Effect of PCS devices on whole body thermal comfort

After each 10-minute cooling period, the changes in T_{sk}, P, T_{eq} and PMV were recorded and averaged. Trials exhibiting a standard deviation greater than 10% were considered unstable and were therefore discarded and repeated. The complete dataset for whole-body T_{sk}, P, T_{eq}, and PMV for all trials and their mean ± standard deviation (SD) is presented in Appendix A.

4.1.1: PMV Analysis

The changes in average PMV for each configuration with different fan speed are shown in Figure 15, where the shaded band represents the thermal neutral zone defines by ASHRAE 55 ($-0.5 \leq$ PMV $\leq +0.5$). The graph demonstrate that all seven cooling configurations reduced the warm discomfort with substantial gradation with the increment of air speed level. Under fan-off condition, PMV was around +1.1 reflecting the warm baseline. Activation of the cooling devices allowed an immediate shift of PMV towards neutrality indicating enhanced convective heat loss aligned with established models of non-uniform cooling.

For C1, a pronounced improvement in whole-body thermal comfort across all operating speeds was introduced with the activation of the PCS. At low speed, PMV decreased from the warm

baseline to approximately +0.3, continuing to approach zero at medium speed, placing thermal sensation within the near-neutral comfort range. At high speed, PMV shifted slightly into negative values, suggesting the onset of mild cooling. A similar trend was observed for C2, although the angular placement made the magnitude of cooling slightly lower than that achieved with direct airflow in C1. PMV reduced to approximately +0.35 to -0.23 from low to high speed.

The two USB fans angled toward the chest (C3) produced moderate and more gradual cooling compared to the bladed fan configurations. At low speed, PMV remained near the upper boundary of the neutral comfort band, indicating acceptable thermal relief. Medium and high speeds progressively reduced PMV to around +0.35 and +0.1, respectively, approaching thermal neutrality without inducing overcooling.

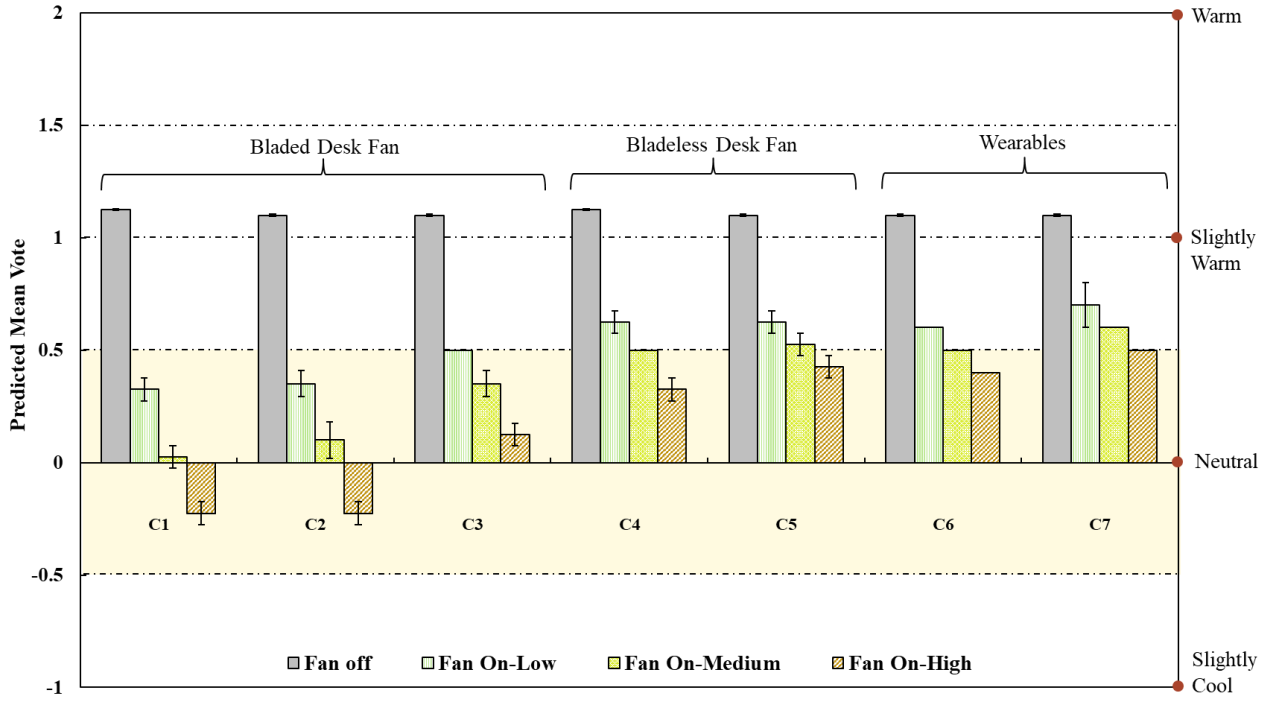

Figure 15: Predicted Mean Vote (PMV) at Fan off and 10th minute of fan-on conditions. The neutral zone represents the ASHRAE 55 -0.5 < PMV < +0.5

The C4 and C5 configurations exhibited lower cooling performance among all tested desk fans, with consistently smaller reductions in PMV compared to bladed fan configurations. For C4, PMV decreased modestly from the warm baseline to approximately +0.65 to +0.33 from low to high airspeed. Though the cooling effect was softer, all the speed levels satisfied the PMV reduction guideline provided by ASHRAE standard 55. C5 demonstrated an even weaker cooling response, with PMV remaining around +0.6 at low speed that couldn't meet the recommended standard reduction but improving to approximately +0.45 at high speed.

The wearable fan configurations show effective improvements in thermal comfort, particularly through localized cooling of thermally sensitive head and neck regions. They showed significant drop when the fan was turned on, but then the improvement in PMV is significantly mild. For the C6, PMV decreased progressively from the warm baseline to approximately +0.6 and decreased to further 0.1 vote with the increment of each speed level.

As thermal comfort improvement from PCS is strongly influenced by the magnitude of air movement, the relationship between PMV reduction (ΔPMV) and the average airspeed measured at the primary occupant location was examined and is presented in Figure 16. This analysis includes only the bladed and bladeless desk fan configurations, as the localized and body-mounted airflow generated by wearable devices could not be reliably represented by a single-point average airspeed measurement. Most configurations achieved PMV reductions exceeding the minimum threshold of 0.5 recommended by ASHRAE Standard 55 for effective PCS operation. The only exception was configuration C5 operating at low speed, which produced a PMV reduction slightly below this criterion. The reason why the PMV reduction was more pronounced in blade fans can be explained through this figure. The initial low speed and increment to medium and high airspeed in bladed fan configurations are much higher than the bladeless one. This big increase in airspeed

also results on greater reduction of PMV. To further understand these effects, the following sections examine the vertical distribution of airspeed and its influence on localized thermal comfort.

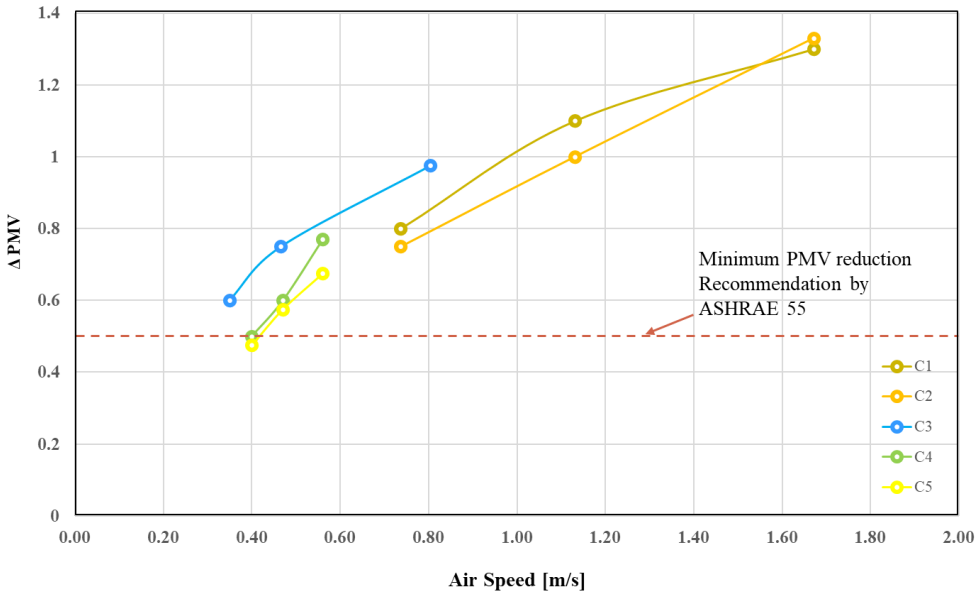

Figure 16: PMV reduction with increased airspeed levels in desk fan configurations (C1-C5)

4.1.2 Equivalent Temperature (Teq) Profile

The temporal variation of T_{eq} for the first trial of each configuration is shown in Figure 17 (a-g). These PMV trends were closely reflected in T_{eq} responses. Under fan-off conditions, T_{eq} was approximately 28.4 °C before the activation of PCS devices produced immediate reductions in Teq, indicating enhanced convective heat removal. Under low-speed operation, T_{eq} decreased from approximately 28.4 °C to about 25.8 °C, corresponding to a reduction of nearly 2.6 °C. Medium-speed operation further reduced T_{eq} to approximately 24.8 °C, and the largest cooling effect was observed at high speed, with T_{eq} approaching 24.0 °C. During fan off period, T_{eq} gradually returned to baseline levels within approximately 15–20 minutes, indicating a transient but reversible cooling effect. For C2, the highest cooling was again observed at high speed, with T_{eq} decreasing 26-24.2 °C from low to high respectively. This slightly lower T_{eq} values relative to C1 indicate that angling

the airflow away from direct chest exposure slightly reduces convective heat loss at the breathing zone, although the overall cooling performance of bladed fans remains significant and effective in shifting thermal sensation toward neutrality.

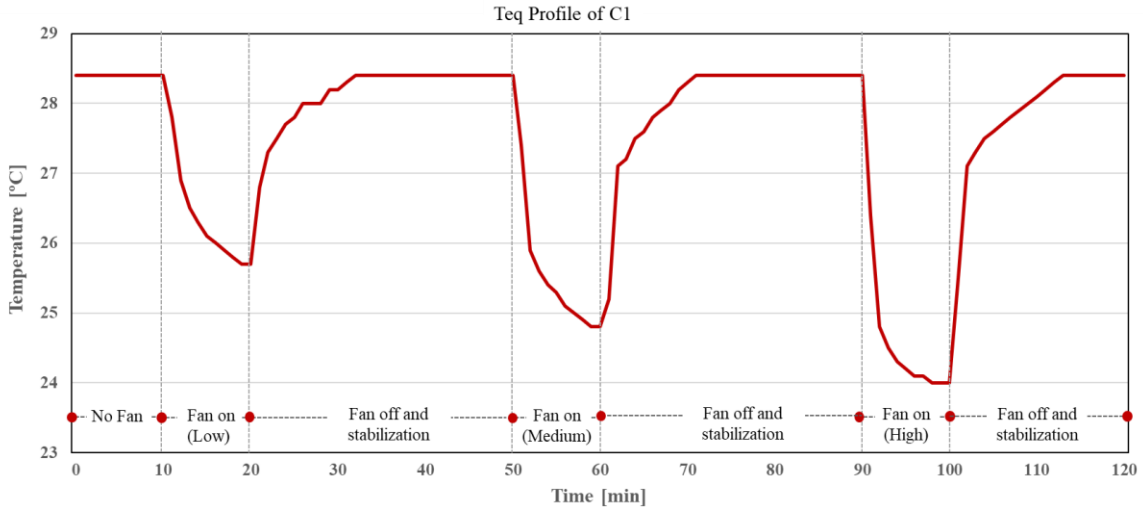

Figure 17(a): Equivalent Temperature (Teq) profile for C1 at three speed levels

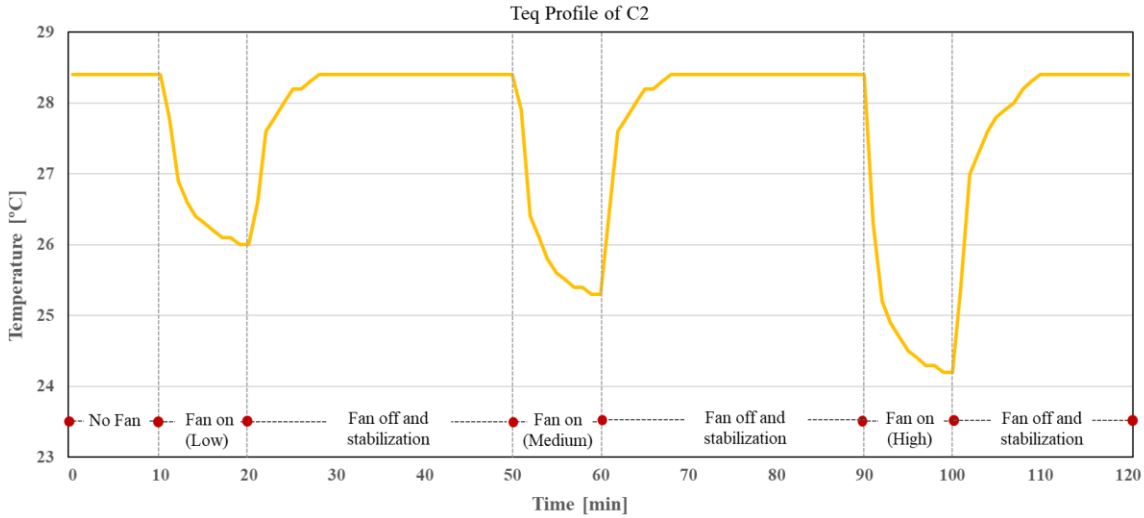

Figure 17(b): Equivalent Temperature (Teq) profile for C2 at three speed levels

T_{eq} responses shows aligned result in C3, decreasing to approximately 26.5 °C under low speed, representing a smaller reduction relative to C1 and C2. Medium and high speeds further lowered T_{eq} to around 25.8 °C and 25.3 °C, respectively. Notably, C3 exhibited smoother temperature transitions across all bladed fan conditions, suggesting that distributing airflow through multiple

low-power jets provides a more stable and controlled cooling effect, with reduced risk of excessive localized convective heat loss.

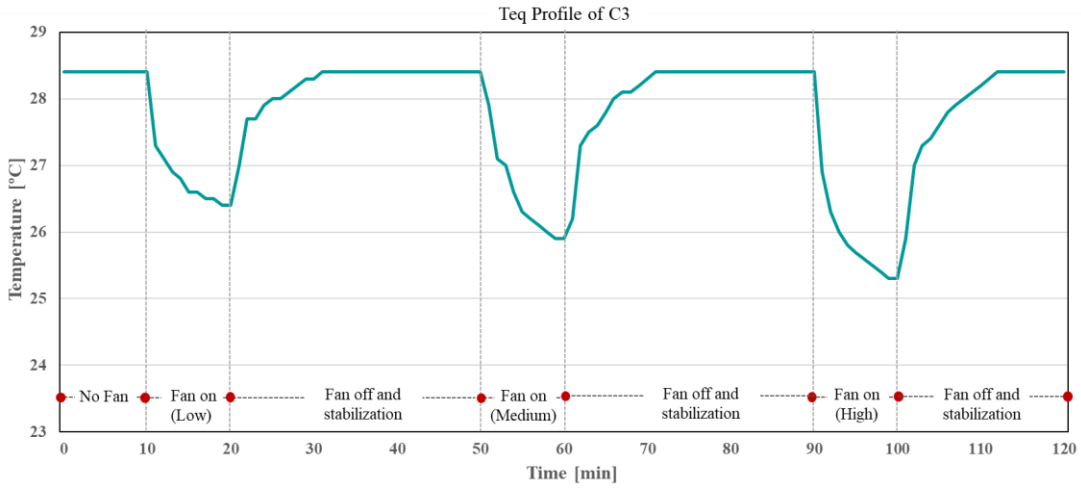

Figure 17(c): Equivalent Temperature (Teq) profile for C3 at three speed levels

The C4 and C5 configurations exhibited lower cooling performance in terms of T_{eq} compared to bladed fan configurations. For C4, T_{eq} decreased from 28.4 °C to approximately 27.0 °C, 26.6 °C, and 26.4 °C at low, medium, and high speeds, respectively. For C5, T_{eq} reductions were limited to approximately 27.2 °C, 26.8 °C, and 26.6 °C across increasing speeds.

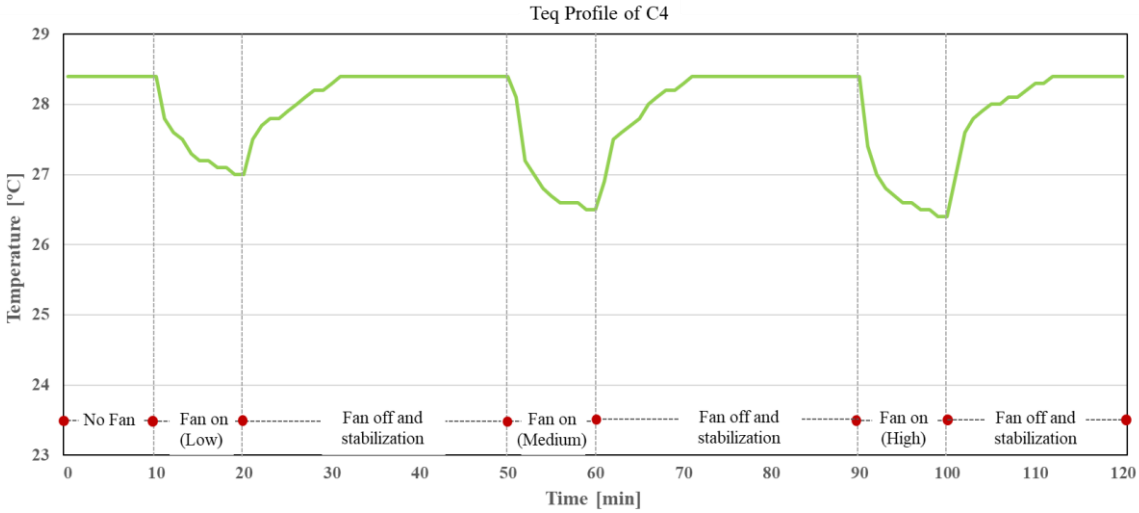

Figure 17(d): Equivalent Temperature (Teq) profile for C4 at three speed levels

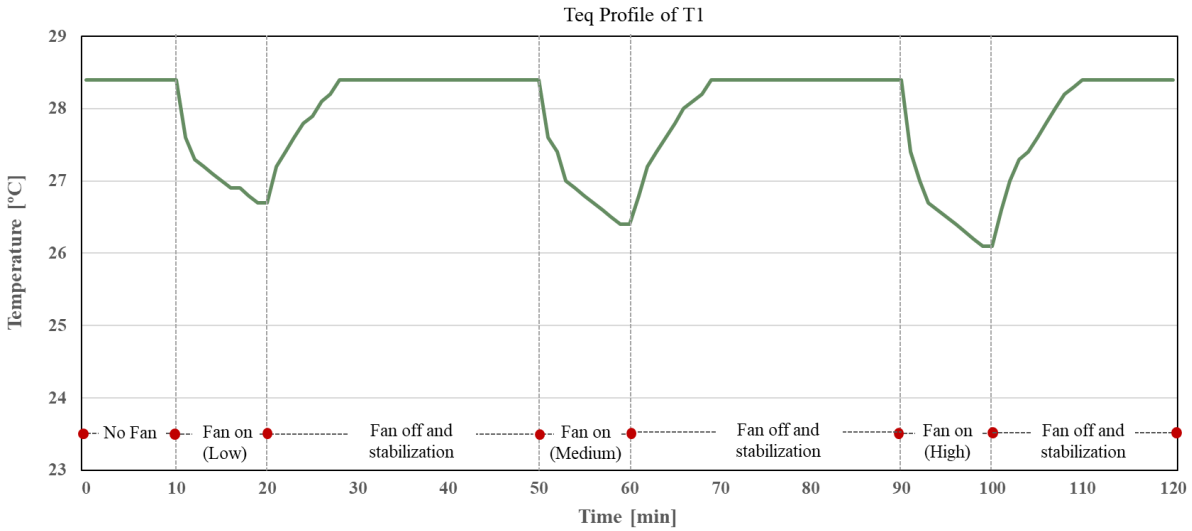

Figure 17(e): Equivalent Temperature (Teq) profile for C5 at three speed levels

For the face fan configuration (C6) T_{eq} decreased 1.7°C from 28.4 °C to 26.7 °C for low speed, for medium and high speed the reduction reached to 26.2 °C, and 26.0 °C respectively. C7 exhibited similar cooling effectiveness, with PMV decreasing to approximately +0.7, +0.6, +0.5 at low, medium, and high speeds, respectively. These T_{eq} profiles support the PMV results that the effectiveness of wearable fans at high speed is close to the effect of low speed bladed desk fan.

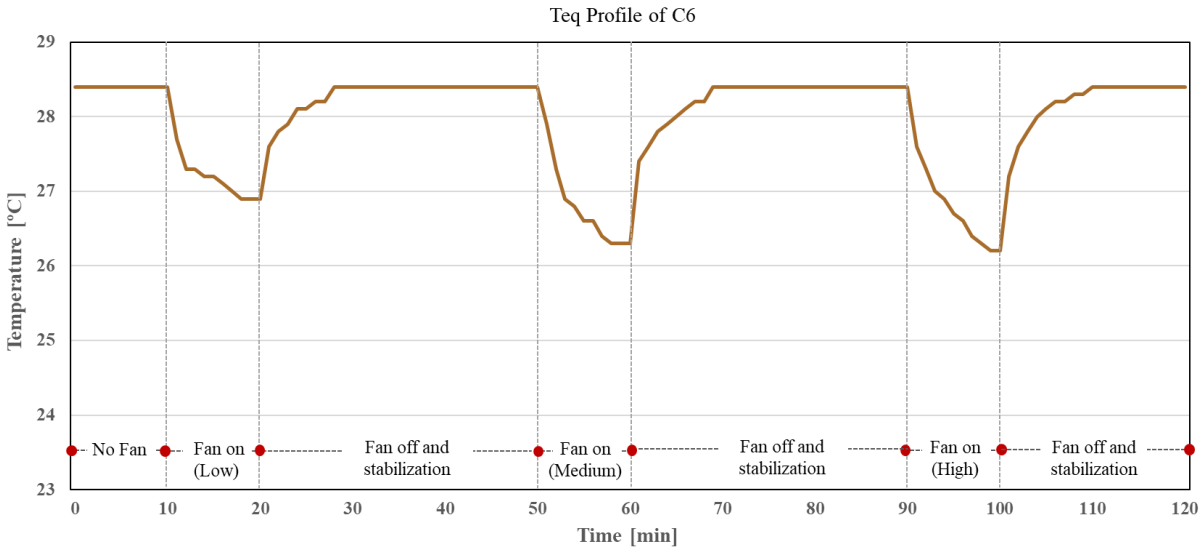

Figure 17(f): Equivalent Temperature (Teq) profile for C6 at three speed levels

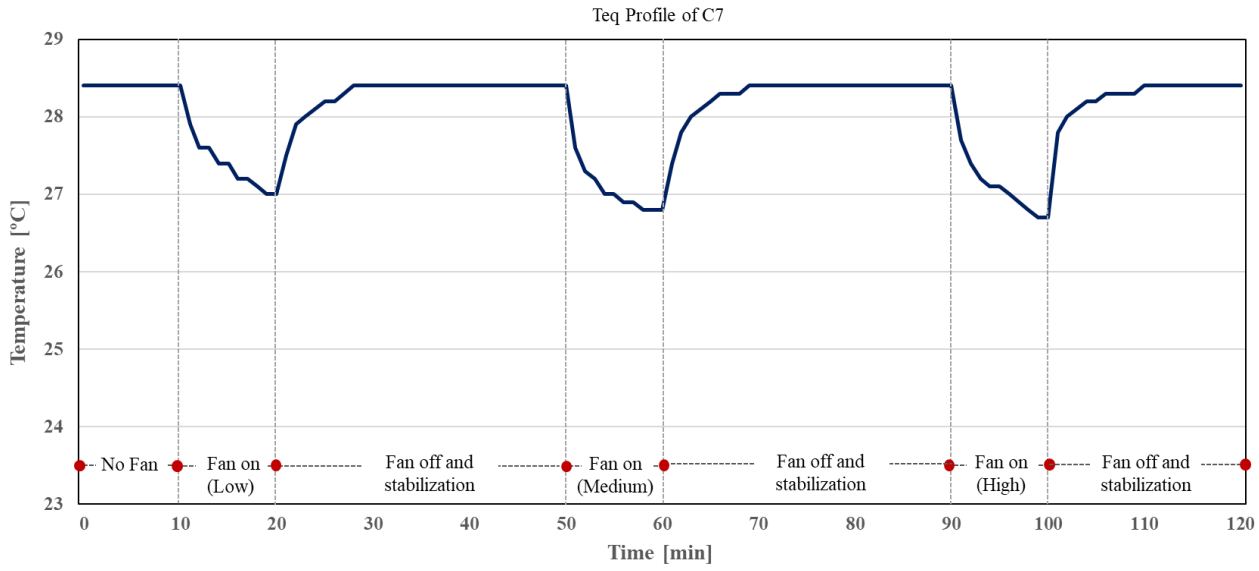

Figure 17(g): Equivalent Temperature (Teq) profile for C7 at three speed levels

Overall, the results demonstrate that the whole body cooling effectiveness of desk and wearable fans is strongly governed by both airflow intensity and distribution. In contrast, adjusting the placement of desk fans from 0º to 45º toward the chest results in only minor differences in whole-body cooling performance, suggesting that airflow structure and magnitude have a more pronounced effect than placement angle. These findings indicate that concentrated high-momentum airflow maximizes cooling effectiveness, whereas diffused or distributed airflow provides more stable but less intense cooling. This trade-off underscores the importance of balancing airflow magnitude and delivery pattern when designing desk fan or air jet integrated workstations specially in energy conscious environment.

4.2 Effect of zonal cooling on overall thermal comfort

This section presents the zonal cooling characteristics based on segmental CP and thermal image of the upper body. The zonal CP values are further grouped to better understand their combined effect on whole-body thermal response.

4.2.1 Zonal CP

Figure 18 gives each configurations wattage CP values, for the individual body parts. The magnitude and spatial distribution of CP varied substantially depending on the airflow delivery mechanism and device type. In general, the highest CP values were concentrated in the breathing zone (face, skull and neck), followed by the upper torso and arms, while the lower body regions exhibited minimal heat loss due to reduced airflow exposure. The graph clearly presents that the bladed fans have a significant cooling effect on torso and hands along with the breathing zone. The bladeless desk fans affect the chest with a mild cooling at torso level. The wearable fan focusses mostly on the zone they target, leaving the other body regions almost unaffected. The thermal image at high speed of each configuration also confirms this fact of zonal cooling in different fan configurations.

C1 and C2 demonstrated the highest corrective power among all tested devices. At high speed, CP values exceeded 6–7 W in the face and 3–4 W in the skull and chest, indicating strong localized convective cooling at exposed upper-body regions. However, the noticeable difference in these two configurations from other configurations is the effect on forearms, hands and stomach. The upper forearms and stomach exhibited CP values of about 4W and 3W at high speed reflecting effective airflow penetration across the frontal torso. In contrast, CP values rapidly decreased toward the lower body, with negligible heat loss observed in the thighs, legs, and feet. This highly non-uniform distribution confirms that bladed desk fans produce strong, directional airflow primarily affecting the upper body and breathing zone, which plays a dominant role in overall thermal sensation.

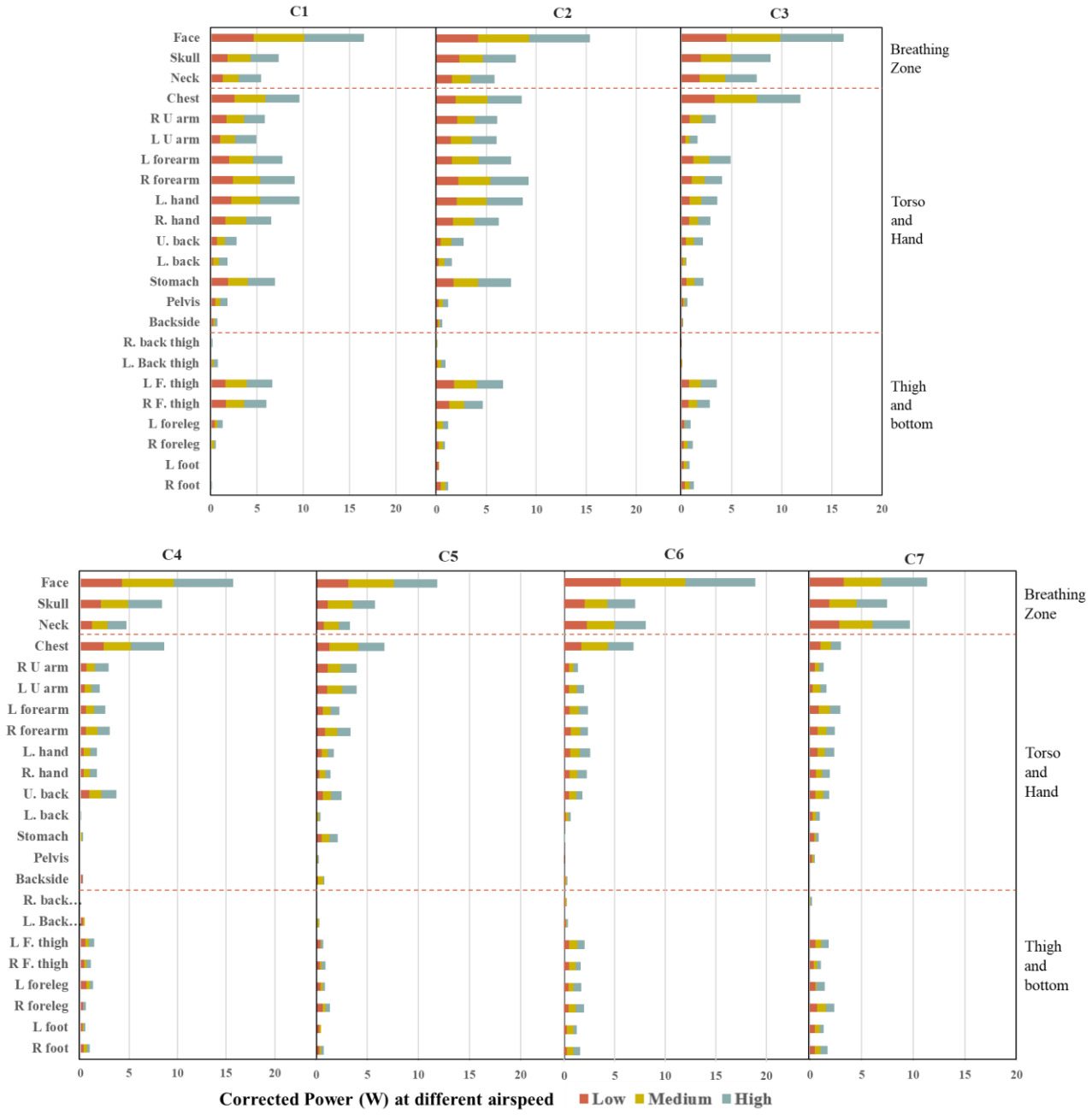

Figure 18: Corrective Power (CP) values of different body parts in terms of local heat loss (Watts) across three fan speed settings (low, medium, high).

C4 and C5 exhibited the highest CP values at face and skull and substantially lower values across all body regions compared to bladed fans. CP values in the Face were around 4-6W from low to high speed and torso and arm regions were generally below 1W, and the lower body remained largely unaffected. The angular bladeless configuration (C5) showed the lowest CP values overall,

supporting the previous finding that angling the airflow further reduces effective convective heat transfer.

The wearable fan configuration C6 and C7 demonstrated highly localized CP distributions concentrated almost exclusively in the breathing zone. Both configurations produced high CP values in the face and skull regions with negligible impact on torso and lower body. C6 showed largest CP values of 6-8W at face from low to high speed and 3-4 W at neck and skull. Compared to C6, configuration C7 exhibited slightly higher CP values across the skull and neck, indicating expanded airflow coverage through the breathing zone. Despite producing lower whole-body CP compared to desk-mounted fans, wearable devices effectively target thermally sensitive regions, which significantly influence thermal perception comparable to desk fans.

Overall, these CP results demonstrate that airflow structure and magnitude have a more pronounced effect than orientation. Bladed desk fans produced the highest overall CP due to strong directional airflow, while bladeless fans provided weaker and more diffuse cooling. Wearable fans, although generating lower whole-body heat loss, delivered highly efficient localized cooling at thermally sensitive regions.

4.2.2 Skin temperature distribution across upper body

Figure 19 represents the thermal image of the manikin after the 10 min fan on period (high speed) to further confirm the zonal cooling characteristics and CP distributions. Compared to the reference (no fan) condition, C1 and C2 show pronounced cooling in the breathing zone, chest, and upper extremities, evidenced by the visibly lower skin temperature distribution across the face, torso, and arms. These visual patterns are consistent with the high corrective power values observed in the torso and hand regions, confirming the ability of bladed fans to deliver extended

cooling towards hands. In contrast, C4 and C5 exhibit more moderate and localized cooling, primarily concentrated in the chest and upper torso, while the arms and lower torso remain largely unaffected.

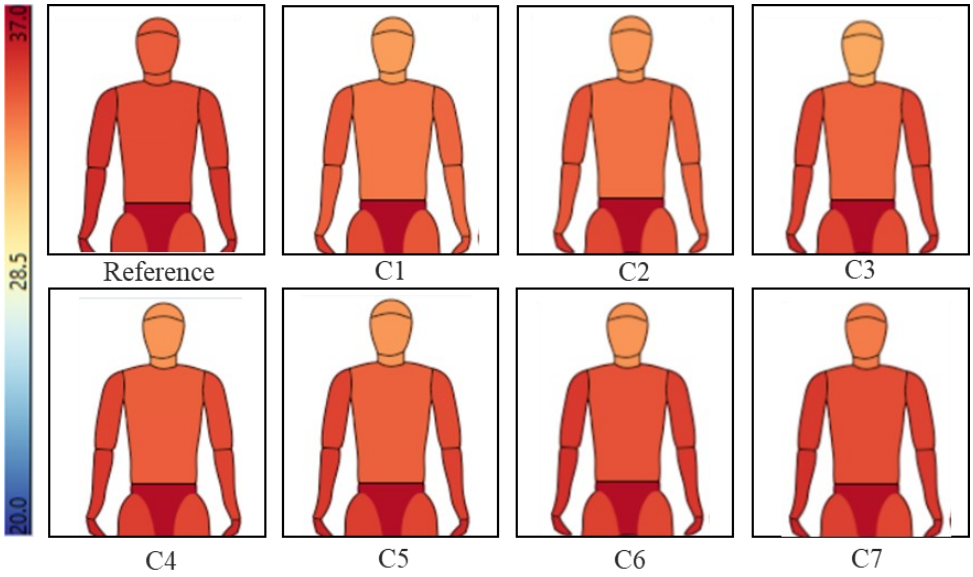

Figure 19: Thermal image of upper body segments at high speed for all 7 configurations

The smaller extent of lighter color regions indicates reduced convective heat transfer compared to bladed fans, validating the milder cooling effect observed in the corrective power analysis. C6 and C7 demonstrate highly localized cooling restricted mainly to the head and neck regions, with minimal changes observed across the torso and extremities. Overall, the thermal images visually validate the zonal CP results, clearly demonstrating that bladed fans provide extensive upper-body cooling, bladeless fans provide moderate chest-focused cooling, and wearable fans deliver highly localized cooling confined to their targeted regions.

4.2.3 Effect of zonal cooling on whole body thermal comfort

To understand the impact of regional cooling on whole body thermal comfort from different airflow pattern more clearly, the most affected zones are grouped together and presented with

whole-body CP in Figure 20. Breathing zone consist of face, skull and neck. Though neck is a separate anatomical section, for better control on the groups, it was considered in the group of breathing zones. Torso contains chest, upper back, lower back, stomach, pelvis and back side. Both upper hands, fore hands and hands fall into the 'hands' group. Figure 20(a) shows the configurations that are directed towards the chest, 20(b) presents those configurations where the fans are angularly (45 degree) directed towards the chest and the zonal and whole body CP for wearables are grouped in figure 20 (c). The figures illustrate how different fan configurations influence CP at the whole-body level and across specific body regions, including the breathing zone, torso, and hand. The configurations where whole-body CP values are comparable despite distinctly different regional cooling patterns are marked in red boxes, demonstrating that similar overall cooling effectiveness can be achieved through different airflow distribution strategies.

In configuration C1, maximum corrective power is shown in hands, while breathing zone and torso shows moderate cooling. At low speed, the overall CP is 28.90 W which is close to the whole body CP achieved by the bladeless fan configuration directed towards chest (C4) at high speed. The trend doesn't change when the fans are directed angularly. C2 exhibits a similar trend, with whole-body CP increasing from 27.12 W to 45.73 W from low to high speed. In configuration C3 the combined effect of two small direct jets resulted the whole body CP of 18.87W to 34.09W with the airspeed increment. Though in this configuration the breathing zone receives substantially higher CP of 10.98 W, while torso and hand CP remains relatively moderate (6.27 W and 6.60 W respectively), the whole body CP value achieved at medium speed (27.29 W) is comparable to the low-speed whole-body CP observed in C1 and C2.

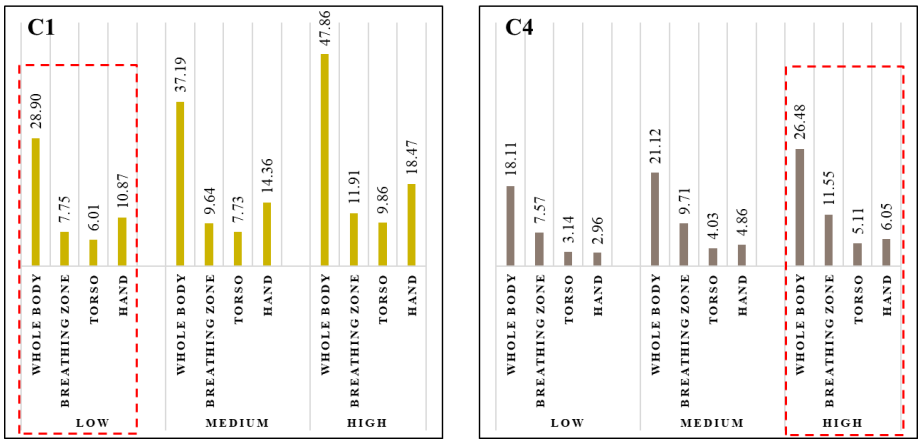

Figure 20(a): Whole body and zonal CP of desk fans directed toward chest

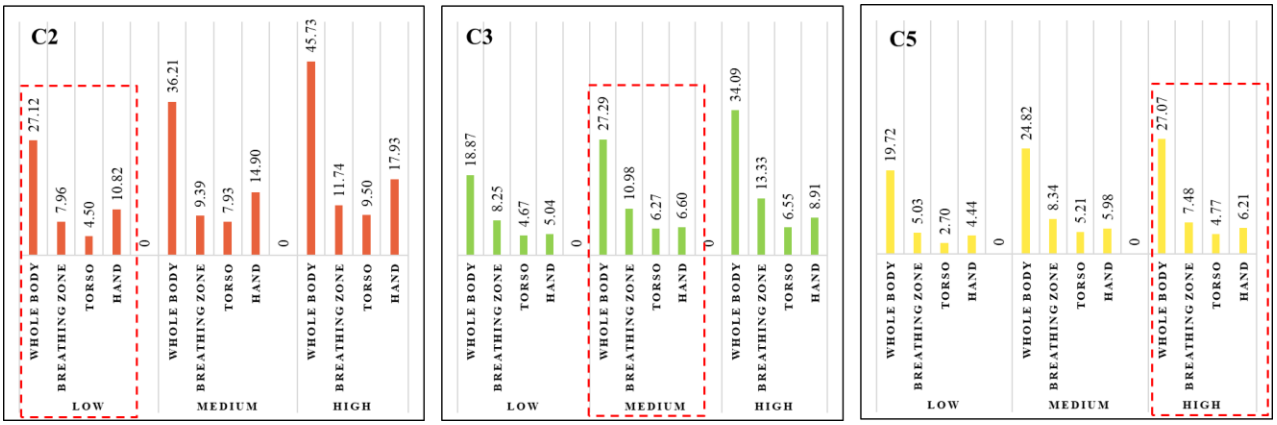

Figure 20(b): Whole body and zonal CP of desk fans angularly (45 degree) directed toward chest

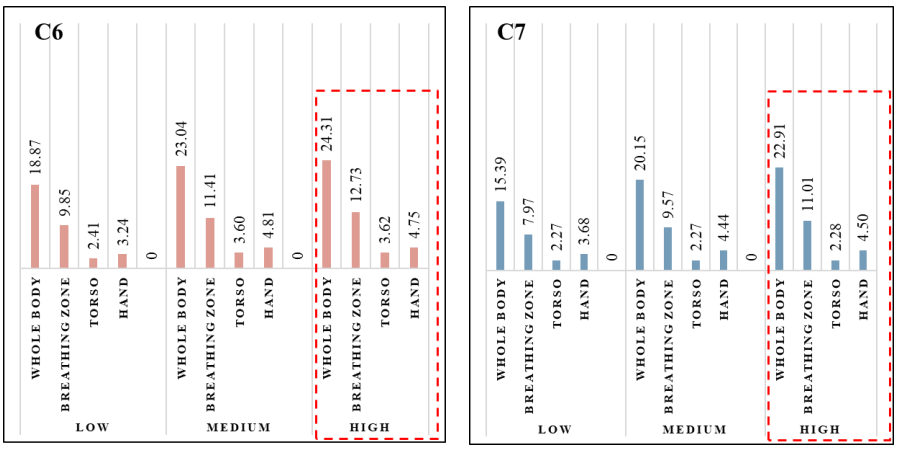

Figure 20(c): Whole body and zonal CP of wearable fans

Similarly, configuration C5 demonstrates comparable whole-body CP values at high speed (27.07 W, red- boxed), closely matching the whole-body CP observed in C3 medium speed, C4 high speed and C1-C2 at low speed. However, regional cooling distribution differs, with moderate breathing zone cooling (7.48 W), lower torso cooling (4.77 W), and moderate hand cooling (6.21 W). This indicates that localized cooling provided by diffused airflow can achieve similar whole-body heat loss while targeting specific regions, but at a higher airflow intensity.

4.3 Cooling efficiency of the PCS configurations

The cooling efficiency of the PCS configurations are described as CP and COP. The whole body CP in terms of EHT and wattage is presented in Table 6. The C1 and C2 configurations have had a great effect on torso, upper and lower arms and hand resulting in a notably higher whole-body CP ranging from 0.93-1.88 for CP_{EHT} and 27.12-48.86 for CP_Q. In contrast, C3 demonstrated moderate cooling performance, with CP_{EHT} increasing from 0.68 to 1.21 as speed increased. C4 and C5 exhibited lower overall corrective power, with CP_{EHT} ranging from 0.61 to 0.89 for C4 and 0.68 to 0.95 for C5, and CP_Q ranging from 18.11 W to 26.48 W and 19.72 W to 27.07 W, respectively. These reduced values reflect the lower airflow momentum and more diffuse air distribution of bladeless fans, which limits their ability to generate strong whole-body convective cooling despite providing localized thermal relief. C6 and C7 produced the lowest whole-body corrective power among all PCS configurations, with CP_{EHT} ranging from 0.61 to 0.85 for C6 and 0.51 to 0.76 for C7. These lower whole-body CP values reflect the highly localized nature of wearable cooling, which primarily targets the face and neck regions and has limited influence on total body heat loss. Nevertheless, both wearable configurations demonstrated consistent increases in CP with fan speed, confirming their ability to provide effective localized cooling with relatively modest whole-body heat removal.

Table 6. Comparison of whole-body corrective power in terms of EHT(CP_{EHT}) and Q(CP_Q) from thermal manikin tests across all configurations.

	Speed	C1	C2	C3	C4	C5
CP_{EHT}	Low	1.05	0.93	0.68	0.61	0.68
	Medium	1.42	1.30	0.96	0.69	0.89
	High	1.88	1.73	1.21	0.89	0.95
CP_Q	Low	28.90	27.12	18.87	18.11	19.72
	Medium	37.19	36.21	27.29	21.12	24.82
	High	47.86	45.73	34.09	26.48	27.07

Figure 21 represents the energy consumption of each configuration of the 10 minute fan on period in the experiment and the calculated COP from that. COP was only calculated for the deskfans as the face and neck fans have rechargable batteries and consume negligible energy. Since COP represents the ratio of useful cooling output to electrical input, its value depends strongly on both the achieved heat loss and the power required to generate airflow. From the graph, it is clearly shown that although a device can generate huge CP, the COP could be very low because of its high energy consumption. Here C1 and C2 have high CP_Q of 28.90-47.86W and 27.12 to 45.73W respectively. However, the conventional bladed fan consumes comperatively higher energy during operation that eventually lowers the COP to less than 1.5. This indicates that although bladed fans provide strong convective cooling, their higher power demand reduces overall energy efficiency.

In contrast, in C3, the total power consumption for both USB powered fans demonstrated substantially lower energy consumption while still providing moderate cooling output, with CP_Q ranging from 18.87–34.09 W. As a result, C3 achieved comparatively higher COP values at every speed level than the conventional bladed fans. C4 and C5 consumed relatively low electrical power but also produced lower cooling output, with CPQ values ranging from 18.11–26.48 W and 19.72–27.07 W, respectively. Despite their reduced cooling capacity, the lower energy consumption allowed these configurations to maintain moderate COP values, reflecting a balance between

cooling effectiveness and energy efficiency. The configurations that were resulting in similar whole body CP despite different airflow mechanism, orientation and targeted zone are marked in red boxes. Among those configurations C3 has the maximum COP, indicating that spitting one large jet into two small jets can provide acceptable thermal comfort with better COP. C4 and C5 at high speed consumes more energy than both usb-powered fan resulting into a lower COP.

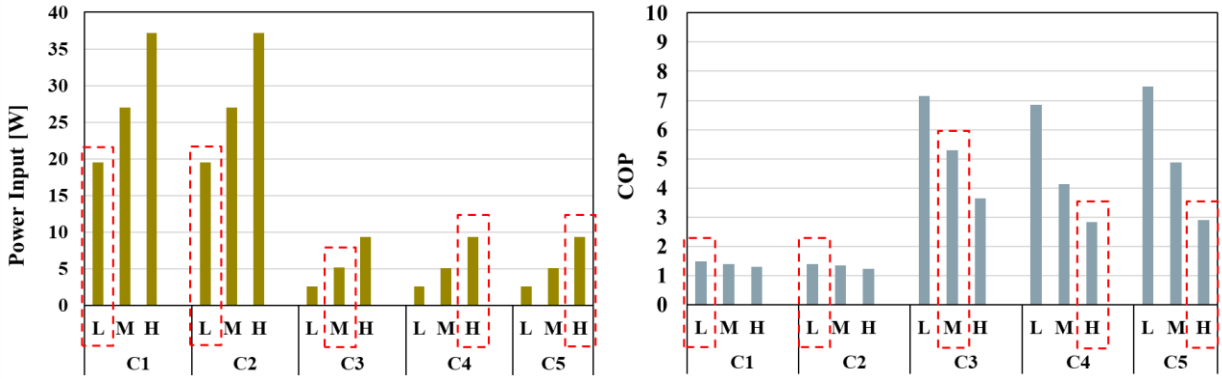

Figure 21: Power input and COP of bladed and bladeless fan configurations

4.4 Air speed Analysis at zonal level

4.4.1 Multilevel air speed exposure at primary occupant (P1)

The measured air velocity distribution indicates a pronounced vertical non-uniformity of airflow generated by the desk fan across the three measurement heights. At the head level (1.1 m), the airspeed increases substantially with fan speed in every configuration. The maximum non-uniformity is shown in Bladed fan configurations where the head level exposure is several times higher than the sitting and ankle level. Whereas the split jet or diffused jet produces moderately low head level airspeed. For C1 and C2, the head level airspeed ranged from 1.66-4.5 m/s from low to high speed. At C3, splitting the large jet into two segments reduced the zonal level non-uniformity and head level exposure came to a range of 0.81 to 2.18 m/s. For C4 and C5, as the

bladeless fan produces diffused airflow, the 1.1m level airspeed is even lower ranging from 0.87-1.39m/s from low to high speeds. These head-level values are significantly higher than the PCS airspeed limits recommended by ASHRAE Standard 55, which suggests a range of approximately 0.3–0.8 m/s when airflow is directed toward the head/ face/ upper body. The results indicate and therefore support the zonal CP results that the tested desk fans produce a concentrated airflow toward the breathing zone and upper body, resulting in strong localized convective cooling at the face, neck, and upper torso regions.

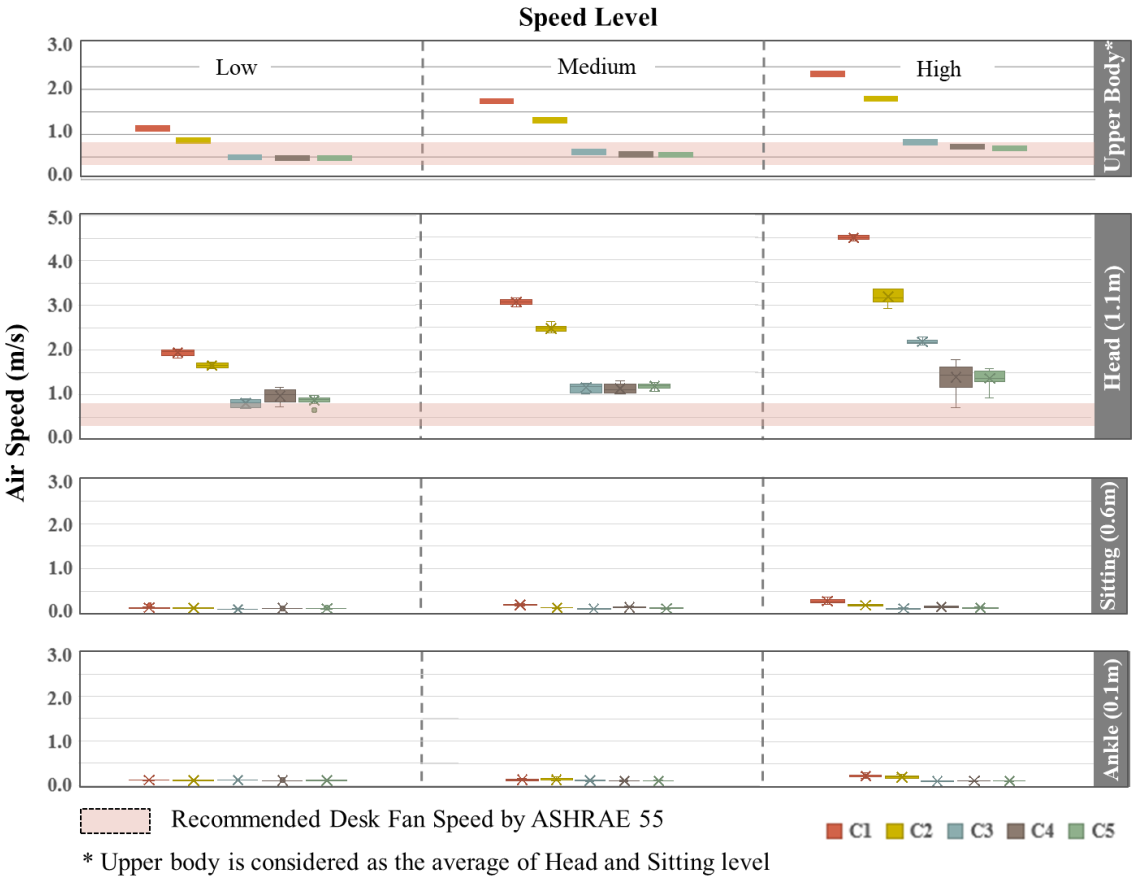

Figure 22: Airspeed at different level for the primary occupant (P1)

In contrast, the airspeed measured at the sitting level (0.6 m) and ankle level (0.1 m) remains substantially lower across all configurations. At the sitting level, velocities are slightly raised (0.35

m/s) by the bladed desk fans, while ankle-level velocities are typically below 0.25 m/s. For C1, C2 and C3 the change in sitting and ankle level airspeed remains almost negligible. The lower body receives minimal airflow exposure, producing a clear vertical gradient in local convective cooling. Such non-uniform airflow distribution can lead to significant differences in local thermal sensation across body region as dominance of airflow at the head level has important implications for perceived thermal comfort.

4.4.2 Spillover effect at Co-worker at P2 and P3

The velocity profiles at P2 (Figure 23) and P3 (Figure 24) represent that the airflow spillover varies substantially in two locations. At P2, averaged airspeed generally remains within 0.2 m/s across all configurations and fan speeds, while at P3 the average exceeds that value in all three speeds for C1 and medium and high speed for C4. Local measurements at adjacent coworker's location (P2) reveal that the maximum spillover consistently occurred at 0.1m level. The direct bladed configurations (C1–C2) and in C4, where airflow is laterally directed maximised the ankle level draught risk for the adjacent occupant. These localized effects are not captured by the averaged value.

At P3, the limitation of average airspeed is more pronounced. Even when the average airspeed suggests moderate exposure, head and torso level airspeed exceeds 0.5m/s for high speed in C1 and 0.3 m/s in high-speed settings in C4 and C5. This indicates that, when the primary occupant is using the desk fan beyond the recommended range of ASHRAE standard 55, the co-worker sitting behind the primary occupant may experience unwanted airflow near sitting and head level particularly for direct, forward-oriented fan configurations.

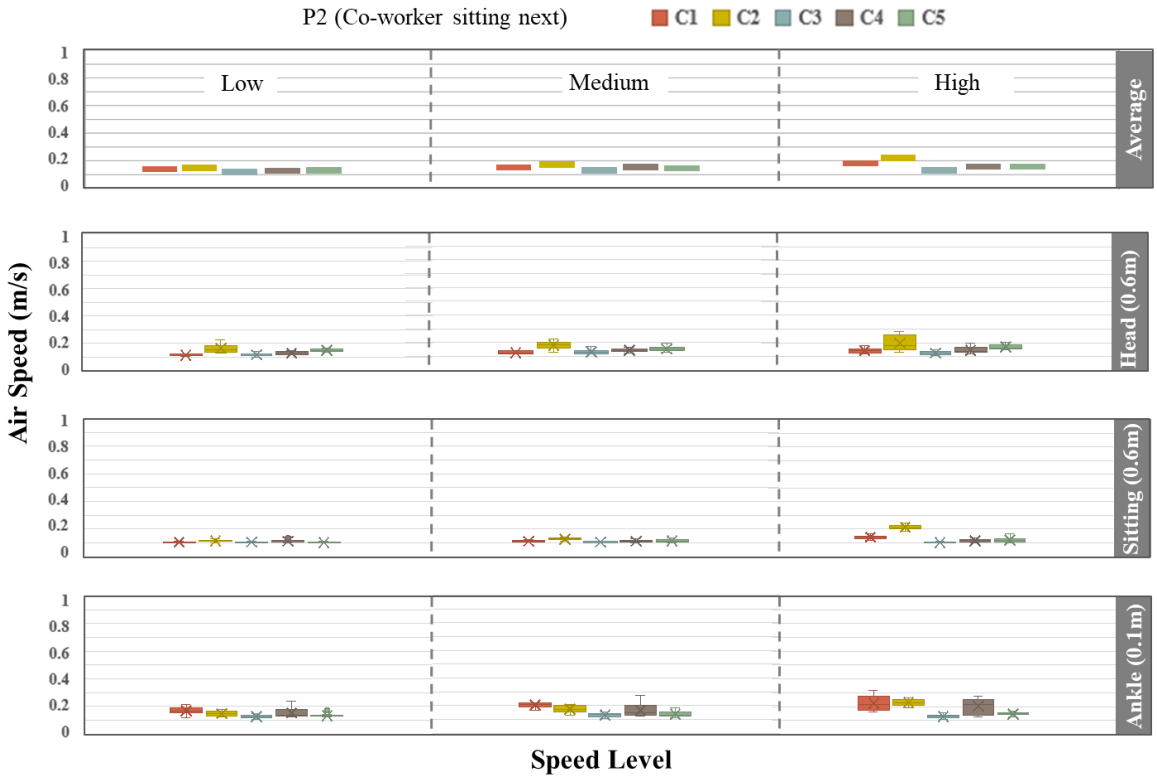

Figure 23: Airspeed at different level for the adjacent coworker (P2)

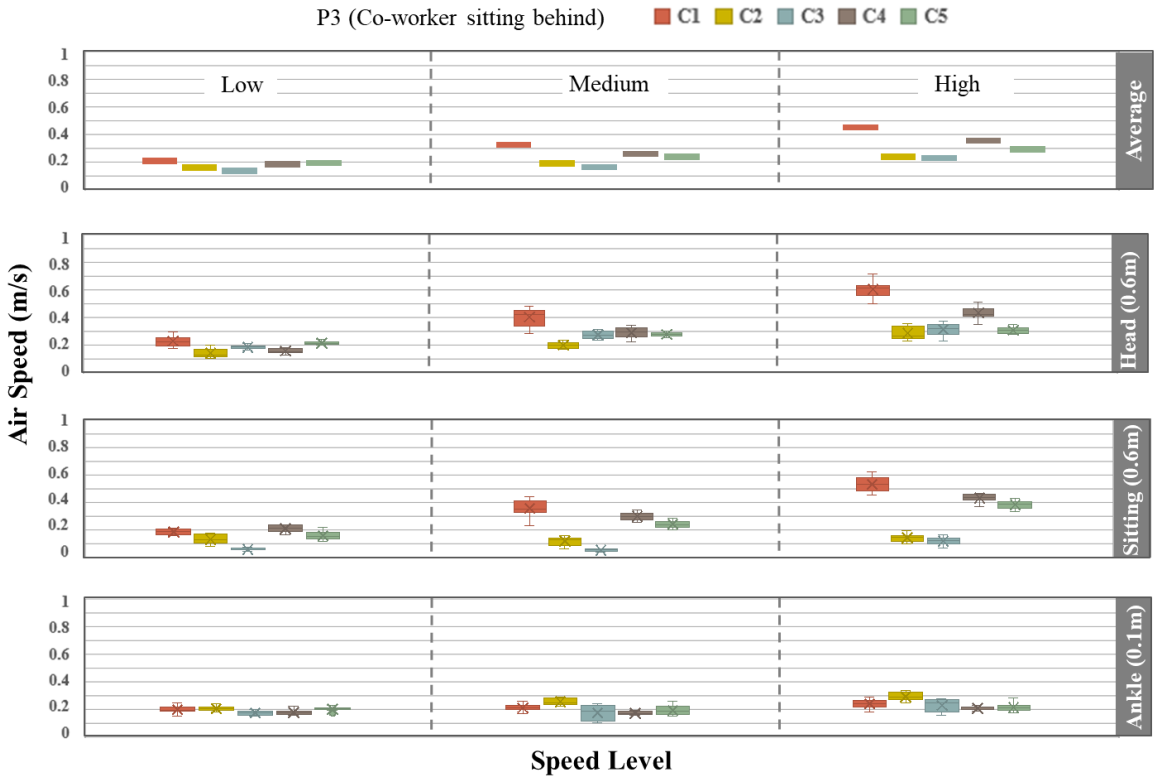

Figure 24: Airspeed at different level for the adjacent coworker (P3)

In both locations, C3 exhibited the minimum spillover at all measured heights. One possible explanation for this is that the two airstreams merged and dissipated before reaching P3, with a combined momentum from both streams, resulting in reduced localised velocities and lower spillover intensity at coworker position.

4.4.3 Draught risk (DR) analysis

The draught risk for the co-worker positions presented in Table 7 further reflects this localized exposure pattern. At position P2, most configurations remain within acceptable limits, with DR values typically below 10–15% across the three measurement heights. These values fall within Category A and B, indicating a relatively low probability of draught discomfort for the neighbouring occupant under most operating conditions. However, some configurations show slightly elevated DR values at ankle level or head level under higher fan speeds, specially for the bladed fans.

Table 7: Calculated draught risk (%) at position P2 and P3 for all configurations.

Configurations	Location	DR(%) at P2			DR (%) at P3		
	Speed	1.1m	0.6m	0.1m	1.1m	0.6m	0.1m
C1	L	5.5	4.9	10.0	13.7	10.2	11.2
	M	6.5	5.4	10.8	25.5	23.1	12.0
	H	8.2	7.5	15.9	32.3	29.8	13.4
C2	L	10.3	5.6	8.2	8.8	8.6	10.6
	M	10.6	6.3	10.2	10.5	7.9	13.8
	H	14.3	11.1	12.5	18.1	9.2	15.3
C3	L	6.0	4.9	6.7	9.5	2.1	8.8
	M	7.3	4.9	7.1	14.3	2.4	12.9
	H	6.5	4.9	6.8	19.1	7.6	14.4
C4	L	6.6	5.7	9.9	8.4	12.0	9.5
	M	7.5	5.6	11.6	16.6	16.0	9.0
	H	8.6	6.0	14.7	23.9	20.7	10.1
C5	L	7.7	4.9	7.0	10.6	9.7	10.0
	M	8.6	5.9	8.0	12.9	13.6	12.0
	H	9.1	6.9	7.6	15.8	19.4	12.0

Category A (<10%) Category B (<20%) Category C (<30%) Beyond

The draught risk becomes more significant at the second co-worker position (P3), where the airflow spillover from the fan interacts differently with the surrounding space. For configuration C1, the draught probability at head level reaches 25.5% at medium speed and increases to 32.3% at high speed. Similarly, the sitting-level DR reaches 23.1% and 29.8% for medium and high speeds, respectively. These values go beyond the typical comfort thresholds and fall within Category C or beyond, indicating a higher risk of draught discomfort for occupants located directly within the lateral spread of the direct airflow jet. Comparable trends are also observed for configurations C2 and C4 at high speeds, where localized airflow leads to DR approaching or exceeding 20% at certain heights.

4. Discussion

The overall analysis confirms that the magnitude and structure of airflow play a significant role in determining the effectiveness of PCS. In every configuration, these findings are consistent with the established principle of air-movement PCS, where increased convective heat transfer at exposed skin reduces equivalent temperature and shifts thermal sensation toward the comfort zone [33]. The conventional bladed desk fans generated large, high-momentum air jets that significantly improved thermal comfort by producing substantial reductions in equivalent temperature and PMV. But at every speed level the airflow exceeds the recommended threshold increasing the risk of overcooling. This finding aligns with the study of He [133], where at 26ºC, with 1.5 m/s average airspeed, 50% occupants mentioned as ‘slightly cool’ in thermal comfort vote. At the same time, configurations that split the airflow into multiple smaller direct jets (e.g. the dual USB powered fan setup) demonstrated that comparable comfort improvements can be achieved through distributed airflow while reducing the risk of excessive localized cooling. In contrast, bladeless desk fans provide diffused airflow and wearable cooling devices provided more targeted cooling.

Although these two provide airflow by two completely different physical mechanism, they result in similar overall thermal comfort improvements with the increment of airspeeds.

The zonal CP analysis and thermal imaging further support the conclusion that whole-body comfort improvement is strongly influenced by localized cooling of upper-body segments. Bladed desk fans produced extended cooling across the breathing zone, chest, arms, and hands, resulting in the highest whole-body CP. This direct, high-momentum airflow increases convective heat loss in the exposed areas and produces strong whole-body comfort improvements. However, excessive localized cooling at the head and extended region may reduce comfort stability and increase draught risk. This behavior aligns with Fanger's [3] heat balance principle, which emphasizes that thermal comfort depends on the balance between heat production and heat loss, and that excessive local convective heat transfer can lead to discomfort even when overall thermal sensation improves. Conversely, distributing airflow across multiple outlets or diffusing the air moderates convective heat transfer and produces a more balanced and stable thermal response. Related observations have been reported in preceding PCS studies, where spatial distribution were identified as more important than maximum air velocity for achieving sustainable thermal comfort [10][42]. Despite affecting fewer body segments, wearable fans still produced meaningful whole-body comfort.

Further zonal CP analysis by grouping close body segments together showed whole-body CP can be achieved through fundamentally different airflow distribution patterns. Bladed fans induce heat loss from breathing zone, torso and hand, whereas bladeless fans provide a diffused airflow with less impact on hands and torso. Wearable fans provide targeted cooling of thermally sensitive regions can achieve similar comfort benefits as broader torso-level cooling. This highlights that with different airflow distribution pattern and targeting varied segments similar whole-body CP

can be achieved. Regional airflow distribution plays a critical role here, rather than the fan placement.

The relationship between CP and COP further highlights the balance between cooling effectiveness and energy efficiency. While bladed desk fans produced the highest CP values, they also consumed more electrical energy, which reduced their overall COP. Conversely, configurations that provided moderate cooling with lower energy input, such as USB fans and bladeless fans, achieved more balanced energy efficiency. Although COP was not explicitly calculated for wearable devices due to their negligible plug-load energy consumption, their localized cooling performance indicates that they can deliver perceptible comfort improvement with minimal energy demand.

A clearer interpretation of the guidance provided in ASHRAE Standard 55 for PCS is necessary. The standard recommends an airspeed range of 0.36–0.8 m/s for desk fans directed toward the head, face, or upper body; however, it does not clearly specify the exact measurement location or method used to evaluate this airspeed. As a result, the guideline creates a level of ambiguity as it can be interpreted in different ways. One interpretation is that the recommended range applies specifically to the head-level airspeed. Another interpretation could be that the guideline refers to the average airspeed across the upper-body region, which could be the average of head and sitting levels, as the desk fan have a significant effect on torso level. In figure 22, this recommended range is presented in red band in both head level and upper body level airspeed to understand the compliance.

The present research demonstrate that the interpretation of the standard significantly influences the compliance assessment of desk fan configurations. When only the head-level airspeed is

considered, all configurations, regardless their location or airspeed exceed the recommended 0.36–0.8 m/s range. In contrast, when the average airspeed of the head and sitting levels is considered, several configurations—particularly the two USB-powered producing split jets at low and medium speeds and bladeless fan producing diffused jets across different intensity levels—fall within the recommended range. Additionally, the PCS guideline in the ASHRAE standard 55 suggests that, under cooling conditions, a PCS should increase the average airspeed by approximately +0.3 m/s. However, the standard does not clearly define the reference location for this increase. It remains unclear whether this criterion should be evaluated at a central room location or directly at the primary occupant's position. In this study, configurations that achieved a +0.3 m/s increase at the occupant location consistently exceeded the recommended 0.36–0.8 m/s range at head level. These ambiguities highlight the need for clearer guidance on measurement locations and evaluation procedures to support the effective implementation of PCS in shared office environments.

The multilevel airspeed measurements show that head-level velocities frequently reach several times higher magnitude from the lower body, indicating the potential for local overcooling or draught discomfort during prolonged exposure. This indicates, level-wise airspeed analysis even when the PCS is only targeted to the upper body is needed to understand the non uniform airflow pattern provided by them. At the same time, elevated airspeed section, ASHRAE Standard 55 permits higher airspeeds without an upper limit when occupants have direct control over the airflow, under the assumption that users can adjust the fan speed to maintain acceptable comfort conditions. The findings suggest that the airflow structure and spatial distribution of air movement should also be considered when evaluating compliance with the guideline, rather than relying solely on a single measurement point.

However, the results of this study indicate that when the primary occupant operates the fan at high speeds, the resulting airflow can extend toward adjacent workstations and increase draught risk for nearby co-workers. In several cases, the calculated draught probability at neighbouring positions exceeds recommended categories. These findings suggest that additional guidance may be necessary for PCS applications in shared office environments. Clearer limits or evaluation procedures for elevated airspeed under user-controlled conditions could help reduce unintended draught exposure for nearby occupants. Fan placement and zonal airflow distribution are critical factors influencing co-worker comfort. Therefore, level-specific airspeed assessment and airflow direction should be carefully considered when evaluating desk-fan PCS performance under ASHRAE Standard 55 guidelines, especially in open-plan office environments.

Overall, the present study demonstrates that PCS effectiveness depends not only on airflow magnitude but also on airflow structure, spatial distribution, and targeted body regions. Direct, high-momentum airflow provides the strongest whole-body cooling but may increase local discomfort, draught risk for coworkers and energy consumption. In contrast, distributed and localized airflow strategies can provide stable and energy-efficient comfort improvements with more energy efficiency and less spillover towards coworkers. These findings support the use of optimized small multi jet direct airflow towards sensitive regions or diffused airflow towards upper body when designing PCS for energy conscious shared office environment to improve practical applications.

Chapter 5 - Conclusion and Future Works

5.1 Findings

This study analysed the effect of airflow structure, device placement and airspeed level on the thermal comfort of primary occupant and coworker spillover under ASHRAE standard 55 recommendations. The key findings can be summarized as follows:

- Whole-body cooling effectiveness of desk and wearable fans is primarily governed by airflow intensity and distribution pattern, whereas adjusting the desk fan position from 0º to 45º toward the chest results in only minor changes in overall cooling performance.
- High-momentum conventional bladed desk fans provide the strongest whole-body cooling. Conventional bladed fans show the largest cooling with PMV reduction of 1-1.5. In energy conscious office environment this might onset risk of overcooling. Splitting direct airflow into multiple smaller jets or providing defused airflow improves comfort while reducing the risk of overcooling and improving comfort stability in energy conscious office environment.
- Breathing zone-torso-hand cooling with a direct airflow in low speed was found equivalent to breathing zone-torso cooling with a diffused airflow in high speed in terms of moderating T_{eq} and PMV. In addition, by targeting the highly thermosensitive face–neck region, wearables achieved whole-body CP_Q improvements nearly equal to those produced by broader torso -breathing-zone cooling by bladeless fan. Conventional bladed fan at low speed, two USB powered fans at medium speed, bladeless and wearable fans at high speed provides similar whole body CP despite targeting the thermosensitive regions differently.

- CP and COP do not peak simultaneously; devices with high cooling output may have lower energy efficiency due to higher power consumption. Conventional bladed fan consumes comperatively higher energy during operation that eventually lowers the COP to less than 1.5. Whereas, USB fan (both) or bladeless fan can provide similar comfort with much lower energy consumption. The dual USB fans showed maximum cooling efficiency with the lowest energy consumption among all other configurations.
- Multilevel airspeed analysis revealed that, to evaluate PCS performance; zonal airflow distribution and level-wise exposure analysis is important to understand more accurate comfort assessment. Conventional bladed fan configurations generated extremely high head level airspeed of 3-4.5 m/s, leading to large zonal CP peaks, whereas lower body exposure remains almost negligible. Long term exposure to this situation may induce local discomfort.
- The coworkers' drought risk was more pronounced at P3 in this experimental setup where head and torso level exceed 0.2 m/s with forward oriented configurations. For configuration C1, the draught probability at head level reaches 25.5% at medium speed and increases to 32.3% at high speed indicating significantly high DR for the coworker.
- Though fan placements and discharge angle has negligible influence on primary occupant's whole body comfort, it strongly influences airflow spillover. Splitting one large jet to two small direct jets (C3) or diffusing the direct jet by bladeless fans (C4-C5) minimise coworker discomfort

Overall, the results indicate that, targeted, diffused and splitting airflow strategies offer a promising pathway for improving thermal comfort while minimizing energy use in shared office operated under an energy conscious setpoints. Compared with highly directional airflow provided

by conventional bladed desk fan, this strategies help cooling the thermally sensitive regions while reducing the spillover effect to the adjacent occupants. Among all the tested configurations, the dual USB fan demonstrated a significantly balanced performance, providing noticeable improvement in occupant comfort consuming relatively low energy and causing minimal unwanted airflow disturbance in the surrounding environment. These findings suggest that appropriately designed and positioned low-power personal fans can support both occupant comfort and energy-efficient operation in shared office spaces.

5.2 Implications of this study

This study can be implemented as baseline for understanding the effect of different airflow mechanism generated by various fan configurations and their effect of zonal and whole body thermal comfort in energy conscious set points. The findings provide evidence on localised cooling highlighting their potential impacts on coworkers. These insights may help to select the PCS suitable for providing comfort while minimising the draught discomfort towards the adjacent coworker.

In addition, the result supports to highlight certain limitations of the existing standards related to PCS application. The current guidelines do not clearly specify how the exact measurement locations and procedure for setting the threshold. It also doesn't consider spatial distribution of airflow produced by the desk fans, which is necessary for understanding the non-uniformity at occupants location as well as the coworkers place. Therefore, the findings of this study suggest that these criteria should be more clearly defined and incorporated into the standards to support the practical implementation of PCS in shared office environments.

5.3 Limitations of the Study

Despite the comprehensive experimental framework, this study has several limitations that should be acknowledged. First, the experiments were conducted in a controlled office space with simplified office layout, which may not fully represent the diversity of real-world open-plan offices where furniture arrangement, occupant movement, and background airflows from HVAC systems can significantly alter airflow patterns. Second, the use of a thermal manikin with fixed physical parameters does not capture subjective human factors such as individual thermal preference, behavioural adaptation, or perceptual tolerance to local draught, as well as fan noise. In addition, coworker exposure were measured at fixed discrete points, which may not reflect the continuous spatial variability of airflow around the occupants. Finally, transient behaviours such as intermittent fan use and occupant posture changes were not considered in this study. Future studies should therefore extend the analysis to real occupied spaces, incorporate subjective comfort assessments and spatial heterogeneity of airflow to further validate and generalise the findings.

5.4 Future Work

Two important extensions can further strengthen the applicability and impact of the findings. First, validation through controlled human-subject experiments is recommended. Although T_{eq}, CP, PMV, and zonal airflow measurements provide robust objective indicators of thermal performance, human perception of comfort involves physiological and psychological responses that cannot be fully captured by manikin-based approaches alone. Future studies should therefore examine thermal sensation and comfort votes, preference responses, and potential draught perception under the most promising configurations identified in this work. Particular attention should be given to comparing multi-region cooling (breathing zone–torso–hand) with breathing-

zone-dominant cooling, as well as evaluating multilevel draught acceptability at coworkers' location in shared settings. Such validation would strengthen the translation of zonal CP and airflow-distribution findings into occupant-centered comfort guidelines.

Second, the incorporation of the experimentally derived performance metrics into building energy simulation models would allow quantification of potential energy savings at the building scale. By integrating fan-induced cooling effects as CP or equivalent temperature adjustments within simulation platforms, it would be possible to evaluate thermostat setpoint extensions and corresponding reductions in cooling loads. Together, these future research directions—human-subject validation and energy simulation integration—would bridge the gap between controlled experimental findings and real-world implementation, advancing the development of evidence-based, occupant-centered, and energy-efficient Personal Comfort System strategies.

Reference:

[1] Y. Tang, H. Yu, K. Zhang, K. Niu, H. Mao, and M. Luo, “Thermal comfort performance and energy-efficiency evaluation of six personal heating/cooling devices,” *Build. Environ.*, vol. 217, p. 109069, Jun. 2022, doi: 10.1016/j.buildenv.2022.109069.

[2] L. Pérez-Lombard, J. Ortiz, and C. Pout, “A review on buildings energy consumption information,” *Energy Build.*, vol. 40, no. 3, pp. 394–398, Jan. 2008, doi: 10.1016/J.ENBUILD.2007.03.007.

[3] P. O. Fanger, A. K. Melikov, H. Hanzawa, and J. Ring, “Air turbulence and sensation of draught,” *Energy Build.*, vol. 12, no. 1, pp. 21–39, Apr. 1988, doi: 10.1016/0378-7788(88)90053-9.

[4] “Developing an adaptive model of thermal comfort and preference.” Accessed: Mar. 09, 2026. [Online]. Available: https://escholarship.org/uc/item/4qq2p9c6

[5] J. F. Nicol and M. A. Humphreys, “Adaptive thermal comfort and sustainable thermal standards for buildings,” *Energy Build.*, vol. 34, no. 6, pp. 563–572, Jul. 2002, doi: 10.1016/S0378-7788(02)00006-3.

[6] M. Frontczak and P. Wargocki, “Literature survey on how different factors influence human comfort in indoor environments,” *Build. Environ.*, vol. 46, no. 4, pp. 922–937, Apr. 2011, doi: 10.1016/j.buildenv.2010.10.021.

[7] J. Kim and R. De Dear, “Workspace satisfaction: The privacy-communication trade-off in open-plan offices,” 2013, doi: 10.1016/j.jenvp.2013.06.007.

[8] E. Arens, M. A. Humphreys, R. de Dear, and H. Zhang, “Are ‘class A’ temperature requirements realistic or desirable?,” *Build. Environ.*, vol. 45, no. 1, pp. 4–10, Jan. 2010, doi: 10.1016/j.buildenv.2009.03.014.

[9] H. Zhang, E. Arens, and W. Pasut, “Air temperature thresholds for indoor comfort and perceived air quality,” *Build. Res. Inf.*, vol. 39, no. 2, pp. 134–144, Mar. 2011, doi: 10.1080/09613218.2011.552703.

[10] H. Zhang, E. Arens, and Y. Zhai, “A review of the corrective power of personal comfort systems in non-neutral ambient environments,” *Build. Environ.*, vol. 91, pp. 15–41, Sep. 2015, doi: 10.1016/j.buildenv.2015.03.013.

[11] W. Song, Z. Zhang, Z. Chen, F. Wang, and B. Yang, “Thermal comfort and energy performance of personal comfort systems (PCS): A systematic review and meta-analysis,” *Energy Build.*, vol. 256, p. 111747, Feb. 2022, doi: 10.1016/j.enbuild.2021.111747.

[12] A. K. Melikov, “Personalized ventilation,” *Indoor Air*, vol. 14, no. SUPPL. 7, pp. 157–167, 2004, doi: 10.1111/j.1600-0668.2004.00284.x.

[13] “(PDF) Moving air for comfort.” Accessed: Mar. 09, 2026. [Online]. Available: https://www.researchgate.net/publication/279556483_Moving_air_for_comfort

[14] H. Zhang, E. Arens, D. E. Kim, E. Buchberger, F. Bauman, and C. Huizenga, “Comfort, perceived air quality, and work performance in a low-power task–ambient conditioning system,” *Build. Environ.*, vol. 45, no. 1, pp. 29–39, Jan. 2010, doi: 10.1016/j.buildenv.2009.02.016.

[15] F. S. Bauman, P. G. Member ASHRAE Thomas Carter, P. V Anne Baughman Edward A Arens,

and S. Member ASHRAE Student Member ASHRAE Member ASHRAE, “Field Study of the Impact of a Desktop Task/Ambient Conditioning System in Office Buildings”.

[16] Y. Zhai, H. Zhang, Y. Zhang, W. Pasut, E. Arens, and Q. Meng, “Comfort under personally controlled air movement in warm and humid environments”, Accessed: Mar. 09, 2026. [Online]. Available: http://www.escholarship.org/uc/item/9s12q89q

[17] M. Luo, E. Arens, H. Zhang, A. Ghahramani, and Z. Wang, “Thermal comfort evaluated for combinations of energy-efficient personal heating and cooling devices,” *Build. Environ.*, vol. 143, pp. 206–216, Oct. 2018, doi: 10.1016/j.buildenv.2018.07.008.

[18] H. Zhang *et al.*, “Using footwarmers in offices for thermal comfort and energy savings,” *Energy Build.*, vol. 104, pp. 233–243, Jul. 2015, doi: 10.1016/j.enbuild.2015.06.086.

[19] T. Hoyt, E. Arens, and H. Zhang, “Extending air temperature setpoints: Simulated energy savings and design considerations for new and retrofit buildings,” *Build. Environ.*, vol. 88, pp. 89–96, Jun. 2015, doi: 10.1016/j.buildenv.2014.09.010.

[20] W. Yao, G. Zhu, Z. Yan, W. Tong, and D. Fan, “Revolutionizing personal thermal management technologies with advanced materials and strategies,” *Appl. Mater. Today*, vol. 44, p. 102719, Jun. 2025, doi: 10.1016/j.apmt.2025.102719.

[21] M. Cabanac, B. Massonnet, and R. Belaiche, “Preferred skin temperature as a function of internal and mean skin temperature,” *J. Appl. Physiol.*, vol. 33, no. 6, pp. 699–703, 1972, doi: 10.1152/jappl.1972.33.6.699.

[22] H. Hensel, “Thermal sensations and thermoreceptors in man,” p. 187, 1982.

[23] J. W. Ring and R. de Dear, “Temperature Transients: A Model for Heat Diffusion through the Skin, Thermoreceptor Response and Thermal Sensation,” *Indoor Air*, vol. 1, no. 4, pp. 448–456, Dec. 1991, doi: 10.1111/j.1600-0668.1991.00009.x.

[24] T. Parkinson and R. De Dear, “Thermal pleasure in built environments: Physiology of alliesthesia,” *Build. Res. Inf.*, vol. 43, no. 3, pp. 288–301, May 2015, doi: 10.1080/09613218.2015.989662.

[25] T. Parkinson, R. De Dear, and C. Candido, “Thermal pleasure in built environments: Alliesthesia in different thermoregulatory zones,” *Build. Res. Inf.*, vol. 44, no. 1, pp. 20–33, Jan. 2016, doi: 10.1080/09613218.2015.1059653.

[26] “Thermal comfort : analysis and applications in environmental engineering : Fanger, P. O : Free Download, Borrow, and Streaming : Internet Archive.” Accessed: Mar. 09, 2026. [Online]. Available: https://archive.org/details/thermalcomfortan0000fang/page/n5/mode/2up

[27] W. Raza, A. Berto, M. Tancon, L. Moro, and M. Azzolin, “Enhancing thermal comfort: a comprehensive review of wearable cooling systems,” *Next Mater.*, vol. 8, no. 5, p. 100762, Jul. 2025, doi: 10.1016/j.nxmate.2025.100762.

[28] Z. Wang *et al.*, “Evaluating the comfort of thermally dynamic wearable devices,” *Build. Environ.*, vol. 167, 2020, doi: 10.1016/j.buildenv.2019.106443.

[29] B. Yang, T. H. Lei, P. Yang, K. Liu, and F. Wang, “On the Use of Wearable Face and Neck Cooling Fans to Improve Occupant Thermal Comfort in Warm Indoor Environments,” *Energies 2021, Vol. 14, Page 8077*, vol. 14, no. 23, p. 8077, Dec. 2021, doi: 10.3390/en14238077.

[30] K. u. Mekrisuh, D. Singh, and Udayraj, “Development and experimental validation of a 3D numerical model to investigate performance of phase change based cooling vest in hot environments,” *Int. J. Therm. Sci.*, vol. 208, Feb. 2025, doi: 10.1016/j.ijthermalsci.2024.109487.

[31] E. Arens, H. Zhang, and C. Huizenga, “Partial- and whole-body thermal sensation and comfort—Part I: Uniform environmental conditions,” *J. Therm. Biol.*, vol. 31, no. 1–2, pp. 53–59, Jan. 2006, doi: 10.1016/j.jtherbio.2005.11.028.

[32] J. D. Cotter and N. A. S. Taylor, “The distribution of cutaneous sudomotor and alliesthesial thermosensitivity in mildly heat-stressed humans: an open-loop approach,” *J. Physiol.*, vol. 565, no. Pt 1, pp. 335–345, May 2005, doi: 10.1113/jphysiol.2004.081562.

[33] “Standard 55 – Thermal Environmental Conditions for Human Occupancy.” Accessed: Mar. 09, 2026. [Online]. Available: https://www.ashrae.org/technical-resources/bookstore/standard-55-thermal-environmental-conditions-for-human-occupancy

[34] “ISO 7730 (2005) Ergonomics of the Thermal Environment—Analytical Determination and Interpretation of Thermal Comfort Using Calculation of the PMV and PPD indices and Local Thermal Comfort Criteria International Organization for Standardization. - Referen….” Accessed: Mar. 09, 2026. [Online]. Available: https://www.scirp.org/reference/referencespapers?referenceid=1205534

[35] D. Fiala, G. Havenith, P. Bröde, B. Kampmann, and G. Jendritzky, “UTCI-Fiala multi-node model of human heat transfer and temperature regulation,” *Int. J. Biometeorol.*, vol. 56, no. 3, pp. 429–441, 2012, doi: 10.1007/s00484-011-0424-7.

[36] J. F. Nicol and M. A. Humphreys, “THERMAL COMFORT AS PART OF A SELF-REGULATING SYSTEM.,” *Build Res Pr.*, vol. 1, no. 3, pp. 174–179, 1973, doi: 10.1080/09613217308550237.

[37] “(PDF) Understanding the adaptive approach to thermal comfort.” Accessed: Mar. 09, 2026. [Online]. Available: https://www.researchgate.net/publication/279888246_Understanding_the_adaptive_approach_to_thermal_comfort

[38] B. W. Olesen and G. S. Brager, “A better way to predict comfort,” *ASHRAE J.*, vol. 46, no. 8, pp. 20–28, 2004.

[39] H. Zhang, “Human Thermal Sensation and Comfort in Transient and Non-Uniform Thermal Environments,” Sep. 01, 2003.

[40] H. Zhang, E. Arens, C. Huizenga, and T. Han, “Thermal sensation and comfort models for non-uniform and transient environments: Part I: Local sensation of individual body parts,” *Build. Environ.*, vol. 45, no. 2, pp. 380–388, Feb. 2010, doi: 10.1016/j.buildenv.2009.06.018.

[41] W. Pasut, H. Zhang, E. Arens, and Y. Zhai, “Energy-efficient comfort with a heated/cooled chair: Results from human subject tests,” *Build. Environ.*, vol. 84, pp. 10–21, Jan. 2015, doi: 10.1016/j.buildenv.2014.10.026.

[42] R. Rawal, M. Schweiker, O. B. Kazanci, V. Vardhan, Q. Jin, and L. Duanmu, “Personal Comfort Systems: A review on comfort, energy, and economics,” *Energy Build.*, vol. 214, p. 109858, May 2020, doi: 10.1016/j.enbuild.2020.109858.

[43] H. Wang, Z. Xu, B. Ge, and J. Li, “Experimental study on a phase change cooling garment to improve thermal comfort of factory workers,” *Build. Environ.*, vol. 227, p. 109819, Jan. 2023, doi: 10.1016/j.buildenv.2022.109819.

[44] X. L. Wang *et al.*, “Hybrid evaporative-fan cooling vest: multi-scale cooling performance evaluation,” *Energy Build.*, vol. 351, p. 116704, Jan. 2026, doi: 10.1016/j.enbuild.2025.116704.

[45] C. Hu, Z. Wang, R. Bo, C. Li, and X. Meng, “Effect of the cooling clothing integrating with phase change material on the thermal comfort of healthcare workers with personal protective equipment during the COVID-19,” *Case Stud. Therm. Eng.*, vol. 42, no. 9, p. 102725, Feb. 2023, doi: 10.1016/j.csite.2023.102725.

[46] C. Gao, K. Kuklane, F. Wang, and I. Holmér, “Personal cooling with phase change materials to improve thermal comfort from a heat wave perspective,” *Indoor Air*, vol. 22, no. 6, pp. 523–530, 2012, doi: 10.1111/j.1600-0668.2012.00778.x.

[47] E. Rahimi, A. Babapoor, G. Moradi, S. Kalantari, and M. Monazzam Esmaeelpour, “Personal cooling garments and phase change materials: A review,” *Renew. Sustain. Energy Rev.*, vol. 190, Feb. 2024, doi: 10.1016/j.rser.2023.114063.

[48] B. Liu, H. Wang, H. Lin, Y. Su, G. Wei, and Z. Xu, “Effect of phase change cooling vest on related thermal regulation factors in moderately hot environments,” *Build. Environ.*, vol. 242, p. 110566, Aug. 2023, doi: 10.1016/j.buildenv.2023.110566.

[49] W. Pasut, H. Zhang, E. Arens, S. Kaam, and Y. Zhai, “Effect of a heated and cooled office chair on thermal comfort,” *HVAC R Res.*, vol. 19, no. 5, pp. 574–583, Jul. 2013, doi: 10.1080/10789669.2013.781371.

[50] S. Shahzad, K. Calautit, S. Wei, P. W. Tien, J. Calautit, and B. Hughes, “Analysis of the thermal comfort and energy performance of a thermal chair for open plan office,” *J. Sustain. Dev. Energy, Water Environ. Syst.*, vol. 8, no. 2, pp. 373–395, 2020, doi: 10.13044/j.sdewes.d7.0298.

[51] H. Yang, B. Cao, and Y. Zhu, “Study on the effects of chair heating in cold indoor environments from the perspective of local thermal sensation,” *Energy Build.*, vol. 180, pp. 16–28, Dec. 2018, doi: 10.1016/j.enbuild.2018.09.003.

[52] J. Chao, S. Li, Z. Zhang, M. Wang, and W. Hou, “Differences in heating effects of three personalized heating devices under various indoor temperatures: Table heating pad, cushion heating pad and leg heating pad,” *Indoor Built Environ.*, vol. 33, no. 3, pp. 571–582, Mar. 2024, doi: 10.1177/1420326X231218365.

[53] Z. Vlaović, B. Iliev, and D. Domljan, “Assessments of Thermal Sensation While Sitting on Office Chairs of Different Seat and Backrest Designs,” *Appl. Sci. 2025, Vol. 15, Page 6127*, vol. 15, no. 11, p. 6127, May 2025, doi: 10.3390/app15116127.

[54] G. Yu, Z. Gu, Z. Yan, and H. Chen, “Investigation and comparison on thermal comfort and energy consumption of four personalized seat heating systems based on heated floor panels,” *Indoor Built Environ.*, vol. 30, no. 8, pp. 1252–1267, Oct. 2020, doi: 10.1177/1420326X20939145.

[55] Y. He *et al.*, “Creating alliesthesia in cool environments using personal comfort systems,” *Build. Environ.*, vol. 209, no. 4, p. 108642, Feb. 2022, doi: 10.1016/j.buildenv.2021.108642.

[56] W. Luo, R. Kramer, Y. de Kort, P. Rense, and W. van Marken Lichtenbelt, “The effects of a novel

personal comfort system on thermal comfort, physiology and perceived indoor environmental quality, and its health implications - Stimulating human thermoregulation without compromising thermal comfort," *Indoor Air*, vol. 32, no. 1, Jan. 2022, doi: 10.1111/ina.12951.

[57] S. Y. Qin, X. Cui, C. Yang, and L. W. Jin, "Thermal comfort analysis of radiant cooling panels with dedicated fresh-air system," *Indoor Built Environ.*, vol. 30, no. 10, pp. 1596–1608, Dec. 2021, doi: 10.1177/1420326X20961142.

[58] J. Miriel, L. Serres, and A. Trombe, "Radiant ceiling panel heating-cooling systems: Experimental and simulated study of the performances, thermal comfort and energy consumptions," *Appl. Therm. Eng.*, vol. 22, no. 16, pp. 1861–1873, Nov. 2002, doi: 10.1016/S1359-4311(02)00087-X.

[59] Z. Ma, D. Zhao, F. Wang, and R. Yang, "A novel thermal comfort and energy saving evaluation model for radiative cooling and heating textiles," *Energy Build.*, vol. 258, Mar. 2022, doi: 10.1016/j.enbuild.2022.111842.

[60] S. M. Hooshmand, H. Zhang, H. Javidanfar, Y. Zhai, and A. Wagner, "A review of local radiant heating systems and their effects on thermal comfort and sensation," *Energy Build.*, vol. 296, p. 113331, Oct. 2023, doi: 10.1016/j.enbuild.2023.113331.

[61] Udayraj, Z. Li, Y. Ke, F. Wang, and B. Yang, "A study of thermal comfort enhancement using three energy-efficient personalized heating strategies at two low indoor temperatures," *Build. Environ.*, vol. 143, pp. 1–14, Oct. 2018, doi: 10.1016/j.buildenv.2018.06.049.

[62] Y. He *et al.*, "Creating alliesthesia in cool environments using personal comfort systems," *Build. Environ.*, vol. 209, Dec. 2021, doi: 10.1016/j.buildenv.2021.108642.

[63] W. Su, B. Yang, B. Zhou, F. Wang, and A. Li, "A novel convection and radiation combined terminal device: Its impact on occupant thermal comfort and cognitive performance in winter indoor environments," *Energy Build.*, vol. 246, p. 111123, Sep. 2021, doi: 10.1016/j.enbuild.2021.111123.

[64] P. D. T. Arachchi Appuhamilage, H. B. Rijal, and S. Shahzad, "Localized thermal control for global impact: A meta-analytical review of thermal comfort and energy performance of personal comfort systems," *Appl. Energy*, vol. 403, Jan. 2026, doi: 10.1016/j.apenergy.2025.127051.

[65] Z. Lei, "Review of application of thermal manikin in evaluation on thermal and moisture comfort of clothing," *J. Eng. Fiber. Fabr.*, vol. 14, Apr. 2019, doi: 10.1177/1558925019841548.

[66] T. . T. Y. Fukazawa, T. Fukazawa, and Y. Tochihara, "The Thermal Manikin; a Useful and Effective Device for Evaluating Human Thermal Environments," *J. Human-Environment Syst.*, vol. 18, no. 1, pp. 021–028, Jan. 2015, doi: 10.1618/jhes.18.021.

[67] A. Psikuta *et al.*, "Thermal manikins controlled by human thermoregulation models for energy efficiency and thermal comfort research – A review," *Renew. Sustain. Energy Rev.*, vol. 78, pp. 1315–1330, 2017, doi: 10.1016/j.rser.2017.04.115.

[68] I. Simova, R. A. Angelova, D. Markov, R. Velichkova, and P. Stankov, "Thermal Manikins-General Features and Applications," *Proc. 2021 6th Int. Symp. Environ. Energies Appl. EFEA 2021*, Mar. 2021, doi: 10.1109/EFEA49713.2021.9406231.

[69] I. Holmér, "Thermal manikin history and applications," *Eur. J. Appl. Physiol.*, vol. 92, no. 6, pp. 614–618, Sep. 2004, doi: 10.1007/s00421-004-1135-0.

[70] E. Paredes Barros *et al.*, “User-centric electrical vehicle thermal conditioning strategy based on close comfort elements in cold environment: Thermal manikin and human participants assessment,” *Case Stud. Therm. Eng.*, vol. 64, no. 6, p. 105435, Dec. 2024, doi: 10.1016/j.csite.2024.105435.

[71] K. W. D. Cheong, W. J. Yu, R. Kosonen, K. W. Tham, and S. C. Sekhar, “Assessment of thermal environment using a thermal manikin in a field environment chamber served by displacement ventilation system,” *Build. Environ.*, vol. 41, no. 12, pp. 1661–1670, Dec. 2006, doi: 10.1016/j.buildenv.2005.06.018.

[72] D. D. Ion-guţă *et al.*, “Advanced Thermal Manikin for Thermal Comfort Assessment in Vehicles and Buildings,” *Appl. Sci. 2022, Vol. 12, Page 1826*, vol. 12, no. 4, p. 1826, Feb. 2022, doi: 10.3390/app12041826.

[73] M. R. Georgescu, A. Cernei, I. Nastase, P. Danca, D. Guta, and I. Ursu, “Development and Use of a New Architecture of Thermal Manikin for Assessing Local Thermal Comfort,” *2023 11th Int. Conf. ENERGY Environ. CIEM 2023*, 2023, doi: 10.1109/CIEM58573.2023.10349780.

[74] Z. El akili, Y. Bouzidi, A. Merabtine, G. Polidori, and J. Kauffmann, “Assessment of thermal comfort of frail people in a sitting posture under non-uniform conditions using a thermal manikin,” *Build. Environ.*, vol. 221, Aug. 2022, doi: 10.1016/j.buildenv.2022.109334.

[75] A. Tanabe *et al.*, “UC Berkeley Indoor Environmental Quality (IEQ) Title Evaluating thermal environments by using a thermal manikin with controlled skin surface temperature Permalink https://escholarship.org/uc/item/22k424vp Publication Date EVALUATING THERMAL ENVIRONMENTS …,” 1994, Accessed: Mar. 09, 2026. [Online]. Available: www.ashrae.org

[76] “Temperature And Human Life by Winslow, C.-E. A., And L. P. Herrington: Very Good Hardcover (1949) 1st Edition | Arroyo Seco Books, Pasadena, Member IOBA.” Accessed: Mar. 09, 2026. [Online]. Available: https://www.abebooks.com/first-edition/Temperature-Human-Life-Winslow-C.-E-Herrington/22316289795/bd

[77] J. Fan and Y. S. Chen, “Measurement of clothing thermal insulation and moisture vapour resistance using a novel perspiring fabric thermal manikin,” *Meas. Sci. Technol.*, vol. 13, no. 7, pp. 1115–1123, Jan. 2002, doi: 10.1088/0957-0233/13/7/320.

[78] D. Tama and M. J. Abreu, “Evaluating the thermal comfort properties of Rize’s traditional hemp fabric (Feretiko) using a thermal manikin Selection and peer-review under responsibility of the scientific committee of the 4th International Con-ference on Natural Fibers-Smart Sustain…,” 2019, doi: 10.1016/j.matpr.2019.10.063.

[79] E. Foda and K. Sirén, “Evaluating the thermal comfort performance of heating systems using a thermal manikin with human thermoregulatory control,” *Indoor Built Environ.*, vol. 25, no. 1, pp. 191–202, Feb. 2016, doi: 10.1177/1420326X14541822.

[80] J. Pokorný, B. Kopečková, J. Fišer, and M. JÍcha, “Simulator with integrated HW and SW for prediction of thermal comfort to provide feedback to the climate control system,” *EPJ Web Conf.*, vol. 180, p. 02085, 2018, doi: 10.1051/epjconf/201818002085.

[81] R. Vilain, M. L. Pereira, V. Felix, and A. Tribess, “Thermal comfort and local discomfort in an operating room ventilated with spiral diffuser jet,” *HVAC R Res.*, vol. 19, no. 8, pp. 1016–1022, Nov. 2013, doi: 10.1080/10789669.2013.838438.

[82] H. O. Nilsson and I. Holmér, “Comfort climate evaluation with thermal manikin methods and computer simulation models,” *Indoor Air*, vol. 13, no. 1, pp. 28–37, 2003, doi: 10.1034/j.1600-0668.2003.01113.x.

[83] “Test Method for Measuring the Evaporative Resistance of Clothing Using a Sweating Manikin,” Jul. 2022, doi: 10.1520/F2370-22.

[84] F. ; Wang *et al.*, “CLOTHING REAL EVAPORATIVE RESISTANCE DETERMINED BY MEANS OF A SWEATING THERMAL MANIKIN: A NEW ROUND-ROBIN STUDY,” vol. 1, 2014.

[85] “(PDF) A database of static clothing thermal insulation and vapor permeability values of non-Western ensembles for use in ASHRAE Standard 55, ISO 7730, and ISO 9920.” Accessed: Mar. 09, 2026. [Online]. Available: https://www.researchgate.net/publication/282954979_A_database_of_static_clothing_thermal_insulation_and_vapor_permeability_values_of_non-Western_ensembles_for_use_in_ASHRAE_Standard_55_ISO_7730_and_ISO_9920

[86] I. Holmer and S. Elnas, “Physiological evaluation of the resistance to evaporative heat transfer by clothing,” *Ergonomics*, vol. 24, no. 1, pp. 63–74, 1981, doi: 10.1080/00140138108924831.

[87] A. Psikuta, L. C. Wang, and R. M. Rossi, “Prediction of the physiological response of humans wearing protective clothing using a thermophysiological human simulator,” *J. Occup. Environ. Hyg.*, vol. 10, no. 4, pp. 222–232, Apr. 2013, doi: 10.1080/15459624.2013.766562.

[88] F. Wang, “Measurements of clothing evaporative resistance using a sweating thermal manikin: an overview,” *Ind. Health*, vol. 55, no. 6, p. 473, 2017, doi: 10.2486/indhealth.2017-0052.

[89] “Thermal Manikins for Precise Thermal Testing | P.T. - read more.” Accessed: Mar. 09, 2026. [Online]. Available: https://pt-teknik.dk/thermal-manikins/

[90] S. ; Li *et al.*, “Study on the Performance of Personal Heating in Extremely Cold Environments Using a Thermal Manikin,” *Build. 2023, Vol. 13, Page 362*, vol. 13, no. 2, p. 362, Jan. 2023, doi: 10.3390/buildings13020362.

[91] A. Psikuta, K. Kuklane, A. Bogdan, G. Havenith, S. Annaheim, and R. M. Rossi, “Opportunities and constraints of presently used thermal manikins for thermo-physiological simulation of the human body,” *Int. J. Biometeorol.*, vol. 60, no. 3, pp. 435–446, Mar. 2016, doi: 10.1007/s00484-015-1041-7.

[92] J. P. Rugh *et al.*, “Predicting human thermal comfort in a transient nonuniform thermal environment,” *Eur. J. Appl. Physiol.*, vol. 92, no. 6, pp. 721–727, Sep. 2004, doi: 10.1007/s00421-004-1125-2.

[93] J. Yang, W. Weng, and M. Fu, “Coupling of a Thermal Sweating Manikin and a Thermal Model for Simulating Human Thermal Response,” *Procedia Eng.*, vol. 84, no. 4, pp. 893–897, Jan. 2014, doi: 10.1016/j.proeng.2014.10.512.

[94] C. Huizenga, Z. Hui, and E. Arens, “A model of human physiology and comfort for assessing complex thermal environments,” *Build. Environ.*, vol. 36, no. 6, pp. 691–699, Jul. 2001, doi: 10.1016/S0360-1323(00)00061-5.

[95] D. Fiala, K. J. Lomas, and M. Stohrer, “Computer prediction of human thermoregulatory and

temperature responses to a wide range of environmental conditions," *Int. J. Biometeorol.*, vol. 45, no. 3, pp. 143–159, Sep. 2001, doi: 10.1007/s004840100099.

[96] S. I. Tanabe, K. Kobayashi, J. Nakano, Y. Ozeki, and M. Konishi, "Evaluation of thermal comfort using combined multi-node thermoregulation (65MN) and radiation models and computational fluid dynamics (CFD)," *Energy Build.*, vol. 34, no. 6, pp. 637–646, Jul. 2002, doi: 10.1016/S0378-7788(02)00014-2.

[97] "Newton Thermal Manikin System | Manikins | ThermetricsThermal Manikin - Newton - Thermetrics." Accessed: Mar. 09, 2026. [Online]. Available: https://thermetrics.com/products/manikin/newton-thermal-manikin/

[98] M. G. M. Richards and N. G. Mattle, "Defense Technical Information Center Compilation Part Notice ADP012411 TITLE: A Sweating Agile Thermal Manikin [SAM] Developed to Test Complete Clothing Systems Under Normal and Extreme Conditions TITLE: Blowing Hot and Cold: Protecting Against Climatic …".

[99] E. Foda and K. Sirén, "A new approach using the Pierce two-node model for different body parts," *Int. J. Biometeorol.*, vol. 55, no. 4, pp. 519–532, Jul. 2011, doi: 10.1007/s00484-010-0375-4.

[100] E. Foda and K. Sirén, "A thermal manikin with human thermoregulatory control: implementation and validation," *Int. J. Biometeorol.*, vol. 56, no. 5, pp. 959–971, Sep. 2012, doi: 10.1007/s00484-011-0506-6.

[101] "an-effective-temperature-scale-based-on-a-simple-model-of-3pdn3o8nxv.pdf."

[102] J. Shinoda, M. P. Bivolarova, C. Bidstrup, T. Hvitved, and J. Toftum, "Development and application of a thermoregulatory control for a thermal manikin: A comparative study of the thermal response of young and elderly individuals," *Energy Build.*, vol. 328, p. 115110, Feb. 2025, doi: 10.1016/j.enbuild.2024.115110.

[103] Y. Takahashi *et al.*, "Thermoregulation model JOS-3 with new open source code," *Energy Build.*, vol. 231, no. 6, p. 110575, Jan. 2021, doi: 10.1016/j.enbuild.2020.110575.

[104] M. Ivanov and S. Mijorski, "CFD Modelling of Flow Interaction in the Breathing Zone of a Virtual Thermal Manikin," *Energy Procedia*, vol. 112, pp. 240–251, Mar. 2017, doi: 10.1016/j.egypro.2017.03.1093.

[105] N. P. Gao, H. Zhang, and J. L. Niu, "Investigating indoor air quality and thermal comfort using a numerical thermal manikin," *Indoor Built Environ.*, vol. 16, no. 1, pp. 7–17, Feb. 2007, doi: 10.1177/1420326X06074667.

[106] J. A. J. Stolwijk and J. B. Pierce, "A MATHEMATICAL MODEL OF PHYSIOLOGICAL TEMPERATURE REGULATION IN MAN 4. Title and Subtitle A MATKElrlATICALp MODEL OF PHYSIOLQGICAL "F'ERATUHE IGGULATION I N b@. N 7. Author(sJ 13. Type of Report and Period Covered 14. Sponsoring Agency Code".

[107] S. T., X. L., O. K., and T. S.I., "Development of human thermoregulation model JOS applicable to different types of human body, sex and age," 2003. Accessed: Mar. 09, 2026. [Online]. Available: https://www.aivc.org/resource/development-human-thermoregulation-model-jos-applicable-different-types-human-body-sex-and

[108] Y. Kobayashi and S. I. Tanabe, "Development of JOS-2 human thermoregulation model with

detailed vascular system," *Build. Environ.*, vol. 66, pp. 1–10, Aug. 2013, doi: 10.1016/j.buildenv.2013.04.013.

[109] "Welcome to Python.org." Accessed: Mar. 09, 2026. [Online]. Available: https://www.python.org/

[110] R. Rissetto, M. Schweiker, and A. Wagner, "Personalized ceiling fans: Effects of air motion, air direction and personal control on thermal comfort," *Energy Build.*, vol. 235, p. 110721, Mar. 2021, doi: 10.1016/j.enbuild.2021.110721.

[111] R. Rissetto and M. Schweiker, "Exploring Information and Comfort Expectations Related to the Use of a Personal Ceiling Fan," *Build. 2024, Vol. 14, Page 262*, vol. 14, no. 1, p. 262, Jan. 2024, doi: 10.3390/buildings14010262.

[112] A. Lipczynska, S. Schiavon, and L. T. Graham, "Thermal comfort and self-reported productivity in an office with ceiling fans in the tropics," *Build. Environ.*, vol. 135, pp. 202–212, May 2018, doi: 10.1016/j.buildenv.2018.03.013.

[113] S. W. Hsiao, H. H. Lin, and C. H. Lo, "A study of thermal comfort enhancement by the optimization of airflow induced by a ceiling fan," *J. Interdiscip. Math.*, vol. 19, no. 4, pp. 859–891, Jul. 2016, doi: 10.1080/09720502.2016.1225935.

[114] Y. Zhai, Y. Zhang, H. Zhang, W. Pasut, E. Arens, and Q. Meng, "Human comfort and perceived air quality in warm and humid environments with ceiling fans," *Build. Environ.*, vol. 90, pp. 178–185, Aug. 2015, doi: 10.1016/j.buildenv.2015.04.003.

[115] M. Luo *et al.*, "Ceiling-fan-integrated air-conditioning: thermal comfort evaluations," *Build. Cities*, vol. 2, no. 1, pp. 928–951, 2021, doi: 10.5334/bc.137.

[116] W. Chen *et al.*, "Ceiling-fan-integrated air conditioning: Airflow and temperature characteristics of a sidewall-supply jet interacting with a ceiling fan," *Build. Environ.*, vol. 171, Mar. 2020, doi: 10.1016/j.buildenv.2020.106660.

[117] H. Wang, G. Wang, and X. Li, "Implementation of demand-oriented ventilation with adjustable fan network," *Indoor Built Environ.*, vol. 29, no. 4, pp. 621–635, Apr. 2020, doi: 10.1177/1420326X19897114.

[118] Y. Zhai, E. Arens, K. Elsworth, and H. Zhang, "Selecting air speeds for cooling at sedentary and non-sedentary office activity levels," *Build. Environ.*, vol. 122, pp. 247–257, Sep. 2017, doi: 10.1016/j.buildenv.2017.06.027.

[119] S. H. Mun, Y. Kwak, Y. Kim, and J. H. Huh, "A Comprehensive Thermal Comfort Analysis of the Cooling Effect of the Stand Fan Using Questionnaires and a Thermal Manikin," *Sustain. 2019, Vol. 11, Page 5091*, vol. 11, no. 18, p. 5091, Sep. 2019, doi: 10.3390/su11185091.

[120] M. S. Ali *et al.*, "Design and Performance Evaluation of a Novel Portable Pedestal Fan With Cooling Effects by Peltier Modules," *Int. J. Energy Res.*, vol. 2025, no. 1, p. 6044104, Jan. 2025, doi: 10.1155/er/6044104.

[121] B. Yang, S. Schiavon, C. Sekhar, D. Cheong, K. W. Tham, and W. W. Nazaroff, "Cooling efficiency of a brushless direct current stand fan," *Build. Environ.*, vol. 85, pp. 196–204, Feb. 2015, doi: 10.1016/j.buildenv.2014.11.032.

[122] Y.-J. Kim, J.-E. Yeo, S.-H. Mun, and J.-H. Huh, "Thermal Comfort Evaluation of Local Air Stream by a Stand Fan in Summer," *J. Archit. Inst. Korea Plan. Des.*, vol. 32, no. 8, pp. 141–148,

Aug. 2016, doi: 10.5659/jaik_pd.2016.32.8.141.

[123] A. K. Melikov, T. Sakoi, S. Kolencíková, and N. Tominaga, “Impact of Air Movement on Eye Symptoms,” 2013. Accessed: Mar. 09, 2026. [Online]. Available: https://orbit.dtu.dk/en/publications/impact-of-air-movement-on-eye-symptoms/

[124] J. Lyu, Y. Shi, H. Du, and Z. Lian, “Sex-based thermal comfort zones and energy savings in spaces with joint operation of air conditioner and fan,” *Build. Environ.*, vol. 246, Dec. 2023, doi: 10.1016/j.buildenv.2023.111002.

[125] M. González-Torres, L. Pérez-Lombard, J. F. Coronel, I. R. Maestre, and D. Yan, “Energy savings and thermal comfort in a zero energy office building with fans in Singapore,” *Build. Environ.*, vol. 243, p. 110674, Sep. 2023, doi: 10.1016/j.egyr.2021.11.280.

[126] M. André, S. Schiavon, and R. Lamberts, “Implementation of desk fans in open office: Lessons learned and guidelines from a field study,” *Build. Environ.*, vol. 259, p. 111681, Jul. 2024, doi: 10.1016/j.buildenv.2024.111681.

[127] S. Norouziasl, M. S. Islam, A. Jafari, A. Bhattacharya, and Y. Zhu, “Optimizing and predicting occupant thermal comfort in indoor office environment: The role of desk fan air velocity,” *Build. Environ.*, vol. 282, p. 113241, Aug. 2025, doi: 10.1016/j.buildenv.2025.113241.

[128] F. A. Ilmiawan, S. A. Zaki, M. K. Singh, and W. Khalid, “Effect of preferable wind directions on personal thermal comfort of occupants in the air-conditioned office in hot-humid climate,” *Build. Environ.*, vol. 254, p. 111390, Apr. 2024, doi: 10.1016/j.buildenv.2024.111390.

[129] “383311 @ redi.cedia.edu.ec.” [Online]. Available: https://redi.cedia.edu.ec/document/383311

[130] Y. He, W. Chen, Z. Wang, and H. Zhang, “Review of fan-use rates in field studies and their effects on thermal comfort, energy conservation, and human productivity,” *Energy Build.*, vol. 194, pp. 140–162, Jul. 2019, doi: 10.1016/j.enbuild.2019.04.015.

[131] Udayraj, Z. Li, Y. Ke, F. Wang, and B. Yang, “Personal cooling strategies to improve thermal comfort in warm indoor environments: Comparison of a conventional desk fan and air ventilation clothing,” *Energy Build.*, vol. 174, pp. 439–451, Sep. 2018, doi: 10.1016/j.enbuild.2018.06.065.

[132] Y. He, N. Li, X. Wang, M. He, and D. He, “Comfort, Energy Efficiency and Adoption of Personal Cooling Systems in Warm Environments: A Field Experimental Study,” *Int. J. Environ. Res. Public Heal. 2017, Vol. 14, Page 1408*, vol. 14, no. 11, p. 1408, Nov. 2017, doi: 10.3390/ijerph14111408.

[133] M. He, N. Li, Y. He, D. He, and C. Song, “The influence of personally controlled desk fan on comfort and energy consumption in hot and humid environments,” *Build. Environ.*, vol. 123, pp. 378–389, Oct. 2017, doi: 10.1016/j.buildenv.2017.07.021.

[134] M. A. Belyamani *et al.*, “Local wearable cooling may improve thermal comfort, emotion, and cognition,” *Build. Environ.*, vol. 254, p. 111367, Apr. 2024, doi: 10.1016/j.buildenv.2024.111367.

[135] Y. Su, E. O’Donnell, S. P. Hoekstra, and C. A. Leicht, “Facial cooling improves thermal perceptions and maintains the interleukin-6 response during passive heating: A sex comparison,” *Temp. (Austin, Tex.)*, vol. 12, no. 1, pp. 40–54, 2024, doi: 10.1080/23328940.2024.2406730.

[136] J. Wang, S. Yu, G. Yang, J. Kang, and S. Yang, “Study on head and neck local cooling for thermal comfort in high-temperature mining environments,” *Case Stud. Therm. Eng.*, vol. 75, p. 107029,

Nov. 2025, doi: 10.1016/j.csite.2025.107029.

[137] F. Wang, Y. Tang, Y. Ke, Q. Zheng, and T. H. Lei, "Ice slurry ingestion for enhanced occupant thermal comfort in warm/hot indoor environments: A comparative study with an energy-efficient desk fan," *Build. Environ.*, vol. 253, p. 111350, Apr. 2024, doi: 10.1016/j.buildenv.2024.111350.

[138] P. Wegertseder-Martinez, I. Berges-Alvarez, and B. Piderit-Moreno, "Evaluation of Synchronous Use of Portable Personal Comfort and Environment Conditioning Systems in Real Office Occupancy Conditions," *Build. 2024, Vol. 14, Page 1820*, vol. 14, no. 6, p. 1820, Jun. 2024, doi: 10.3390/buildings14061820.

[139] S. Lu and E. Cochran Hameen, "An Interactive Task Conditioning System Featuring Personal Comfort Models and Non-Intrusive Sensing Techniques: A Field Study in Shanghai," *Technol. 2021, Vol. 9, Page 90*, vol. 9, no. 4, p. 90, Nov. 2021, doi: 10.3390/technologies9040090.

[140] L. Yu, Z. Xu, T. Zhang, X. Guan, and D. Yue, "Energy-efficient personalized thermal comfort control in office buildings based on multi-agent deep reinforcement learning," *Build. Environ.*, vol. 223, p. 109458, Sep. 2022, doi: 10.1016/j.buildenv.2022.109458.

[141] S. Schiavon, A. Krikor Melikov, and S. Member ASHRAE Fellow ASHRAE, "Introduction of a Cooling-Fan Efficiency Index," vol. 15, no. 6, 2009, Accessed: Mar. 09, 2026. [Online]. Available: www.ashrae.org

[142] A. ; Simone and B. W. Olesen, "Preferred Air Velocity and Local Cooling Effect of desk fans in warm environments," 2013.

[143] K. W. Tham and J. Pantelic, "Performance evaluation of the coupling of a desktop personalized ventilation air terminal device and desk mounted fans," *Build. Environ.*, vol. 45, no. 9, pp. 1941–1950, 2010, doi: 10.1016/j.buildenv.2010.01.019.

[144] H. Alsaad and C. Voelker, "Performance evaluation of ductless personalized ventilation in comparison with desk fans using numerical simulations," *Indoor Air*, vol. 30, no. 4, pp. 776–789, 2020, doi: 10.1111/ina.12672.

[145] S. H. Mun, Y. J. Kim, and J. H. Huh, "Analysis on the actual cooling effect of the standing fan: A comparative study of heat loss and thermal comfort for body segments," *Build. Simul. Conf. Proc.*, vol. 3, pp. 1655–1660, 2017, doi: 10.26868/25222708.2017.145.

[146] K. Miura, K. Takagi, and K. Ikematsu, "Evaluation of two cooling devices for construction workers by a thermal manikin," *Fash. Text.*, vol. 4, no. 1, 2017, doi: 10.1186/s40691-017-0108-y.

[147] D. J. Fannon, "Developing low-energy personal thermal comfort systems: design, performance, testing, and research methods," *Cent. Built Environ. UC Berkeley*, 2015, [Online]. Available: http://www.tandfonline.com/doi/abs/10.1080/09613218.2011.556008

[148] M. Kong, T. Q. Dang, J. Zhang, and H. E. Khalifa, "Micro-environmental control for efficient local cooling," *Build. Environ.*, vol. 118, pp. 300–312, 2017, doi: 10.1016/j.buildenv.2017.03.040.

[149] T. Han, L. Huang, S. Kelly, C. Huizenga, and Z. Hui, "Virtual thermal comfort engineering," *SAE Tech. Pap.*, 2001, doi: 10.4271/2001-01-0588.

[150] "Equivalent Temperature," Oct. 2001, doi: 10.4271/J2234_200110.

[151] D. P. Wyon, S. Larsson, B. Forsgren, and I. Lundgren, "Standard Procedures for Assessing

Vehicle Climate with a Thermal Manikin," *SAE Tech. Pap.*, Feb. 1989, doi: 10.4271/890049.

[152] N. DiFonzo and P. Bordia, "Reproduced with permission of the copyright owner . Further reproduction prohibited without," *J. Allergy Clin. Immunol.*, vol. 130, no. 2, p. 556, 1998, [Online]. Available: http://dx.doi.org/10.1016/j.jaci.2012.05.050

[153] M. Hepokoski, A. Curran, S. Gullman, and D. Jacobsson, "Coupling a Passive Sensor Manikin with a Human Thermal Comfort Model to Predict Human Perception in Transient and Asymmetric Environments," *SAE Int. J. Passeng. Cars - Mech. Syst.*, vol. 10, no. 1, pp. 135–140, 2017, doi: 10.4271/2017-01-0178.

[154] E. Barna and L. Bánhidi, "Combined effect of two local discomfort parameters studied with a thermal manikin and human subjects," *Energy Build.*, vol. 51, pp. 234–241, 2012, doi: 10.1016/j.enbuild.2012.05.015.

[155] M. Veselý, P. Molenaar, M. Vos, R. Li, and W. Zeiler, "Personalized heating – Comparison of heaters and control modes," *Build. Environ.*, vol. 112, pp. 223–232, 2017, doi: 10.1016/j.buildenv.2016.11.036.

[156] Y. He, N. Li, L. Zhou, K. Wang, and W. Zhang, "Thermal comfort and energy consumption in cold environment with retrofitted Huotong (warm-barrel)," *Build. Environ.*, vol. 112, pp. 285–295, 2017, doi: 10.1016/j.buildenv.2016.11.044.

[157] L. Huang, Q. Ouyang, Y. Zhu, and L. Jiang, "A study about the demand for air movement in warm environment," *Build. Environ.*, vol. 61, pp. 27–33, 2013, doi: 10.1016/j.buildenv.2012.12.002.

[158] "Rowenta Turbo Silence Extreme+ Mechanical Oscillating Table/Desk Fan, 4-Speed | Canadian Tire." Accessed: Mar. 09, 2026. [Online]. Available: https://www.canadiantire.ca/en/pdp/rowenta-turbo-silence-extreme-mechanical-oscillating-table-desk-fan-4-speed-1430042p.html#nl-product-details

[159] "Koonie F491." Accessed: Mar. 09, 2026. [Online]. Available: https://device.report/koonie/f491

[160] "ULTTY Bladeless Fan Air Purifier R21 White US Edition." Accessed: Mar. 09, 2026. [Online]. Available: https://u-ultty.com/products/r21-white-us?srsltid=AfmBOoqKq8ms0BZynjMJODfrU9aiRZ4kViX-W-tjYUGSFtgQU9GYKxpJ

[161] "JISULIFE Portable Neck Fan, Hands Free Bladeless Hanging Sport Fan, 4000 mAh Battery Operated Wearable Personal Fan, Leafless, Rechargeable, Headphone Design, USB Powered,5 Speeds-Dark Green : Amazon.ca: Home." Accessed: Mar. 09, 2026. [Online]. Available: https://www.amazon.ca/Portable-Bladeless-Operated-Rechargeable-Headphone/dp/B08911JGGW/ref=sr_1_1_sspa?crid=2EUZV4BO2MZIE&dib=eyJ2IjoiMSJ9.stYzfViw9XkKIwLchImPipPOS5EHpT6sNpVVVT7O8Xsrsz0uvlqkUgK2fvtSd1xRA1GtZLo5M5-W-DK7i7qA7UIU6Mm21JuLKoqOhOTVykxAIrbIsGu6f9yVAe1TVT6EykDlwss7U4fOWqpS5fr-q0Er3gaC1jRQ9Or5_ZtZc-R1CftTMSXjr2iMDoV4ALEBit4EgsZUyNUjwvgY5G7nyqrFDkaTTlOF-WvLEIkzyxU.E_70Qaugd77zJvE4CzhZYWJmn_fAEISfAdd6TitzDT4&dib_tag=se&keywords=neck%2Bfan&qid=1773077067&s=kitchen&sprefix=neck%2Bfan%2Ckitchen%2C181&sr=1-1-spons&sp_csd=d2lkZ2V0TmFtZT1zcF9hdGY&th=1

APPENDICES

Appendix A:

A1: Whole-body physiological metrics for configuration_C1

C1_Deskfan_towards chest (Ta: 25±1°)						
Speed	Trial	Date	Tsk (°C)	P(W/m²)	Teq (°C)	PMV
0	1	26-Jul	34.8	46.4	28.3	1.1
	2	27-Jul	34.9	43.9	28.7	1.2
	3	29-Jul	34.8	46	28.3	1.1
	4	3-Aug	34.8	46.1	28.5	1.1
Average			**34.83**	**45.60**	**28.45**	**1.13**
StDev			**0.05**	**1.15**	**0.19**	**0.05**
Low	1	26-Jul	34.5	63	25.7	0.3
	2	27-Jul	34.6	60.5	26.2	0.4
	3	29-Jul	34.5	63.4	25.7	0.3
	4	3-Aug	34.6	63.5	25.8	0.3
Average			**34.55**	**62.60**	**25.85**	**0.33**
StDev			**0.06**	**1.42**	**0.24**	**0.05**
Medium	1	26-Jul	34.3	65.5	24.8	0
	2	27-Jul	34.5	65.9	25.3	0.1
	3	29-Jul	34.4	69.4	24.7	0
	4	3-Aug	34.4	69.1	24.9	0
Average			**34.40**	**67.48**	**24.93**	**0.03**
StDev			**0.08**	**2.06**	**0.26**	**0.05**
High	1	26-Jul	34.2	73	24	-0.2
	2	27-Jul	34.2	73.3	24.1	-0.2
	3	29-Jul	34.2	74.8	23.8	-0.3
	4	3-Aug	34.3	73.9	24.1	-0.2
Average			**34.23**	**73.75**	**24.00**	**-0.23**
StDev			**0.05**	**0.79**	**0.14**	**0.05**

A2: Whole-body physiological metrics for configuration_C2

C2_Deskfan_Angular towards chest (Ta: 25±1°)						
Speed	Trial	Date	Tsk (°C)	P(W/m²)	Teq (°C)	PMV
0	1	26-Jul	34.8	45.8	28.5	1.1
	2	27-Jul	34.8	45.6	28.4	1.1
	3	3-Aug	34.8	46.7	28.4	1.1
	4	5-Aug	34.8	47.1	28.3	1.1
Average			**34.80**	**46.30**	**28.40**	**1.10**
StDev			**0.00**	**0.72**	**0.08**	**0.00**
Low	1	26-Jul	34.6	61.6	26	0.4
	2	27-Jul	34.6	61.6	26.1	0.4
	3	3-Aug	34.6	63.7	25.7	0.3
	4	5-Aug	34.6	62.1	26	0.3
Average			**34.60**	**62.25**	**25.95**	**0.35**
StDev			**0.00**	**0.99**	**0.17**	**0.06**
Medium	1	26-Jul	34.5	63.2	25.6	0.2
	2	27-Jul	34.5	69.1	25.2	0.1
	3	3-Aug	34.4	70.6	24.8	0
	4	5-Aug	34.5	67.5	25.1	0.1
Average			**34.48**	**67.60**	**25.18**	**0.10**
StDev			**0.05**	**3.19**	**0.33**	**0.08**
High	1	26-Jul	34.3	73	24.2	-0.2
	2	27-Jul	34.3	73.3	24.2	-0.2
	3	3-Aug	34.3	74.1	23.9	-0.3
	4	5-Aug	34.3	72.4	24.1	-0.2
Average			**34.30**	**73.20**	**24.10**	**-0.23**
StDev			**0.00**	**0.71**	**0.14**	**0.05**

A3: Whole-body physiological metrics for configuration_C3

C3_USB powered (2)_desk_Angular towards chest (Ta: 25±1°)						
Speed	Trial	Date	Tsk (°C)	P(W/m²)	Teq (°C)	PMV
0	1	21-Jul	34.8	46.5	28.4	1.1
	2	22-Jul	34.8	46.4	28.3	1.1
	3	23-Jul	34.8	45.9	28.4	1.1
	4	25-Jul	34.8	46.7	28.3	1.1
Average			**34.80**	**46.38**	**28.35**	**1.10**
Std Dev			**0.00**	**0.34**	**0.06**	**0.00**
Low	1	21-Jul	34.6	59.3	26.4	0.5
	2	22-Jul	34.6	57.2	26.6	0.5
	3	23-Jul	34.6	59	26.5	0.5
	4	25-Jul	34.7	54.4	26.6	0.5
Average			**34.63**	**57.48**	**26.53**	**0.50**
Std Dev			**0.05**	**2.25**	**0.10**	**0.00**
Medium	1	21-Jul	34.5	62.4	25.9	0.3
	2	22-Jul	34.6	61.4	26.1	0.4
	3	23-Jul	34.6	63.5	26	0.3
	4	25-Jul	34.6	62.4	26	0.4
Average			**34.58**	**62.43**	**26.00**	**0.35**
Std Dev			**0.05**	**0.86**	**0.08**	**0.06**
High	1	21-Jul	34.5	66.3	25.3	0.1
	2	22-Jul	34.5	68.4	25	0.1
	3	23-Jul	34.5	66.4	25.2	0.1
	4	25-Jul	34.5	64.6	25.5	0.2
Average			**34.5**	**66.425**	**25.25**	**0.125**
Std Dev			**0.00**	**1.55**	**0.21**	**0.05**

A4: Whole-body physiological metrics for configuration_C4

C4_Bladeless_desk_towards chest (Ta: 25±1°)						
Speed	Trial	Date	Tsk (°C)	P(W/m²)	Teq (°C)	PMV
0	1	21-Jul	34.8	46.6	28.3	1.1
	2	24-Jul	34.8	47.2	28.3	1.1
	3	25-Jul	34.8	45.9	28.3	1.1
	4	29-Aug	34.8	47	28.3	1.1
Average			**34.80**	**46.68**	**28.30**	**1.10**
Std Dev			**0.00**	**0.57**	**0.00**	**0.00**
Low	1	21-Jul	34.7	57.3	26.8	0.6
	2	24-Jul	34.7	56.2	26.7	0.6
	3	25-Jul	34.7	57.1	26.9	0.6
	4	29-Aug	34.6	58.7	26.7	0.6
Average			**34.68**	**57.33**	**26.78**	**0.60**
Std Dev			**0.05**	**1.03**	**0.10**	**0.00**
Medium	1	21-Jul	34.6	58.3	26.5	0.5
	2	24-Jul	34.7	60.4	26.4	0.5
	3	25-Jul	34.7	58.3	26.6	0.5
	4	29-Aug	34.7	59.4	26.4	0.5
Average			**34.68**	**59.10**	**26.48**	**0.50**
Std Dev			**0.05**	**1.01**	**0.10**	**0.00**
High	1	21-Jul	34.6	62.1	26	0.3
	2	24-Jul	34.6	63	25.9	0.3
	3	25-Jul	34.7	60.4	24.3	0.4
	4	29-Aug	34.6	63.5	25.8	0.3
Average			**34.63**	**62.25**	**25.50**	**0.33**
Std Dev			**0.05**	**1.36**	**0.80**	**0.05**

C5_BladeLess_desk_Angular to chest (Ta: 25±1°)						
Speed	Trial	Date	Tsk (°C)	P(W/m²)	Teq (°C)	PMV
0	1	22-Jul	34.8	46.7	28.3	1.1
	2	23-Jul	34.9	35.6	28.4	1.1
	3	25-Jul	34.9	46.3	28.5	1.1
	4	4-Aug	34.8	47.1	28.3	1.1
Average			**34.85**	**43.93**	**28.38**	**1.10**
Std Dev			**0.06**	**5.56**	**0.10**	**0.00**
Low	1	22-Jul	34.7	57.2	26.7	0.6
	2	23-Jul	34.7	51	26.7	0.6
	3	25-Jul	34.7	57.4	26.8	0.6
	4	4-Aug	34.7	56.5	27	0.7
Average			**34.70**	**55.53**	**26.80**	**0.63**
Std Dev			**0.00**	**3.04**	**0.14**	**0.05**
Medium	1	22-Jul	34.6	60.2	26.4	0.5
	2	23-Jul	34.6	58.5	26.6	0.5
	3	25-Jul	34.6	58	26.5	0.5
	4	4-Aug	34.7	57.4	26.9	0.6
Average			**34.63**	**58.53**	**26.60**	**0.53**
Std Dev			**0.05**	**1.20**	**0.22**	**0.05**
High	1	22-Jul	34.6	62.1	26.1	0.4
	2	23-Jul	34.6	57.8	26.3	0.4
	3	25-Jul	34.6	60.8	26.2	0.4
	4	4-Aug	34.7	58.7	26.6	0.5
Average			**34.63**	**59.85**	**26.30**	**0.43**
Std Dev			**0.05**	**1.96**	**0.22**	**0.05**

C6_Face fan (Ta: 25±1°)						
Speed	Trial	Date	Tsk (°C)	P(W/m²)	Teq (°C)	PMV
0	1	29-Jul	34.8	46.5	28.3	1.1
	2	30-Jul	34.8	47	28.3	1.1
	3	31-Jul	34.8	46.3	28.3	1.1
	4	1-Aug	34.8	46.7	28.3	1.1
Average			**34.80**	**46.63**	**28.30**	**1.10**
StDev			**0.00**	**0.30**	**0.00**	**0.00**
Low	1	29-Jul	34.7	55.9	26.7	0.6
	2	30-Jul	34.7	60.4	26.8	0.6
	3	31-Jul	34.7	55.3	26.9	0.6
	4	1-Aug	34.7	59.3	26.7	0.6
Average			**34.70**	**57.73**	**26.78**	**0.60**
StDev			**0.00**	**2.51**	**0.10**	**0.00**
Medium	1	29-Jul	34.7	61.4	26.4	0.5
	2	30-Jul	34.7	61.2	26.6	0.5
	3	31-Jul	34.7	59.8	26.6	0.5
	4	1-Aug	34.7	58.3	26.6	0.5
Average			**34.70**	**60.18**	**26.55**	**0.50**
StDev			**0.00**	**1.44**	**0.10**	**0.00**
High	1	29-Jul	34.6	61.9	26.4	0.4
	2	30-Jul	34.6	61	26.1	0.4
	3	31-Jul	34.6	60.5	26.2	0.4
	4	1-Aug	34.6	60.3	26.3	0.4
Average			**34.60**	**60.93**	**26.25**	**0.40**
StDev			**0.00**	**0.71**	**0.13**	**0.00**

C7_Neck Fan (Ta: 25±1°)						
Speed	Trial	Date	Tsk (°C)	P(W/m²)	Teq (°C)	PMV
0	1	29-Jul	34.8	47.5	28.3	1.1
	2	30-Jul	34.8	46.7	28.3	1.1
	3	31-Jul	34.9	45.1	28.5	1.1
	4	3-Aug	34.8	46.7	28.3	1.1
Average			**34.8**	**46.5**	**28.4**	**1.1**
Std Dev			**0.0**	**0.9**	**0.1**	**0.0**
Low	1	29-Jul	34.7	54.6	27	0.7
	2	30-Jul	34.7	53.6	26.9	0.6
	3	31-Jul	34.8	54.8	27.2	0.7
	4	3-Aug	34.7	59.2	26.7	0.6
Average			**34.7**	**55.6**	**27.0**	**0.7**
Std Dev			**0.0**	**2.2**	**0.2**	**0.1**
Medium	1	29-Jul	34.7	58.3	26.9	0.6
	2	30-Jul	34.7	59.6	26.8	0.6
	3	31-Jul	34.7	57.2	26.8	0.6
	4	3-Aug	34.7	58.3	26.6	0.5
Average			**34.7**	**58.4**	**26.8**	**0.6**
Std Dev			**0.0**	**0.9**	**0.1**	**0.0**
High	1	29-Jul	34.7	59.3	26.6	0.5
	2	30-Jul	34.7	59.8	26.6	0.5
	3	31-Jul	34.7	60.5	26.4	0.5
	4	3-Aug	34.6	60.3	26.3	0.4
Average			**34.7**	**60.0**	**26.5**	**0.5**
Std Dev			**0.0**	**0.5**	**0.1**	**0.0**

Appendix B: Zonal Heat Loss Data

B1: Zonal heat loss for configuration _C1

Zonal Heat Loss																							
Speed	**Trial**	**L foot**	**R foot**	**L fore leg**	**R fore leg**	**L F. thigh**	**R F. thigh**	**Pelvis**	**L. Back thigh**	**Face**	**Skull**	**L. hand**	**R. hand**	**L fore arm**	**R fore arm**	**L U arm**	**Back side**	**R U arm**	**Chest**	**Stomach**	**U. back**	**L. back**	**Neck**	**R. back thigh**
0	1	100.2	93.8	55.8	49.9	44	40	36	29.5	82.5	70	60.8	56.5	48.3	41.9	45.5	36.6	39.2	41.3	29.9	31.6	21.8	66.5	30
	2	98.6	92.3	50.1	47.2	42.8	36.9	26.2	32.3	86.5	71.6	60.7	50.3	52.2	41.9	45.3	27.4	33.4	35.9	29.4	28.6	19	70.2	23.9
	3	103.9	103.9	53.3	48.9	42.8	36.3	22.9	27.5	90.8	77.7	63.8	61.9	56.1	44.6	46.5	26.4	37.4	42.1	25.2	29	20.5	87	23.1
	4	97.2	98.3	52.6	47.8	41.9	38.4	25.6	27.8	100.5	71.4	66.7	58.4	55.6	50.2	47.2	25.2	43.4	36.6	27.1	31.6	20.6	82.6	26.6
	Avg	**99.98**	**97.08**	**52.95**	**48.45**	**42.88**	**37.90**	**27.68**	**29.28**	**90.08**	**72.68**	**63.00**	**56.78**	**53.05**	**44.65**	**46.13**	**28.90**	**38.35**	**38.98**	**27.90**	**30.20**	**20.48**	**76.58**	**25.90**
Low	1	95.8	96.3	55	50.2	61.6	57	46.1	33.4	199	103.9	121.3	95.6	100.3	100.2	57.4	36.2	59.3	63.7	48.4	39	22.1	106.8	26.4
	2	98.1	95.7	58.8	46.2	53.1	51.8	38.3	28.8	197.8	100.6	110	93.2	94.5	98.2	58.3	29.8	55.2	69.3	44.6	34.4	24.1	107.8	25.1
	3	103.4	96.7	54.7	51.3	63.1	55.5	36.7	29	213.5	107.5	120.1	84.9	101.8	100.4	59.5	32.9	61.6	69.5	49.5	37.5	24	110.3	24.5
	4	104.7	98.6	57.4	49.5	60.3	54.8	38.9	30.3	213.8	111.5	105.9	100.2	101.4	101	58.3	28.8	58	67.6	52.4	38.2	23.1	111.8	27.5
	Avg	**100.50**	**96.83**	**56.48**	**49.30**	**59.53**	**54.78**	**40.00**	**30.38**	**206.03**	**105.88**	**114.33**	**93.48**	**99.50**	**99.95**	**58.38**	**31.93**	**58.53**	**67.53**	**48.73**	**37.28**	**23.33**	**109.18**	**25.88**
Mediun	1	97.1	100.6	55.8	51.2	64.8	59.9	44.5	34	208.3	101.6	125.9	108	104.1	112.2	59.5	34.6	62.7	71.9	46.7	39.2	25.7	108.2	27.6
	2	95.1	95.7	54.5	48.1	65.8	58.3	37.8	31.5	223.9	115.8	128.2	104.1	110	113.1	64.8	29.8	61	75.3	50.1	40.9	27.1	119.2	19.9
	3	93	93.2	56.1	52	68	59.3	42.1	30	240.4	125.1	146.2	100.4	121.1	115.4	67.3	30.5	67.5	81.2	54.9	42	29.3	121.6	26.5
	4	103.7	96.8	56.2	51.6	67.5	57.5	43.7	30.8	236.1	128.3	141.3	119.5	115.6	113.5	69.5	30.3	53.8	76.5	56.4	39.2	26.7	127.6	26.9
	Avg	**97.23**	**96.58**	**55.65**	**50.73**	**66.53**	**58.75**	**42.03**	**31.58**	**227.18**	**117.70**	**135.40**	**108.00**	**112.70**	**113.55**	**65.28**	**31.30**	**61.25**	**76.23**	**52.03**	**40.33**	**27.20**	**119.15**	**25.23**
High	1	96.4	103.5	59.7	44	72.6	63.1	49	36.6	250	130.4	164	130.2	129.5	132.8	72.4	33.3	56.1	79.5	52.1	44.9	30	134.8	28.7
	2	99.7	100.8	54.5	51	72.1	63.6	44.7	34.7	245.9	123.5	155.1	121.4	128	137.3	72.2	31.8	65	80.2	61.8	44.2	32.6	137.7	28.3
	3	101.9	98.9	60.8	53.8	71	65	48.9	34.1	248.2	128.6	169.2	108.3	125.3	128.8	75	33.4	73.1	82	62.7	45.5	32.2	138.2	27.1
	4	103.7	96.9	57.2	51.6	72.7	60.7	49.3	30.9	257.7	134.6	156.7	122.1	124.2	127	76	31.7	68.4	79.1	66.5	41.5	29.1	137.3	28.2
	Avg	**100.43**	**100.03**	**58.05**	**50.10**	**72.10**	**63.10**	**47.98**	**34.08**	**250.45**	**129.28**	**161.25**	**120.50**	**126.75**	**131.48**	**73.90**	**32.55**	**65.65**	**80.20**	**60.78**	**44.03**	**30.98**	**137.00**	**28.08**

B2: Zonal heat loss for configuration _C2

Zonal Heat Loss																							
Speed	**Trial**	**L foot**	**R foot**	**L fore leg**	**R fore leg**	**L F. thigh**	**R F. thigh**	**Pelvis**	**L. Back thigh**	**Face**	**Skull**	**L. hand**	**R. hand**	**L forearm**	**R forearm**	**L U arm**	**Backside**	**R U arm**	**Chest**	**Stomach**	**U. back**	**L. back**	**Neck**	**R. back thigh**
0	1	97.9	92.2	51.7	46.7	42.3	47.1	25.8	29.3	96.4	68.4	63.5	59.6	51.4	48.3	51.8	27.1	39.8	37.1	27.6	30	20.4	71.9	26.3
	2	101.5	94.7	52.5	50.9	42.8	38.4	39.7	30.6	76.2	67.6	58.7	50.5	52	42.2	44.5	35.7	38.5	36.7	28.8	31.7	22.1	69.8	29.5
	3	112.3	100.9	56.2	51.1	42.5	46.9	24.1	28.8	99.7	69.5	69.5	49.3	46.5	44.5	43.4	24.1	30.1	39.8	22.7	29	19	74.6	28.1
	4	104.3	94	53.4	47.7	46.3	38	26.8	27.3	105.5	75.6	71.9	59.6	56.5	43.2	49.4	27.5	36.6	40.1	29.9	35.7	22	74.5	27.1
	Avg	**104.00**	**95.45**	**53.45**	**49.10**	**43.48**	**42.60**	**29.10**	**29.00**	**94.45**	**70.28**	**65.90**	**54.75**	**51.60**	**44.55**	**47.28**	**28.60**	**36.25**	**38.43**	**27.25**	**31.60**	**20.88**	**72.70**	**27.75**
Low	1	98	96.5	49.8	49.6	63.3	56.3	36	29.7	193.8	107.5	111.6	87.9	100.9	104.8	61.7	30.9	44.7	68.3	46.6	40.1	23.5	114.6	25.9
	2	118.1	117.2	56.2	53.1	56.1	64.3	45.6	30.9	196.2	134.9	93.7	88.5	50.1	63.8	67.9	34.3	83	42.1	45.7	31	22.1	106.2	28.7
	3	109.1	102.5	54.4	55.4	65.4	53.1	32.1	29.8	209.3	101.3	119.7	89.2	104.5	105	64.7	27.7	57.6	62.7	46.2	37.6	24	111.1	26.6
	4	105.6	97.4	54.7	46	61.6	48.5	36.5	29.5	193.8	106.3	124.6	106.1	92.6	106.9	63.1	28.4	58.2	65.2	45.1	37.1	22.5	109.5	25.7
	Avg	**107.70**	**103.40**	**53.78**	**51.03**	**61.60**	**55.55**	**37.55**	**29.98**	**198.28**	**112.50**	**112.40**	**92.93**	**87.03**	**95.13**	**64.35**	**30.33**	**60.88**	**59.58**	**45.90**	**36.45**	**23.03**	**110.35**	**26.73**
Mediun	1	113.6	116.1	61.8	54.7	69.2	56.7	36.4	33.8	216.6	120.5	126	95.8	109.3	116.8	73	28.7	58.7	72.2	53.8	43.1	29.2	125.7	26.7
	2	101.5	98.2	56.7	51.4	71.8	58	47.1	35.1	220.9	109.4	122.3	96.2	111.7	117.1	72.3	34.4	58	75.4	52.8	46	27.2	115	29.7
	3	105.6	105.1	62.2	53.8	68.1	60.4	41.6	33.6	229.9	114.2	140.7	107	121.4	122.8	75.7	30.6	60.3	73.5	59.6	42.4	26.5	121.1	29.8
	4	101	99	53.2	49.8	62.3	58.3	45.7	29.3	224.1	109.9	151.2	114.9	114	121.9	68.9	29.1	54.6	76.5	55.1	40.7	26.6	119.1	25.4
	Avg	**105.43**	**104.60**	**58.48**	**52.43**	**67.85**	**58.35**	**42.70**	**32.95**	**222.88**	**113.50**	**135.05**	**103.48**	**114.10**	**119.65**	**72.48**	**30.70**	**57.90**	**74.40**	**55.33**	**43.05**	**27.38**	**120.23**	**27.90**
High	1	100.4	94.6	57.3	51.2	72.1	65.8	47.6	36.2	241.8	132.8	143.7	108.5	124.5	131.1	73	30.2	64.4	84.6	60.5	43.1	31.4	133.7	27.4
	2	98.6	99.2	58.5	51.7	72.3	64.4	50.4	35.3	241.7	130.3	141.4	105.8	125.7	131.8	81.1	34.9	62.1	80.5	61.2	47.8	30.2	127.7	29.6
	3	106.6	106	58.7	50.9	75.9	61.7	48.5	29.7	249.1	132.8	154.6	114.7	135.2	138.7	82.3	31.2	61	69.5	67.9	46	26.8	132.9	29.7
	4	98.1	101.5	58.2	50.7	62.6	56.9	51.8	31.8	251.1	127.9	163.8	118.7	122.8	132	73.9	31.3	64	72	67.2	45.8	27.9	134.7	27.8
	Avg	**100.93**	**100.33**	**58.18**	**51.13**	**70.73**	**62.20**	**49.58**	**33.25**	**245.93**	**130.95**	**150.88**	**111.93**	**127.05**	**133.40**	**77.58**	**31.90**	**62.88**	**76.65**	**64.20**	**45.68**	**29.08**	**132.25**	**28.63**

B3: Zonal heat loss for configuration _C3

Zonal Heat Loss																							
Speed	Trial	L foot	R foot	L fore leg	R fore leg	L F. thigh	R F. thigh	Pelvis	L. Back thigh	Face	Skull	L. hand	R. hand	L forearm	R fore arm	L U arm	Back side	R U arm	Chest	Stomach	U. back	L. back	Neck	R. back thigh
0	1	108.7	98.8	53.8	50	41.8	36.3	27	28.8	94.5	74	66.9	58.5	58.2	43.6	46.7	29.6	39.5	41.4	27.3	31.1	22.8	70.1	26.1
	2	106.6	97.3	53	50.3	45.2	38.9	31	28.3	96.5	72.8	64.9	52.5	51.7	42.5	45.6	31.2	40.1	41	26.9	31.7	21.4	70.3	26.2
	3	104.7	98.8	58.6	50.8	37.4	36.7	28	26.9	91.2	74.1	54.3	56.5	38.1	40.9	46.9	34.2	41.7	39.4	24	32.3	20.9	77.9	29.7
	4	97.3	93.3	52.4	47.7	42.4	38.5	26.3	28.6	89.5	86.6	71.8	62.8	61.2	47.9	44.9	25.8	37.7	42.6	29.1	31.6	20.8	78.8	28.4
	Avg	**104.33**	**97.05**	**54.45**	**49.70**	**41.70**	**37.60**	**28.08**	**28.15**	**92.93**	**76.88**	**64.48**	**57.58**	**52.30**	**43.73**	**46.03**	**30.20**	**39.75**	**41.10**	**26.83**	**31.68**	**21.48**	**74.28**	**27.60**
Low	1	109.2	100.4	54.4	51.8	53.2	44.5	32.5	28.1	199.8	119.5	88	79	87.8	66.6	51.4	31.3	49.8	79.8	34.7	37.4	24.1	117.3	26.2
	2	109.1	102.9	55.2	51.8	42.1	40.8	31.9	28.3	220.6	108.2	74.7	70.4	68.8	68.5	52.6	32.1	49.4	75.5	32.4	36.8	23.7	111.7	25.8
	3	107	101.5	57.5	49.9	51.7	53.4	36.8	28.9	205	113.4	87.2	78.6	70.7	67.4	47.1	34.2	48.9	79.1	28.9	34.5	23.4	123.9	28.9
	4	110.4	109.9	60.1	53.6	51.6	42.7	28.3	30.5	192.9	109.7	84.9	73.3	91.7	67.1	52.3	27.4	51.8	79.5	34	37.9	20.7	128.2	25.7
	Avg	**108.93**	**103.68**	**56.80**	**51.78**	**49.65**	**45.35**	**32.38**	**28.95**	**204.58**	**112.70**	**83.70**	**75.33**	**79.75**	**67.40**	**50.85**	**31.25**	**49.98**	**78.48**	**32.50**	**36.65**	**22.98**	**120.28**	**26.65**
Mediun	1	108.4	102.2	46.7	50.1	58	45.8	34.9	27.8	229	139.8	93.4	82.1	102.2	68.6	48.2	33.8	50.5	90.4	34.8	42	24	138.9	27.1
	2	108.9	101.3	56.8	50.4	48.8	44	31	26.9	238.8	131.8	81.3	77.2	75.7	81.2	51.4	30.8	54.5	88.4	36.9	37.8	23.8	134.6	27.2
	3	114.2	114.1	57.1	56	54.5	48.4	34.5	26.7	233.8	134	98.2	84	86.8	77	49.2	33	55.4	84.1	31.1	40.7	25.5	135.2	26.8
	4	108.1	106.5	59	55.2	55	46.9	31.5	24.1	210.7	124.6	93.2	69.1	95.8	70.2	54.9	27	56.3	87.7	39.4	42.4	24.1	142.9	24.8
	Avg	**109.90**	**106.03**	**54.90**	**52.93**	**54.08**	**46.28**	**32.98**	**26.38**	**228.08**	**132.55**	**91.53**	**78.10**	**90.13**	**74.25**	**50.93**	**31.15**	**54.18**	**87.65**	**35.55**	**40.73**	**24.35**	**137.90**	**26.48**
High	1	106.7	100.5	54.5	53.1	60.6	51.4	36.9	30.2	241.3	151.3	110.6	90.5	104.1	75.9	55	31.8	54.7	94.2	36.2	37.7	24.8	154.2	28.4
	2	116	107.9	63.3	58.1	54.8	51.9	33.4	29.9	275.6	155.6	87.7	83.5	93.5	99.8	58.7	31.1	59.8	90.4	37.1	46.1	20.1	157.8	27.8
	3	111.7	108.7	60.9	54.9	57.6	52.4	37.1	26.5	256.8	150.6	104	92.5	95.2	84	54.1	32.5	54.2	85.3	35.5	38.5	21.1	154.1	28.8
	4	105.8	103.5	59.4	51	59.9	48.7	31.5	25.8	225.2	137	103.6	79.1	112.6	76.7	56.1	28.2	57.5	89.8	39.4	43.7	23.8	146.1	24
	Avg	**110.05**	**105.15**	**59.53**	**54.28**	**58.23**	**51.10**	**34.73**	**28.10**	**249.73**	**148.63**	#####	**86.40**	**101.35**	**84.10**	**55.98**	**30.90**	**56.55**	**89.93**	**37.05**	**41.50**	**22.45**	**153.05**	**27.25**

B4: Zonal heat loss for configuration _C4

Speed	Trial	L foot	R foot	L fore leg	R fore leg	L F. thigh	R F. thigh	Pelvis	L. Back thigh	Face	Skull	L. hand	R. hand	L fore arm	R fore arm	L U arm	Back side	R U arm	Chest	Stomach	U. back	L. back	Neck	R. back thigh
0	1	109.8	101.6	55.2	49.9	42.4	37.5	19.6	26	106.5	72.8	69.2	60.7	59.9	45.7	47.4	22.3	39.3	40.8	26	30.4	20.1	78.7	25.6
	2	103.3	97.7	55.5	47.2	42.9	38.2	23	25.8	97.2	78.8	69.2	58.7	58.4	47.4	47.7	26.5	38.4	42.1	36.3	30.2	21.6	84.1	27.7
	3	97.3	96.7	50.1	50	44.2	38.6	26.2	26.4	92.4	62.2	63.8	62.3	55.9	55.3	42.7	25.3	37	40.7	25.5	23	20.4	76.2	27
	4	105.8	97.3	58.1	56.2	44.7	41.5	41.5	33.2	98.5	68.2	76.1	63.3	58	52.7	53.7	39.1	41.6	44.3	28.6	30.6	24.3	72.5	31.8
	Avg	**104.05**	**98.33**	**54.73**	**50.83**	**43.55**	**38.95**	**27.58**	**27.85**	**98.65**	**70.50**	**69.58**	**61.25**	**58.05**	**50.28**	**47.88**	**28.30**	**39.08**	**41.98**	**29.10**	**28.55**	**21.60**	**77.88**	**28.03**
										211.1														
Low	1	105.5	101	57.3	52.1	46.8	41.5	23.1	37.3		115	78.9	70.3	71.4	66	53.4	28.5	50.2	72.8	27.9	40.9	20.5	116.4	21.1
	2	106.5	96.6	60	52.3	54.9	43.5	24.2	28.6	203.9	110.7	76.1	71.6	69.2	63.6	53.4	26.5	44.3	68.8	22.5	38	22	105.9	27.4
	3	111.6	115.2	63.6	55.9	45.6	43.7	25.7	27.2	201.5	100.7	78.1	66.9	72	61.4	54	39.2	46.2	65.3	25.8	37.1	23.5	102.5	27.3
	4	53.5	47.6	60.6	62	50.1	43.9	40	33.3	222	118.2	79.4	73.1	77.7	73.2	60.5	41.2	51	75.3	34.2	39.9	24.5	115.1	31.2
	Avg	**94.28**	**90.10**	**60.38**	**55.58**	**49.35**	**43.15**	**28.25**	**31.60**	**209.63**	**111.15**	**78.13**	**70.48**	**72.58**	**66.05**	**55.33**	**33.85**	**47.93**	**70.55**	**27.60**	**38.98**	**22.63**	**109.98**	**26.75**
Mediu	1	105.6	100	55.3	52.3	45.5	40.5	21.7	28.1	239	123.2	89.1	78.1	77.1	66.3	51.6	29.7	51.7	76.3	28.4	43.4	14.4	114.1	25.8
	2	106.3	104.2	59.5	49.7	47.9	41.4	24.9	30.2	234.2	122.5	88.4	75.7	80.5	100.4	59.9	26.9	43.5	75.6	32.5	42.9	25	120.3	26.8
	3	109.3	111.1	58.4	43.6	47.6	42.5	26.5	29	223.5	120.5	78.6	71.5	76.8	68.5	57	28.3	51.5	67.9	31	41.4	24.1	116.4	26
	4	109	110.2	58.6	51.6	52.1	45.6	38.8	30.1	239.8	133.8	80.1	74.3	82.9	77.3	66.4	34.2	59.4	79.2	34.2	37	22.3	127.5	30.1
	Avg	**107.55**	**106.38**	**57.95**	**49.30**	**48.28**	**42.50**	**27.98**	**29.35**	**234.13**	**125.00**	**84.05**	**74.90**	**79.33**	**78.13**	**58.73**	**29.78**	**51.53**	**74.75**	**31.53**	**41.18**	**21.45**	**119.58**	**27.18**
High	1	106.1	103.6	57.5	52.4	47.6	42.9	27.9	29.5	256.5	133.8	83.4	77.1	83.9	75.9	59	29.1	58.1	78.5	28.8	48.8	24.1	132.8	25.6
	2	104.9	102.2	57.1	52.3	51.1	45.1	27.4	24.4	253.4	144.8	93.2	82.3	89	85.5	56.5	29	58.7	83.9	32.1	44.4	17.4	132	25.6
	3	107.9	106.2	58.2	54.1	49.1	43	26.1	24.4	242.3	125.8	78.4	76.2	81	75.1	57.4	28.1	53	77.6	31.7	43.7	23.5	116.5	26
	4	105.3	104.2	57.9	54.2	54.7	49.9	36.8	28.8	255.9	148.8	99.5	81.9	94.1	92.9	70.9	33.7	60	87.2	37.6	47.9	22.1	146.2	29.6
	Avg	**106.05**	**104.05**	**57.68**	**53.25**	**50.63**	**45.23**	**29.55**	**26.78**	**252.03**	**138.30**	**88.63**	**79.38**	**87.00**	**82.35**	**60.95**	**29.98**	**57.45**	**81.80**	**32.55**	**46.20**	**21.78**	**131.88**	**26.70**

B5: Zonal heat loss for configuration _C5

Zonal Heat Loss																							
Speed	**Trial**	**L foot**	**R foot**	**L fore leg**	**R fore leg**	**L F. thigh**	**R F. thigh**	**Pelvis**	**L. Back thigh**	**Face**	**Skull**	**L. hand**	**R. hand**	**L fore arm**	**R fore arm**	**L U arm**	**Back side**	**R U arm**	**Chest**	**Stomach**	**U. back**	**L. back**	**Neck**	**R. back thigh**
0	1	104	98.8	55.3	47.8	42.7	37.7	21.2	29	97.4	82.2	67	60.8	61.3	46.9	46.3	25.2	36.9	43.2	25	32.2	20.1	83.3	24.5
	2	108.8	98.3	55.8	49.3	49.3	37.7	23.5	28.6	96.6	81.9	67.1	59.5	57	41.6	22.4	26.2	33.6	41	17.5	34.9	20.8	86.5	26.1
	3	97.4	94	54.7	50	43	39.2	35.2	29.3	90.1	74.3	62.2	58	52.2	42.4	46	34.9	38	42.4	24.9	32.3	20.2	70.4	28.3
	4	105.8	97.3	55.1	50.2	44.1	38.9	22.4	28.9	105.1	75.1	76	73.5	54.6	54.5	44.9	24.2	38	40.3	25.6	27.8	20.6	78.9	23.9
	Avg	**104.00**	**97.10**	**55.23**	**49.33**	**44.78**	**38.38**	**25.58**	**28.95**	**97.30**	**78.38**	**68.08**	**62.95**	**56.28**	**46.35**	**39.90**	**27.63**	**36.63**	**41.73**	**23.25**	**31.80**	**20.43**	**79.78**	**25.70**
Low	1	108.3	100.1	56	51.4	46.3	39.3	22.4	29.2	209.8	113.6	81.5	71.9	73.6	70	57.3	26.7	55.8	71	30.5	38.9	16.7	117.3	25.6
	2	107.2	100.9	56	53.4	48	39.2	26.2	29.4	133.4	76.8	81.7	71.1	62.1	61.8	45.6	29.7	46.1	48.9	25.5	38.7	25.4	75.7	25.4
	3	110.8	104.1	63.6	57.3	49.5	42.8	34.5	32.1	194.4	114.3	75.1	68.1	67.4	61	50.3	35	48.5	42.4	28.1	38.5	20.7	103.3	26.4
	4	112.8	106.5	59.6	56.4	52.5	47.3	25.6	29.8	163.3	93	80.3	68.9	80.1	71.3	56.6	25.5	50.4	63	31.2	39	22.8	99.2	25.9
	Avg	**109.78**	**102.90**	**58.80**	**54.63**	**49.08**	**42.15**	**27.18**	**30.13**	**175.23**	**99.43**	**79.65**	**70.00**	**70.80**	**66.03**	**52.45**	**29.23**	**50.20**	**56.33**	**28.83**	**38.78**	**21.40**	**98.88**	**25.83**
Mediu	1	108.1	101.3	56.1	50.5	45.5	41.1	23.6	29.3	232	132	85.6	80.6	76.1	78	59.7	28.1	51.4	76.8	32.7	42.4	24.9	121.9	26.7
	2	105.9	101.2	58.2	56.2	47.1	37.8	27.6	36.7	198.4	122.7	82.6	78.1	71.4	68.2	56.7	28	51.9	73.7	31.9	40.1	18.7	120.1	24.4
	3	101.9	95.8	54.7	46.6	42.5	42.1	35.7	27.9	207.3	120.6	81	73.6	73.7	79.7	58.1	57.3	53.8	75.9	31.4	39.7	23.2	110.2	25.6
	4	110.9	102.7	59.1	54.6	45.9	39.8	22.9	26.8	202.5	114.8	83	74.4	78.1	69.9	56.8	25.8	50.6	67.3	32.7	40.8	21.3	110.2	24.2
	Avg	**106.70**	**100.25**	**57.03**	**51.98**	**45.25**	**40.20**	**27.45**	**30.18**	**210.05**	**122.53**	**83.05**	**76.68**	**74.83**	**73.95**	**57.83**	**34.80**	**51.93**	**73.43**	**32.18**	**40.75**	**22.03**	**115.60**	**25.23**
High	1	96.4	99.9	56.3	56.2	47.9	42.3	28.2	35.6	241.5	143.5	83.8	78.8	79	76.2	63	28.3	55.1	79.9	31	48.8	23.5	123.9	26.1
	2	104.4	103	56.8	52.2	44.4	41.1	28.7	27.7	136.4	79.2	76.5	69.8	70.5	71.8	54	29.6	47.1	52.5	28	41.7	21.6	71	24.1
	3	100.5	96.3	55	49.7	48.6	46.1	31.3	27.2	222	135.8	80.3	78.7	79.5	85.3	58.3	31.7	58.1	78.4	36.1	43.4	23.5	122.7	25.7
	4	113.2	109.7	60.8	54.5	46.9	38.4	24.4	29.4	208.7	116	82.5	72.9	74.5	75	53.3	25.6	60.7	70.5	33	40.5	21.5	111.2	24.7
	Avg	**103.63**	**102.23**	**57.23**	**53.15**	**46.95**	**41.98**	**28.15**	**29.98**	**202.15**	**118.63**	**80.78**	**75.05**	**75.88**	**77.08**	**57.15**	**28.80**	**55.25**	**70.33**	**32.03**	**43.60**	**22.53**	**107.20**	**25.15**

B6: Zonal heat loss for configuration _C6

Zonal Heat Loss																								
Speed	**Trial**	**L foot**	**R foot**	**L fore leg**	**R fore leg**	**L F. thigh**	**R F. thigh**	**Pelvis**	**L. Back thigh**	**Face**	**Skull**	**L. hand**	**R. hand**	**L fore arm**	**R fore arm**	**L U arm**	**Back side**	**R U arm**	**Chest**	**Stomach**	**U. back**	**L. back**	**Neck**	**R. back thigh**
0	1	105.8	99.4	56.8	47.3	44.6	37.5	23.7	39.8	104.1	86.2	64.6	60.6	51.6	44.6	43.8	25.5	38.4	38.8	28.4	30.4	18.4	85.8	27
	2	105.7	97.8	55.9	50.1	43	41	24.2	30.5	105.5	76.8	70	59.4	56.2	43.1	46.8	28.3	37.5	39.7	25.3	28.8	19.7	81.6	26.1
	3	112.8	99.3	53.9	49.7	41.5	37.6	18.3	24.9	97.9	82.3	67.6	59.5	53.5	42.3	43.5	22.2	36.3	37.3	20.7	28.3	16.9	84.1	25.2
	4	107.1	98.8	58.1	50.8	50.1	45.2	25.3	30.7	85.5	76.5	72.1	69.8	55.5	55.7	50.5	45.1	46.2	54.7	25.1	29.3	27.1	26	27.1
	Avg	**107.85**	**98.83**	**56.18**	**49.48**	**44.80**	**40.33**	**22.88**	**31.48**	**98.25**	**80.45**	**68.58**	**62.33**	**54.20**	**46.43**	**46.15**	**30.28**	**39.60**	**42.63**	**24.88**	**29.20**	**20.53**	**69.38**	**26.35**
Low	1	105.2	98	57.3	51.7	47.4	42.3	29.5	27.5	156	118.9	84.4	75.9	68.8	61.9	45.1	28.5	46.6	55.3	30.2	29.9	20.9	141.3	25.6
	2	123.9	114.9	65.5	59.3	50.3	45.2	26.5	31.3	255.4	112.4	84.4	75.9	67.4	63.3	54.6	27.8	44.8	59.3	27.4	37.1	22.5	135.4	28.3
	3	121	104.8	63.2	54.1	52.5	40	23.6	23.8	140.8	110.8	83.3	71.8	77.1	60.9	47.1	27	45.8	46.7	28.9	33.4	23.2	141.2	23.3
	4	118.3	112.1	56.6	56.3	51.6	49.7	34.9	32.7	169.8	116	90.8	78.4	84.1	67.9	50.6	32.4	45.4	53.9	30.8	39.9	26.2	141.8	28.8
	Avg	**117.10**	**107.45**	**60.65**	**55.35**	**50.45**	**44.30**	**28.63**	**28.83**	**180.50**	**114.53**	**85.73**	**75.50**	**74.35**	**63.50**	**49.35**	**28.93**	**45.65**	**53.80**	**29.33**	**35.08**	**23.20**	**139.93**	**26.50**
Mediur	1	113.8	113.1	61.1	58.9	49.1	41.8	25.8	30.2	161.1	138.9	79.4	74.8	75.8	66.4	54.5	27.9	43.9	50.1	31.2	38.5	23.5	157.8	26.5
	2	122.5	112.8	54.4	53.5	53.8	45.1	25.6	30.6	258.2	112.2	88	77.3	78.5	68.6	58.8	28.7	46.9	71.2	26.9	38.2	25	144.4	27.2
	3	115.4	109	52.7	58.1	51.1	42.8	23.3	27.3	173.7	134.7	88.4	78.1	82.5	64.5	50.4	26.2	45.5	44.7	26.1	33.2	23	162	26
	4	116.8	104.1	61.4	57.7	49.8	44.9	31	33.5	163.8	131.6	82.5	76.3	77.4	69.2	57.6	30.2	42.7	50.5	23.9	40.2	25.1	140	26.5
	Avg	**117.13**	**109.75**	**57.40**	**57.05**	**50.95**	**43.65**	**26.43**	**30.40**	**189.20**	**129.35**	**84.58**	**76.63**	**78.55**	**67.18**	**55.33**	**28.25**	**44.75**	**54.13**	**27.03**	**37.53**	**24.15**	**151.05**	**26.55**
High	1	119	113.1	65.6	59.6	53	38.9	25.2	31.7	172	130.4	89.7	79.7	75.5	62.6	55.9	28.3	43.2	52.2	28.7	37.9	24.2	153.8	28.2
	2	105.6	111.9	63	50.2	52.3	45.4	28	32	271.2	117	94.5	83.5	72.5	64.2	54.3	29.8	45.8	61.5	25	37	23.5	153.6	28.3
	3	117.7	104.7	61.8	59.5	49.6	45.1	24.3	29.4	206.6	149.9	88.1	82.9	84.4	65.4	49.7	29.1	45.2	44.5	27.7	39.6	26.1	171.1	27.3
	4	116.6	118.6	62.3	57.6	52.3	46.4	29.5	32	185.1	142.7	88.1	74.3	80.3	65.7	53.1	29.6	43.8	55.6	30.6	28.8	25.3	161.3	28.3
	Avg	**114.73**	**112.08**	**63.18**	**56.73**	**51.80**	**43.95**	**26.75**	**31.28**	**208.73**	**135.00**	**90.10**	**80.10**	**78.18**	**64.48**	**53.25**	**29.20**	**44.50**	**53.45**	**28.00**	**35.83**	**24.78**	**159.95**	**28.03**

B7: Zonal heat loss for configuration _C7

Zonal Heat Loss																							
Speed	**Trial**	**L foot**	**R foot**	**L fore leg**	**R fore leg**	**L F. thigh**	**R F. thigh**	**Pelvis**	**L. Back thigh**	**Face**	**Skull**	**L. hand**	**R. hand**	**L fore arm**	**R fore arm**	**L U arm**	**Back side**	**R U arm**	**Chest**	**Stomach**	**U. back**	**L. back**	**Neck**	**R. back thigh**
0	1	101.9	96.6	56.6	47.6	43.9	37.1	33.7	28.7	94.5	69.1	69.6	65.7	57	40	45.1	33	39.9	40.6	26.5	31.1	20.3	66.4	27.7
	2	105.7	97.8	55.9	50.1	43	41	25.3	30.5	105.5	76.8	70	59.4	56.2	43.1	46.8	28.3	37.5	32.7	25.3	28.8	19.7	81.6	26.1
	3	103.7	103.2	53.9	49.2	44.5	39.3	25.6	27.1	102.4	70.7	64.9	57.4	53.6	47.9	45.3	24	37.8	40.9	27.3	30.9	22.7	74.7	27
	4	119.6	102.1	54.8	52	43	37	32.4	29.1	96.8	71.7	56.1	56	47.5	47.5	45.9	32.7	40.1	40.1	25.1	29.4	21.8	69.7	26.5
	Avg	**107.73**	**99.93**	**55.30**	**49.73**	**43.60**	**38.60**	**29.25**	**28.85**	**99.80**	**72.08**	**65.15**	**59.63**	**53.58**	**44.63**	**45.78**	**29.50**	**38.83**	**38.58**	**26.05**	**30.05**	**21.13**	**73.10**	**26.83**
Low	1	101.5	100.6	56.3	51.5	50.2	41.9	31.8	30.9	227.8	100.9	73.2	66.7	62	53.5	53.1	33.3	43.9	61.5	25.5	36.3	22.9	121.1	29.2
	2	123.9	114.9	65.5	59.3	50.3	45.2	26.5	31.3	255.4	112.4	84.4	75.9	67.4	63.3	54.6	27.8	44.8	59.3	27.4	37.1	22.5	135.4	28.3
	3	111.1	100.2	53.7	47.9	44.7	41.8	25.8	29.3	249.4	103.4	77.7	72.2	68.7	60.3	46.4	27.5	45.5	53.6	21.8	33.7	25.3	135.1	24.7
	4	116	104.4	60.1	55	49.1	45	35.9	30.5	224.5	119.3	78.9	73.6	64.3	61.3	51	35.3	45.3	56.7	25.4	35.4	20	126.6	29.6
	Avg	**113.13**	**105.03**	**58.90**	**53.43**	**48.58**	**43.48**	**30.00**	**30.50**	**239.28**	**109.00**	**78.55**	**72.10**	**65.60**	**59.60**	**51.28**	**30.98**	**44.88**	**57.78**	**25.03**	**35.63**	**22.68**	**129.55**	**27.95**
Medium	1	116.5	116.8	61	59.9	51	47.2	30.8	31.6	255.5	116.4	86.1	78.3	77.4	68.8	52.9	31.4	38.7	66.4	27.4	41	24.4	132.4	29.3
	2	122.5	112.8	54.4	53.5	53.8	45.1	25.6	30.6	258.2	112.2	88	77.3	78.5	68.5	58.8	28.7	46.9	71.2	26.9	38.2	25	144.8	27.2
	3	118	104.1	58.6	53.9	53	44.8	26.3	29.1	268.9	114.8	83.9	77.6	73.8	62.4	53.7	28.4	42.9	66.3	22.5	36	25.1	148.1	27.6
	4	121.6	113.4	65.8	57	50.8	46.4	34.1	33.2	255.4	113.2	88.5	78	74.4	65.1	55.3	33.2	47	66.7	26.5	35.9	21.7	140.3	27.8
	Avg	**119.65**	**111.78**	**59.95**	**56.08**	**52.15**	**45.88**	**29.20**	**31.13**	**259.50**	**114.15**	**86.63**	**77.80**	**76.03**	**66.20**	**55.18**	**30.43**	**43.88**	**67.65**	**25.83**	**37.78**	**24.05**	**141.40**	**27.98**
High	1	115.9	118	62.5	60	51.5	46.4	28.7	33.4	271.8	125	86.2	77.6	72.7	60.6	51.9	31.5	41.6	71	29.6	38	21.5	150.4	26.9
	2	105.6	111.9	63	50.2	52.3	45.4	28	32	271.2	117	94.5	83.5	72.5	64.2	54.3	29.8	45	61.5	27.8	37	23.5	153.6	28.3
	3	110.7	109.3	63.6	58.5	50.1	38.8	27.9	29	270	120.4	88.1	79.8	73.7	64.4	50	28.6	44.9	68.4	23.3	36.1	25	149.9	24.9
	4	124.6	112.4	57.2	58.2	50.6	44.4	31.9	30.3	278.9	125	88.1	80.2	75.3	62.9	61.7	35.2	45.4	66.8	26.7	36.8	26	148.1	28.2
	Avg	**114.20**	**112.90**	**61.58**	**56.73**	**51.13**	**43.75**	**29.13**	**31.18**	**272.98**	**121.85**	**89.23**	**80.28**	**73.55**	**63.03**	**54.48**	**31.28**	**44.23**	**66.93**	**26.85**	**36.98**	**24.00**	**150.50**	**27.08**

Appendix C: Wind Speed

C1: Vertical windspeed at P1

1.1m															
Time	C1			C2			C3			C4			C5		
(min)	L	M	H	L	M	H	L	M	H	L	M	H	L	M	H
1	1.83	3.14	4.57	1.69	2.38	3.34	0.92	1.02	2.15	0.73	1.02	1.58	0.81	1.08	1.17
2	1.94	3.11	4.51	1.67	2.47	2.92	0.89	1.04	2.16	0.85	1.14	1.79	0.99	1.10	0.94
3	1.88	2.96	4.44	1.58	2.48	3.23	0.72	1.05	2.16	1.11	1.20	1.48	0.94	1.15	1.35
4	1.93	3.06	4.47	1.73	2.50	3.33	0.70	1.20	2.25	1.09	1.30	1.72	0.90	1.24	1.33
5	2.01	3.10	4.50	1.64	2.62	3.35	0.85	1.23	2.17	1.05	1.22	0.72	0.92	1.23	1.37
6	2.00	2.95	4.51	1.61	2.41	3.10	0.72	1.24	2.15	0.80	1.01	1.57	0.65	1.19	1.44
7	2.00	3.10	4.42	1.59	2.54	3.10	0.82	1.20	2.11	0.86	1.05	1.32	0.92	1.27	1.37
8	1.88	3.05	4.57	1.64	2.43	3.00	0.81	1.18	2.20	0.97	1.07	1.14	0.86	1.23	1.53
9	1.98	3.04	4.47	1.73	2.38	3.36	0.81	1.17	2.29	1.13	1.08	1.18	0.84	1.20	1.58
10	1.99	3.02	4.53	1.70	2.49	3.08	0.89	1.25	2.14	1.16	1.28	1.39	0.89	1.19	1.55
0.6m															
Time	C1			C2			C3			C4			C5		
(min)	L	M	H	L	M	H	L	M	H	L	M	H	L	M	H
1	0.14	0.19	0.24	0.12	0.14	0.21	0.12	0.12	0.11	0.12	0.14	0.16	0.13	0.11	0.15
2	0.19	0.20	0.24	0.14	0.14	0.21	0.12	0.13	0.11	0.13	0.13	0.14	0.13	0.14	0.14
3	0.14	0.20	0.28	0.13	0.14	0.21	0.11	0.12	0.10	0.13	0.16	0.15	0.15	0.13	0.14
4	0.13	0.19	0.27	0.13	0.13	0.19	0.12	0.11	0.11	0.13	0.14	0.16	0.12	0.11	0.13
5	0.15	0.18	0.27	0.13	0.13	0.18	0.12	0.11	0.11	0.13	0.16	0.16	0.13	0.12	0.13
6	0.15	0.20	0.35	0.13	0.14	0.17	0.11	0.10	0.10	0.13	0.17	0.14	0.12	0.13	0.13
7	0.14	0.23	0.38	0.12	0.13	0.20	0.11	0.10	0.10	0.14	0.16	0.17	0.11	0.12	0.13
8	0.13	0.23	0.28	0.13	0.14	0.19	0.11	0.11	0.11	0.13	0.15	0.17	0.13	0.13	0.14
9	0.13	0.18	0.22	0.14	0.14	0.19	0.10	0.11	0.10	0.13	0.15	0.17	0.12	0.14	0.16
10	0.14	0.20	0.32	0.13	0.15	0.18	0.10	0.10	0.11	0.13	0.16	0.17	0.11	0.14	0.15
0.1m															
Time	C1			C2			C3			C4			C5		
(min)	L	M	H	L	M	H	L	M	H	L	M	H	L	M	H
1	0.12	0.11	0.22	0.11	0.14	0.22	0.13	0.12	0.13	0.11	0.12	0.13	0.12	0.13	0.12
2	0.11	0.12	0.26	0.12	0.13	0.18	0.13	0.12	0.13	0.11	0.12	0.13	0.10	0.12	0.12
3	0.12	0.15	0.22	0.11	0.12	0.18	0.13	0.12	0.12	0.11	0.13	0.13	0.11	0.12	0.12
4	0.12	0.14	0.22	0.11	0.12	0.19	0.13	0.12	0.13	0.11	0.13	0.12	0.12	0.12	0.12
5	0.13	0.15	0.22	0.11	0.15	0.21	0.12	0.13	0.12	0.11	0.12	0.12	0.11	0.12	0.13
6	0.13	0.17	0.19	0.12	0.16	0.25	0.12	0.14	0.11	0.12	0.11	0.12	0.12	0.12	0.13
7	0.12	0.15	0.22	0.12	0.15	0.23	0.13	0.15	0.12	0.12	0.12	0.13	0.11	0.12	0.13
8	0.12	0.16	0.30	0.13	0.17	0.21	0.12	0.16	0.13	0.11	0.12	0.12	0.12	0.13	0.13
9	0.13	0.14	0.26	0.12	0.20	0.19	0.12	0.14	0.15	0.11	0.12	0.12	0.11	0.13	0.13
10	0.13	0.13	0.21	0.12	0.14	0.27	0.13	0.12	0.15	0.11	0.11	0.13	0.11	0.12	0.12

C2: Vertical windspeed at P2

1.1m															
Time	C1			C2			C3			C4			C5		
(min)	L	M	H	L	M	H	L	M	H	L	M	H	L	M	H
1	0.11	0.12	0.12	0.18	0.15	0.17	0.10	0.12	0.15	0.12	0.15	0.13	0.14	0.20	0.16
2	0.11	0.12	0.15	0.21	0.17	0.26	0.11	0.12	0.12	0.12	0.14	0.13	0.16	0.17	0.18
3	0.11	0.13	0.15	0.13	0.17	0.26	0.12	0.13	0.14	0.12	0.15	0.17	0.14	0.15	0.17
4	0.11	0.12	0.13	0.14	0.20	0.19	0.11	0.12	0.13	0.13	0.16	0.20	0.14	0.14	0.16
5	0.11	0.14	0.12	0.16	0.22	0.15	0.11	0.14	0.12	0.14	0.14	0.18	0.14	0.16	0.17
6	0.11	0.12	0.12	0.16	0.13	0.28	0.11	0.17	0.11	0.14	0.14	0.13	0.16	0.15	0.16
7	0.12	0.14	0.15	0.17	0.21	0.16	0.11	0.13	0.12	0.14	0.14	0.12	0.16	0.16	0.15
8	0.12	0.13	0.14	0.23	0.17	0.15	0.14	0.14	0.13	0.15	0.12	0.14	0.14	0.15	0.16
9	0.13	0.14	0.18	0.14	0.19	0.13	0.13	0.12	0.12	0.12	0.13	0.13	0.16	0.13	0.20
10	0.11	0.12	0.18	0.16	0.20	0.23	0.12	0.15	0.12	0.13	0.17	0.14	0.16	0.14	0.20
0.6m															
Time	C1			C2			C3			C4			C5		
(min)	L	M	H	L	M	H	L	M	H	L	M	H	L	M	H
1	0.10	0.12	0.14	0.12	0.11	0.21	0.11	0.10	0.10	0.11	0.12	0.10	0.11	0.13	0.11
2	0.11	0.12	0.13	0.11	0.13	0.23	0.11	0.11	0.10	0.10	0.13	0.11	0.10	0.11	0.15
3	0.10	0.11	0.14	0.11	0.12	0.21	0.10	0.10	0.10	0.11	0.12	0.13	0.10	0.11	0.16
4	0.10	0.11	0.14	0.13	0.12	0.25	0.10	0.10	0.10	0.11	0.11	0.14	0.11	0.10	0.13
5	0.11	0.11	0.16	0.11	0.14	0.23	0.11	0.10	0.11	0.11	0.12	0.13	0.11	0.12	0.10
6	0.11	0.12	0.17	0.10	0.13	0.21	0.10	0.10	0.11	0.12	0.11	0.12	0.11	0.11	0.10
7	0.11	0.11	0.15	0.11	0.13	0.21	0.11	0.11	0.11	0.14	0.10	0.12	0.10	0.13	0.12
8	0.11	0.11	0.12	0.12	0.14	0.21	0.10	0.10	0.10	0.12	0.11	0.11	0.11	0.11	0.11
9	0.10	0.11	0.13	0.11	0.12	0.19	0.11	0.11	0.10	0.11	0.10	0.10	0.10	0.11	0.12
10	0.10	0.11	0.14	0.12	0.13	0.22	0.11	0.11	0.10	0.11	0.11	0.11	0.10	0.14	0.12
0.1m															
Time	C1			C2			C3			C4			C5		
(min)	L	M	H	L	M	H	L	M	H	L	M	H	L	M	H
1	0.16	0.19	0.28	0.13	0.13	0.19	0.12	0.13	0.12	0.12	0.21	0.14	0.13	0.11	0.12
2	0.14	0.17	0.23	0.14	0.16	0.25	0.11	0.16	0.11	0.13	0.27	0.12	0.13	0.13	0.13
3	0.12	0.21	0.20	0.13	0.20	0.20	0.11	0.14	0.11	0.14	0.20	0.13	0.13	0.12	0.15
4	0.17	0.21	0.16	0.15	0.20	0.26	0.12	0.14	0.13	0.13	0.17	0.26	0.13	0.12	0.17
5	0.18	0.19	0.17	0.13	0.17	0.21	0.14	0.15	0.13	0.15	0.15	0.24	0.13	0.13	0.15
6	0.19	0.22	0.18	0.16	0.14	0.23	0.13	0.14	0.14	0.17	0.14	0.25	0.13	0.14	0.15
7	0.17	0.21	0.26	0.17	0.17	0.22	0.14	0.12	0.13	0.19	0.13	0.27	0.17	0.17	0.15
8	0.16	0.22	0.28	0.18	0.19	0.22	0.15	0.12	0.16	0.14	0.15	0.24	0.13	0.19	0.15
9	0.20	0.22	0.32	0.15	0.21	0.25	0.14	0.11	0.14	0.24	0.13	0.20	0.14	0.15	0.15
10	0.22	0.22	0.18	0.17	0.17	0.26	0.12	0.11	0.14	0.14	0.12	0.18	0.13	0.14	0.15

C3: Vertical windspeed at P3

1.1m															
Time	C1			C2			C3			C4			C5		
(min)	L	M	H	L	M	H	L	M	H	L	M	H	L	M	H
1	0.21	0.31	0.56	0.17	0.20	0.36	0.16	0.24	0.24	0.15	0.31	0.41	0.22	0.25	0.29
2	0.25	0.28	0.71	0.17	0.17	0.33	0.18	0.27	0.31	0.18	0.30	0.51	0.21	0.24	0.32
3	0.19	0.33	0.61	0.11	0.16	0.36	0.17	0.26	0.38	0.16	0.28	0.43	0.24	0.28	0.34
4	0.29	0.39	0.63	0.11	0.20	0.27	0.18	0.26	0.28	0.17	0.33	0.42	0.20	0.26	0.36
5	0.23	0.41	0.63	0.16	0.22	0.24	0.17	0.31	0.28	0.15	0.22	0.45	0.21	0.27	0.32
6	0.25	0.43	0.60	0.10	0.17	0.26	0.21	0.30	0.33	0.18	0.25	0.44	0.21	0.29	0.32
7	0.18	0.45	0.61	0.20	0.20	0.28	0.19	0.23	0.32	0.13	0.24	0.41	0.23	0.28	0.31
8	0.22	0.44	0.56	0.12	0.23	0.31	0.18	0.29	0.35	0.15	0.26	0.50	0.20	0.27	0.30
9	0.19	0.41	0.62	0.13	0.19	0.27	0.20	0.26	0.37	0.14	0.33	0.35	0.20	0.26	0.29
10	0.26	0.47	0.50	0.12	0.19	0.25	0.19	0.23	0.34	0.14	0.29	0.42	0.21	0.25	0.29
0.6m															
Time	C1			C2			C3			C4			C5		
(min)	L	M	H	L	M	H	L	M	H	L	M	H	L	M	H
1	0.17	0.24	0.45	0.11	0.14	0.15	0.06	0.1	0.11	0.23	0.34	0.44	0.12	0.21	0.41
2	0.22	0.32	0.57	0.1	0.1	0.16	0.07	0.1	0.13	0.24	0.28	0.37	0.16	0.23	0.38
3	0.19	0.41	0.5	0.11	0.12	0.2	0.08	0.1	0.17	0.24	0.3	0.43	0.14	0.26	0.34
4	0.2	0.34	0.49	0.18	0.16	0.15	0.06	0.1	0.16	0.18	0.35	0.46	0.22	0.29	0.41
5	0.22	0.35	0.62	0.18	0.15	0.11	0.06	0	0.08	0.24	0.26	0.45	0.19	0.23	0.4
6	0.19	0.44	0.58	0.13	0.1	0.19	0.05	0.1	0.11	0.19	0.3	0.42	0.18	0.29	0.35
7	0.18	0.37	0.58	0.08	0.08	0.13	0.06	0.1	0.1	0.22	0.28	0.41	0.17	0.26	0.37
8	0.17	0.35	0.46	0.14	0.14	0.15	0.07	0.1	0.13	0.21	0.31	0.46	0.15	0.23	0.4
9	0.19	0.38	0.49	0.17	0.17	0.11	0.05	0.1	0.13	0.17	0.32	0.45	0.14	0.26	0.36
10	0.16	0.42	0.56	0.15	0.14	0.15	0.06	0.1	0.14	0.2	0.3	0.43	0.14	0.23	0.43
0.1m															
Time	C1			C2			C3			C4			C5		
(min)	L	M	H	L	M	H	L	M	H	L	M	H	L	M	H
1	0.14	0.22	0.17	0.17	0.24	0.31	0.15	0.2	0.2	0.18	0.18	0.21	0.22	0.16	0.27
2	0.18	0.24	0.22	0.2	0.29	0.32	0.17	0.2	0.21	0.15	0.19	0.21	0.2	0.17	0.22
3	0.18	0.26	0.26	0.19	0.23	0.32	0.18	0.2	0.25	0.16	0.2	0.22	0.21	0.2	0.17
4	0.19	0.21	0.25	0.19	0.28	0.27	0.16	0.2	0.25	0.16	0.17	0.21	0.16	0.21	0.19
5	0.24	0.2	0.21	0.2	0.28	0.27	0.17	0.2	0.26	0.22	0.16	0.21	0.18	0.26	0.21
6	0.19	0.23	0.22	0.19	0.24	0.24	0.14	0.2	0.26	0.19	0.16	0.2	0.19	0.22	0.16
7	0.2	0.22	0.25	0.2	0.29	0.25	0.18	0.1	0.26	0.18	0.17	0.19	0.2	0.23	0.22
8	0.23	0.2	0.24	0.18	0.25	0.28	0.19	0.1	0.17	0.15	0.16	0.18	0.19	0.17	0.19
9	0.2	0.17	0.28	0.23	0.24	0.27	0.17	0.1	0.15	0.17	0.17	0.18	0.19	0.18	0.18
10	0.17	0.19	0.2	0.23	0.23	0.26	0.15	0.2	0.17	0.17	0.19	0.19	0.2	0.16	0.2